CURRENT RECORD ANALYSIS AND TIDAL COMPUTATIONS FOR PORT VALDEZ, ALASKA

J. C. Mungall

IMS Report R73-5
Sea Grant Report 73-6

Institute of Marine Science
University of Alaska
Fairbanks, Alaska

INSTITUTE OF MARINE SCIENCE

UNIVERSITY OF ALASKA

FAIRBANKS, ALASKA 99701

CURRENT RECORD ANALYSIS AND TIDAL COMPUTATIONS FOR PORT VALDEZ, ALASKA

J. C. H. Mungall*

IMS Report R73-5
Sea Grant Report 73-6
November 1973

D. W. Hood
Director

---

*Presently at Department of Oceanography, Texas A & M University, College Station, Texas 77843

ACKNOWLEDGEMENTS

This publication is a result of research sponsored by the Alyeska Pipeline Service Company through the Institute of Marine Science, University of Alaska. Final report preparation was assisted in part by the Alaska Sea Grant Program under Grant No. 04-3-158-41 from NOAA Office of Sea Grant, Department of Commerce.

CONTENTS

CHAPTER I

GENERAL DESCRIPTION OF PORT VALDEZ AND ITS TIDES

Description of Port Valdez

The fjord of Port Valdez (Figure 1) is the innermost of several bodies of water that lie between the Gulf of Alaska and the town of Valdez. The center of the fjord lies approximately at 69°07'N and 146°28'W. The dimensions of the fjord are about 3 miles by 12 miles, with the major axis lying East-West.

Port Valdez has a pronounced sill at its entrance, Valdez Narrows, where the minimum sill depth is about 80 fathoms. At this point the entrance is less than 1 mile wide. Between Valdez Narrows and the town of Valdez the fjord is U-shaped in cross-section with depths for the most part lying between 100 and 130 fathoms.

Description of the vertical tides of Port Valdez

The vertical movement of the sea surface in Port Valdez, as far as tidal motions are concerned, appears to be very simple. Little or no variation in tidal amplitude occurs over the surface (see next section), and so one set of harmonic constituents is sufficient to predict the vertical tide anywhere in the fjord. A set of constituents is shown in Table I, along with some additional values of interest. These values, provided by the U.S. Coast and Geodetic Survey, were computed by them from a 29-day record taken in 1901. As can be seen from the factor $F = (K_1 + O_1)/(M_2 + S_2) = 0.43$, the tides of the fjord are of the 'mixed, predominantly semi-diurnal' type.

Although the regular features of the tide seem simple, there may be additional perturbations which should be examined. Storms in the Gulf of Alaska may cause noticeable changes of height, and there may also be smaller seiching oscillations due to local winds. The detection of the presence of such features could only be investigated by continuous tide gauge records.

Some generalizations concerning the tides of Port Valdez

It is to be expected that the vertical tides of the region (i.e. tide heights) should be fairly simple for two reasons: 1) Owing to the considerable depths, the part played by bottom friction will be small. 2) Again, as a result of the considerable depths, the length of the fjord is a small fraction of the theoretical resonant length*, so that little increase in tidal range will occur between the inner limit of the sill and the end of the fjord**. These two factors should result in a tide of pure standing-wave type, with practically no change in tidal range or change of phase between the sill and the end of the fjord. Thus, as a general conclusion, the surface slope along the major axis of the fjord should be virtually negligible at all stages of the tide.

Owing to the sea surface being essentially horizontal at all times, a simple estimation can be made of the flow rate through any section of the fjord. Representing the instantaneous tide height h by

$$h = \hat{h} \sin \omega t,$$

where $\hat{h}$ is the amplitude of the constituent having angular frequency ω (2π/Period), then

$$\frac{\partial h}{\partial t} = \omega \hat{h} \cos \omega t.$$

The maximum rate of change of the tide, $\omega \hat{h}$, occurs as the sea surface passes through mean sea level. If the surface area of the fjord is S, and the

---

*for the M_2 tide, $L = T\sqrt{gH}/4$, or $L = 12.42 \times 3600 \times \sqrt{9.81 \times 130 \times 1.829}/(4 \times 1.853 \times 1000)$ nm so the resonant length L = 291 nautical miles.

**Theoretical amplification between entrance and end of fjord is $1/\cos(90° \times 12/291) = 1.002$.

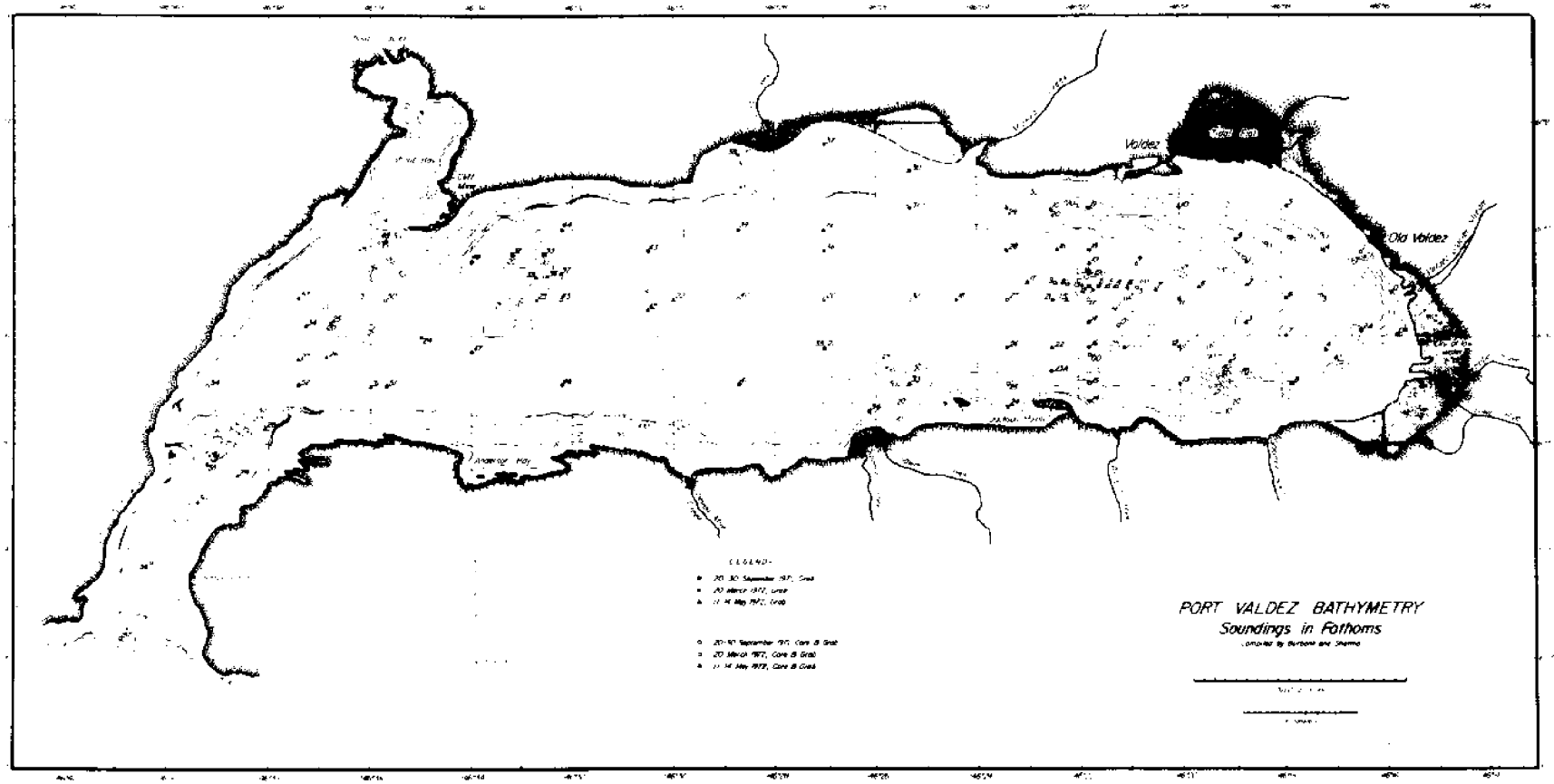

Figure 1. Bathymetry of Port Valdez

TABLE I

TIDAL CONSTITUENTS FOR

PORT VALDEZ*

Location 69°08'N - 146°20'W		Time Zone S + 10
Constituent	Amplitude, ft	κ, degrees÷
K_1	1.657	122.7
O_1	0.970	110.7
(P_1)	(0.548)	(122.7)
(K_2)	(0.414)	(24.7)
(μ_2)	(0.108)	(322.7)
S_2	1.522	24.7
M_2	4.514	353.7
M_4	0.090	141.2
M_6	0.029	190.1
(N_2)	(0.862)	(337.1)**
(L_2)	(0.125)	(10.3)**
(2N)	(0.115)	(320.5)**

Note: values in parentheses are obtained by inference.

Mean sea level 6.3 ft above chart datum
Neap Range = 6.23 ft
Mean Range = 9.65 ft
Spring Range = 12.53 ft

* Source: U. S. Coast and Geodetic Survey

÷ κ (Kappa) is local epoch

** my calculations

cross-sectional area is A, then the maximum depth-mean current $\hat{U}$ is

$$\hat{U} = S \omega \hat{h} / A.$$

As a first example, to estimate the maximum depth mean current associated with the M_2 tide at the entrance, using

$$S = 100 \text{ km}^2$$

$$\omega = 2\pi/(12.42 \times 3600)$$

$$\hat{h} = 1.375 \text{ m}$$

$$A = 1480 \times 100 \text{ m}^2,$$

then $\hat{U} = 13$ cm/sec.

As a second example, one can estimate the maximum depth mean current associated with the M_2 tide, at a distance of some 5-1/2 miles from the closed end of the fjord. With S now equal to 50 km^2 (0.5 x the former value) and A now equal to 9000 x 100 m^2 (6.1 x the former value) the current will be only about 13 x 0.5/6.1 cm/sec, or about 1 cm/sec. Thus one can reasonably conclude that depth mean currents throughout the fjord are likely to be small.

A final simple computation that can be made is one to determine the effect of coriolis force on the sea surface heights at the sides of the fjord. The maximum slope of the sea surface halfway up the fjord can be obtained from

$$\tan \theta = \frac{2 \Omega \sin \phi}{g} U$$

where $\Omega = 2\pi/(24 \times 3600)$ sec^{-1}

ϕ = latitude (61°04')

$g = 981$ cm sec^{-2}

U = current in cm sec^{-1} (1 cm sec^{-1})

or $\tan \theta = 6.5 \times 10^{-8}$.

Since there is essentially zero current when the sea surface is at its maximum, the coriolis force causes no slope across the fjord at this time. When maximum flood or ebb currents occur (at a time when the sea surface is passing through mean sea level), the above slope causes the sea surface at the sides of the fjord to be about $3 \times 10^5 \times 6.5 \times 10^{-8}$ cms (0.2 mm) above or below mean sea level - an insignificant quantity.

As far as the coriolis force is concerned, the only effects of interest are likely to be the lag or lead of the maximum current along the sides, compared to those in the center.

CHAPTER II

DESCRIPTION OF DATA COLLECTION AND ANALYSES TECHNIQUES

Current meter deployment

In December 1971, and again in March 1972, current meters were deployed in Valdez Narrows in the (approximate) location of 61°04'N - 146°40'W. During each deployment the current meters were located on a saddle-point (Figure 2) in some 160 m of water. In each case some 6 days of records were obtained, the relevant dates being 3-9 December 1971 and 12-18 March 1972. Hydrographic data were recorded throughout Port Valdez for the same periods by the Institute of Marine Science, making the current meter records -- otherwise of sadly short length -- of considerable interest.

In an attempt to reduce noise due to motion induced by surface waves, the taught-wire mooring method was used with the string of current meters being supported by a subsurface buoy. During the first (December 1971) deployment, four meters were placed at depths of 10, 20, 80, and 130 m, while during the second (March 1972) deployment, five meters were placed at depths of 10, 20, 40, 80, and 130 m. Braincon Model 381 histogram current meters were used, being set so as to record current speed and direction every 20 minutes.

It is necessary to remark at this point that there exists a possibility that fluctuations with a frequency of greater than 1.5 cph (cycles per hour) may have been aliased into the records. As far as the present investigation is concerned this is probably of no serious consequence.

Analysis philosophy

The shortness of the original records (6 days) is such that limits are necessarily set on the type and quality of information that can be extracted. The main items of interest are probably the behavior of the drift-currents and tidal-frequency currents with depth and time. In this report the dividing line between drift currents and tidal-frequency currents is taken to be 0.04 cph (so that constituents of the diurnal-, semidiurnal-, etc. type are included in the tidal-frequency current group). The most economical of the filters needed for the above separation involves a loss of some 21 hours of data at each end of the record, leaving only some 4 days of record for display and analysis. Meaningful analysis for the diurnal and semidiurnal components of the currents is virtually impossible under these circumstances, so that, for example, little faith can be put in the time delay of the maximum current with depth. All that can be expected are approximate values which must be used with caution. On the positive side, except for their short duration, some useful information is to be found in the drift currents and in particular in their directions and magnitudes as a function of time and depth.

As the current meter data are two-dimensional, in order to avoid the difficulties of programming the filtering and analysis procedures in complex arithmetic, the current vectors must be split up into two components (true North and true East) and then be separately filtered and analysed. Finally, the results of the analysis are recombined to provide information concerning the dimensions of the half-major and half-minor axes, the orientation of the major axis, and the phase of, for example, the maximum inwards current.

Since much of the information of use in the records may be displayed visually, the following computer plots are shown for each current meter.

a) True North component, unsmoothed current (V-NORTH)
b) True East component, unsmoothed current (V-EAST)
c) True North component, smoothed current (VBAR-NORTH)

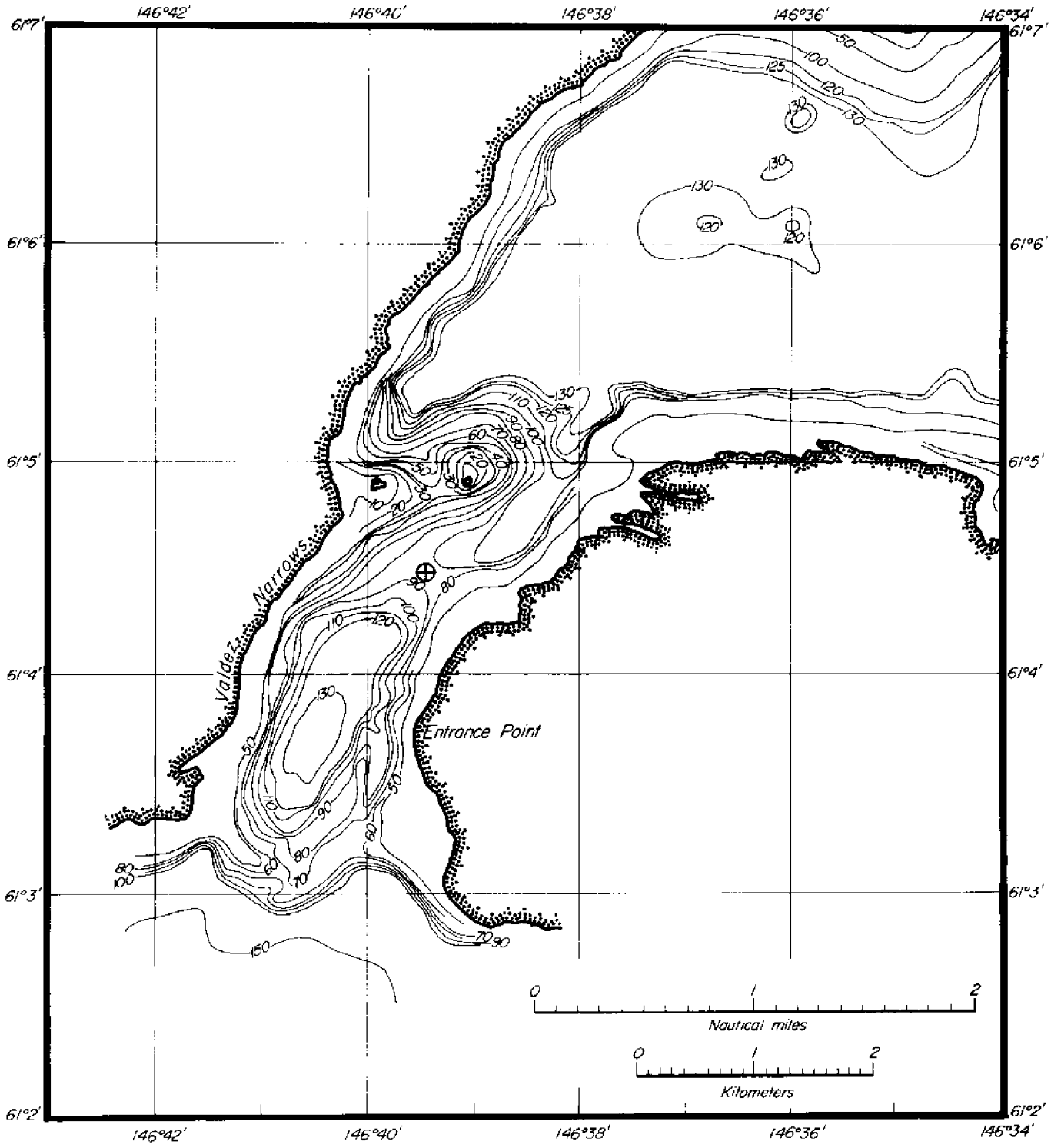

Figure 2. Bathymetry of entrance to Port Valdez showing location of current meters

d) True East component, smoothed current (VBAR-EAST)
e) 40° True component, tidal-frequency current (VCHANNEL)
f) 130° True component, tidal-frequency current (VCHNL + 90)
g) Magnitude, drift current (DRIFT CM/SEC)
h) True direction, drift current (DRIFT ANGLE T)
i) Log Spectra, original current magnitude (LOG (SPECTRA)

All current values are in centimeters per second, and all angles are in true degrees. The value '40°' used above represents the approximate angle of the inwards axis of the fjord entrance. For interest, the tides corresponding to the two periods have been predicted, and are shown at the start of each group of records (the constituents shown in Table I being used).

Filtering procedures

As mentioned previously, the current data were recorded at intervals of 20 minutes. The display and visual interpretation of the data is facilitated by removing some of the high-frequency variations, which may in many cases be random, by means of a low-pass filtering operation (a process often called 'decimation').

A second consideration is that conventional tidal analysis techniques are usually based on the assumption that the data are spaced at hourly intervals. In order to ensure that aliasing does not occur, the hourly data should be such that the highest frequency present in the record should not be greater than 0.5 cph. As the spacing of the original data is such that frequencies can be present of as high as 1.5 cph some form of low-pass filtering is again necessary.

To meet both of the above requirements a numerical low-pass filter was designed that is symmetrical (and thus has no phase distortion) and has the amplitude response shown in Figure 3. As can be seen, the cut-off is around 0.5 cph. The shoulders of the filter are not very sharp; this choice of filter was however necessitated by the fact that symmetrical filters with sharper shoulders result in the loss of increasing amounts of data at the ends of the records. With the above filter only 2 hours are lost at each end.

To simplify the tidal analysis process, and to present the data in forms such that the drift currents may clearly be distinguished from the tidal-frequency components (say, those components containing frequencies equal to or greater than one cycle per lunar day), it is customary to make use of the Doodson low-pass filter (Doodson & Warburg, 1941, p. 110). This symmetrical filter, whose amplitude response is shown in Figure 4, is such that there are very small contributions present from the principal diurnal, semidiurnal, etc., constituents. Furthermore the Doodson filter is particularly economical in that only 19 hours of data are lost at each end of the record. The combined effect of the two filters is such that about 21 hours of data are lost at each end of the records. Thus the original 6-day records are essentially reduced to 4-day records before one can perform the tidal analyses or look at the drift currents. Obviously this truncation is something to be considered in the future when more records are collected.

The need to restrict the truncation of the records to the bare minimum leads to filters without sharp cut-offs. The actual net effect of the combined filtering operation on the tidal frequency components is seen in Figure 5, while that affecting the drift currents is seen in Figure 6. It is necessary to remember this when analysing the filtered data for tidal constituents; the resulting computed amplitudes must be multiplied by the reciprocal of the combined amplitude response associated with each particular frequency.

For general interest results of an intermediate part of the filtering process used to obtain the basic drift components (VMEAN-NORTH and VMEAN-EAST), and to obtain the basic tidal frequency components (VDIURNAL-NORTH and VDIURNAL-EAST) are shown in Figure 7 for the 10 meter 5 December 1971 current record. The original unsmoothed and decimated records corresponding to this record can be seen in Figure 9. To be noted are the truncations occurring in the two steps, and the effect of filtering in each step.

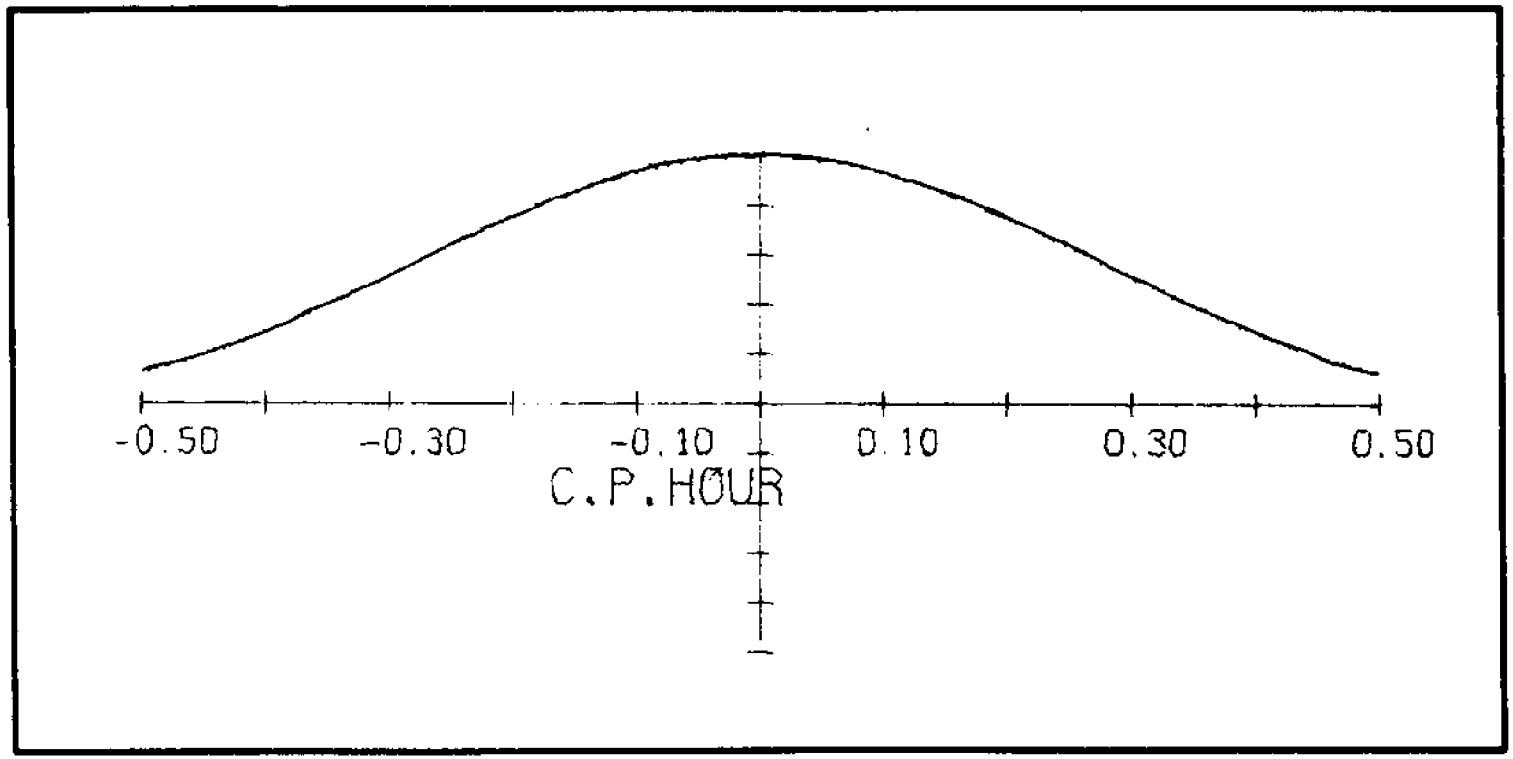

Figure 3. Amplitude response of decimation filter

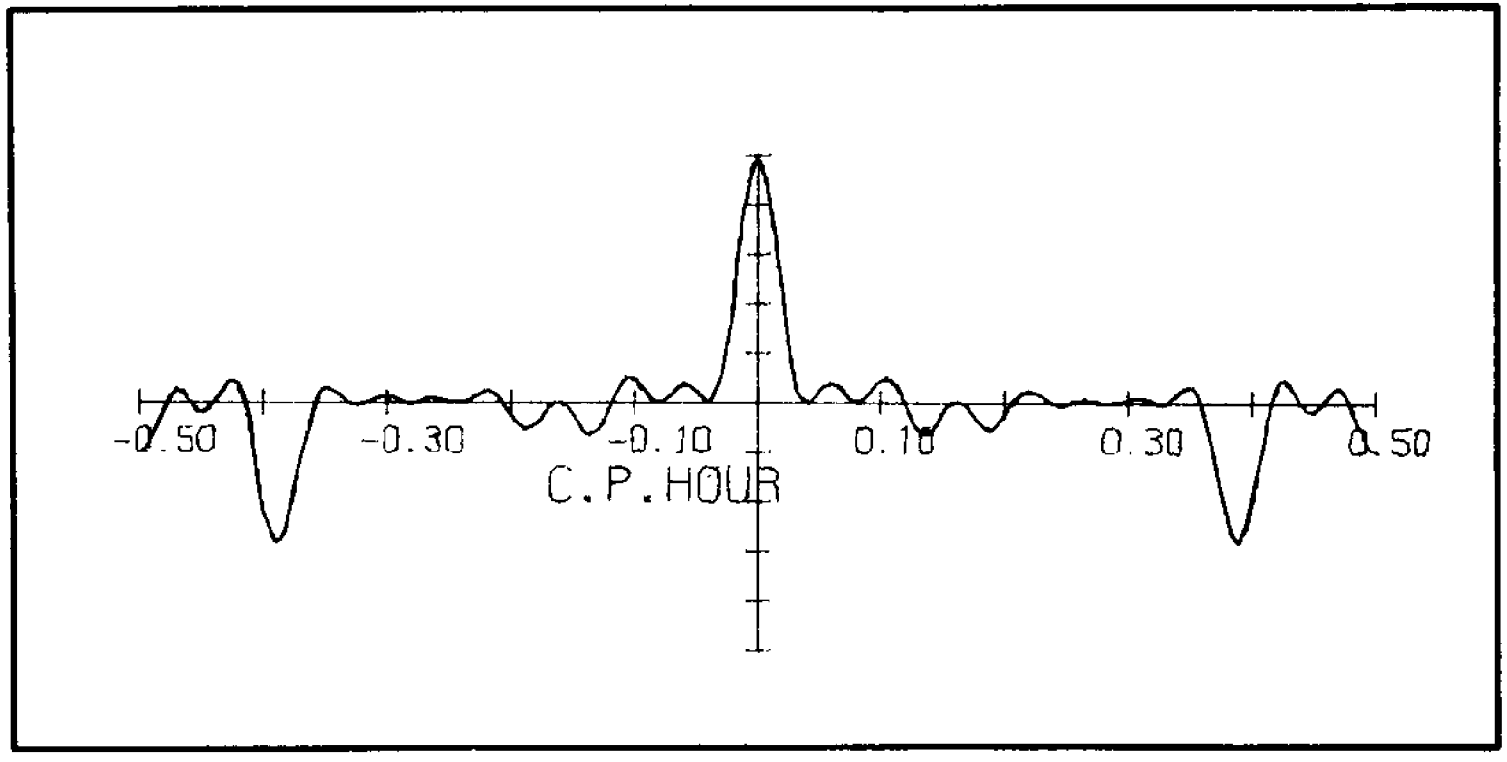

Figure 4. Amplitude response of Doodson low-pass tidal filter

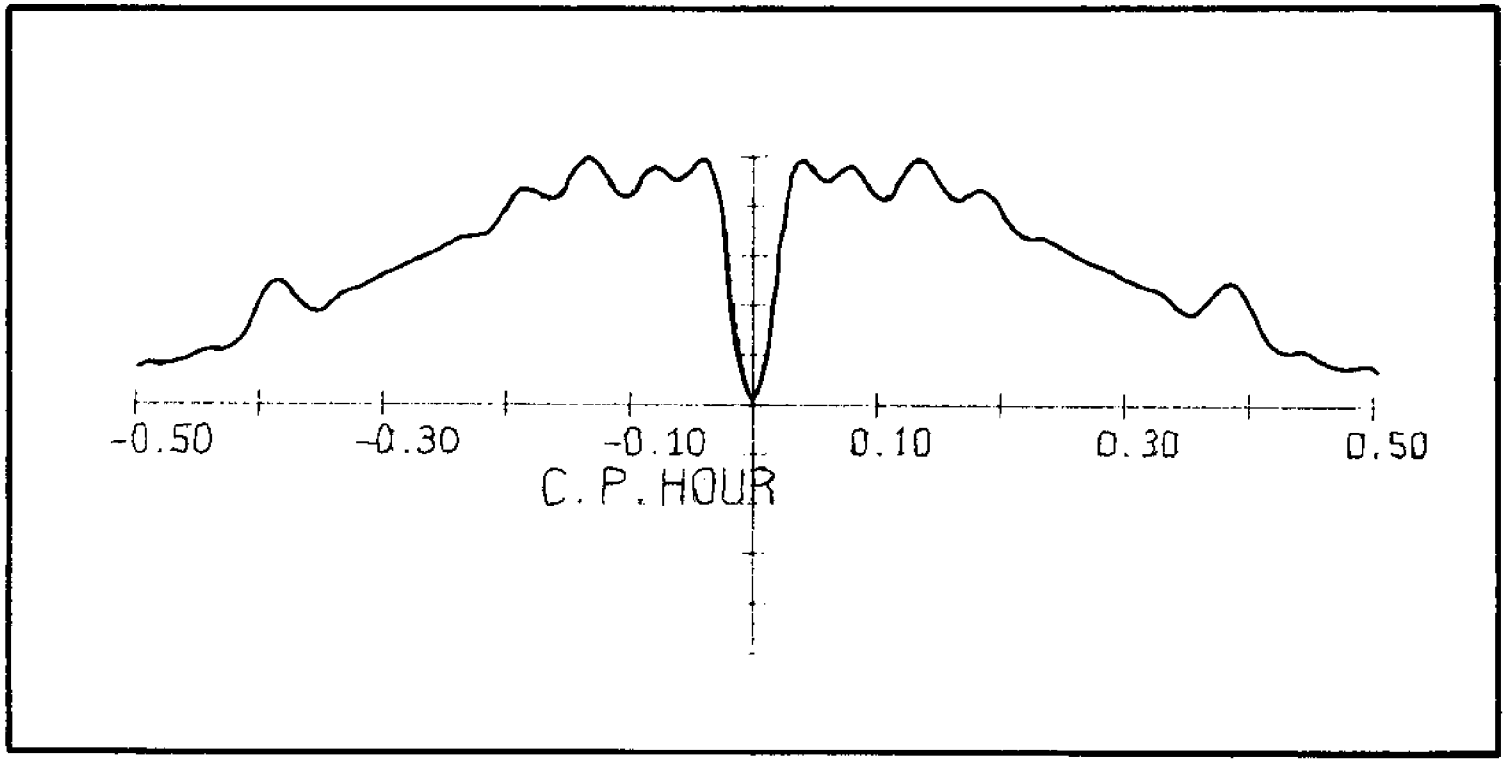

Figure 5. Amplitude response of operations leading to data containing tidal frequencies

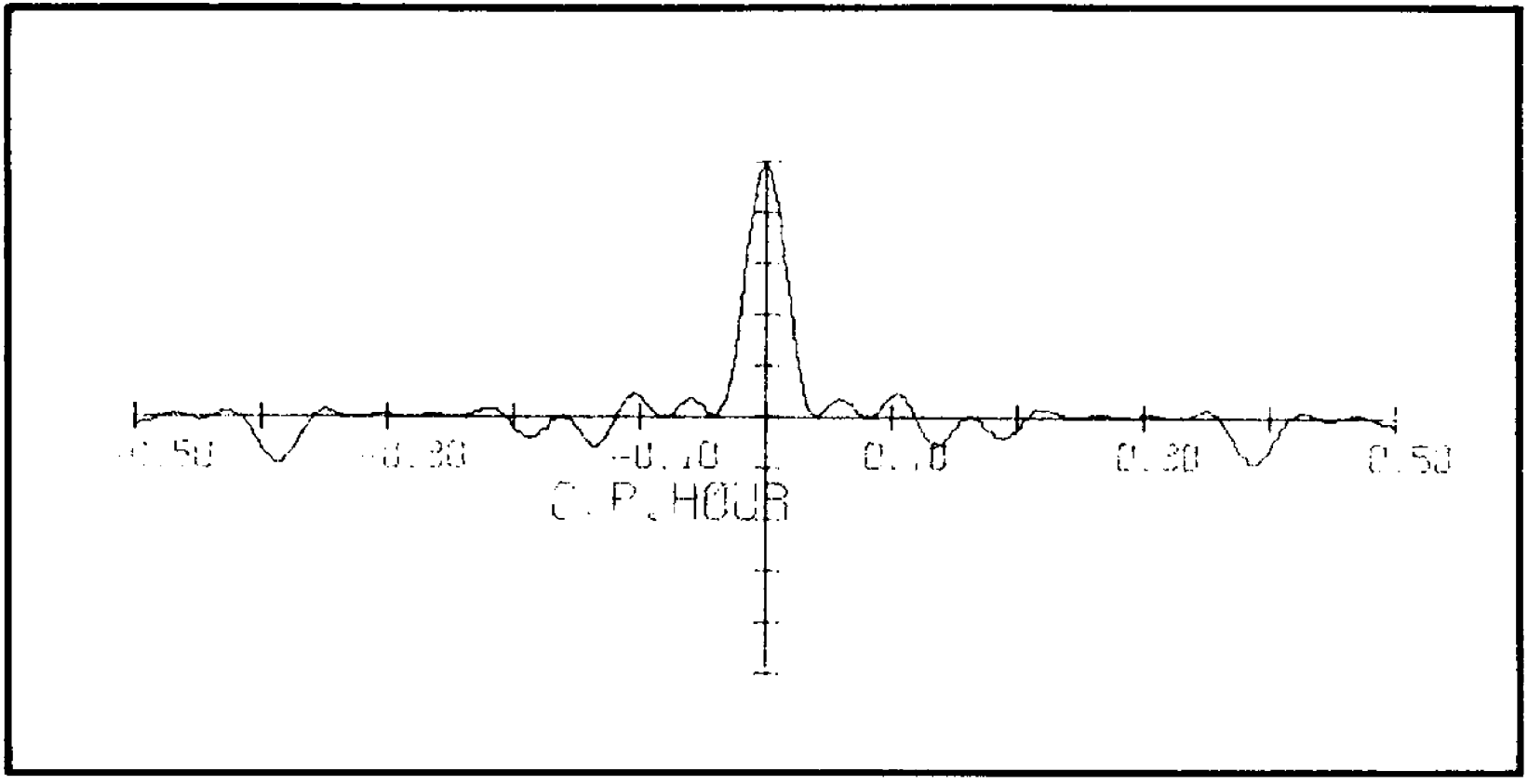

Figure 6. Amplitude response of operations leading to data containing drift frequencies

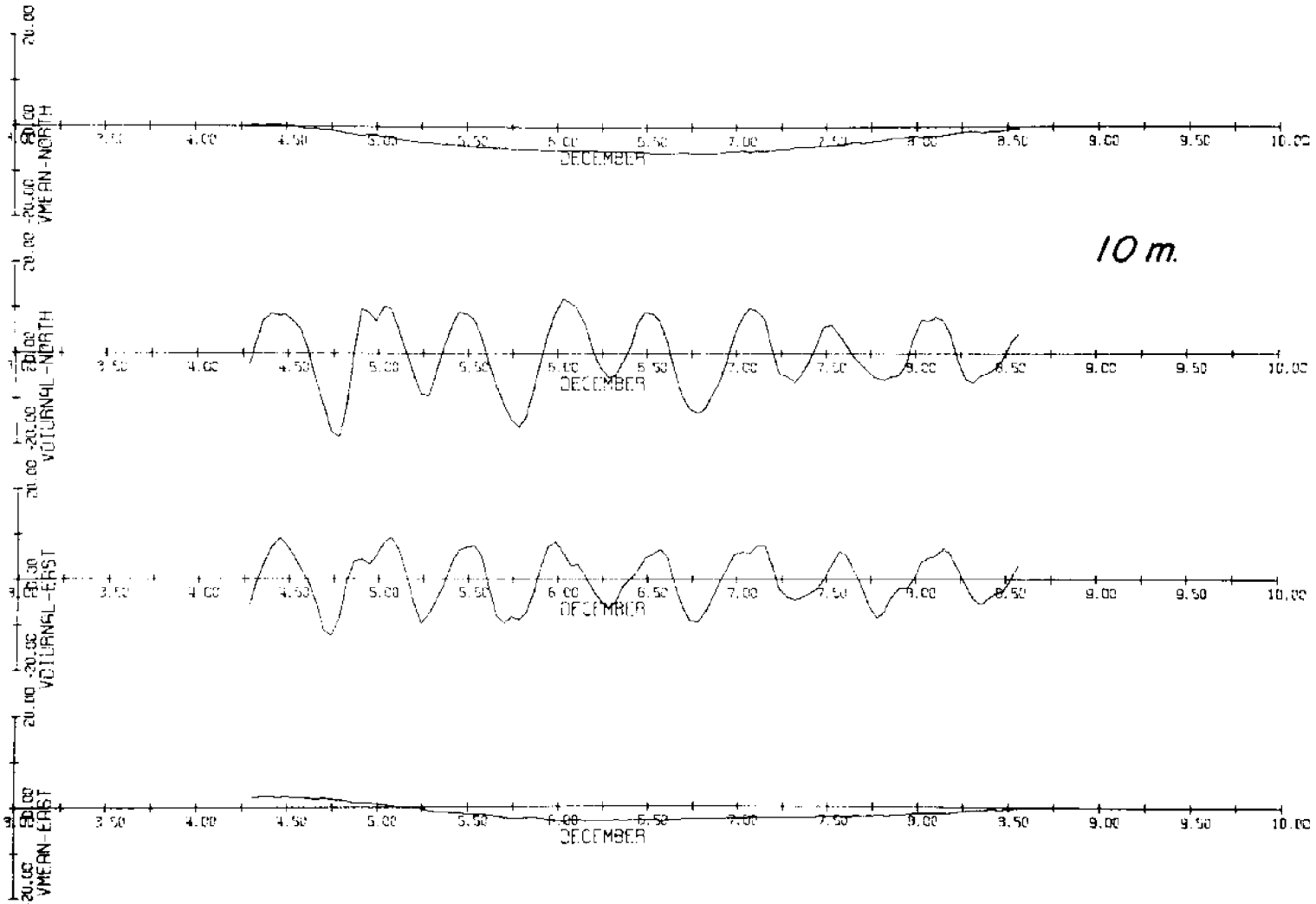

Figure 7. Example of intermediate calculations showing the North and East components of drift and tidal frequencies

TABLE II. Constituents, angular frequency and correction factors used in the harmonic analysis program.

Constituent	Angular frequency, degrees/hour	Correction factor
M.S.L.	0	x 1/1.0
K_1	15.04	x 1/0.988
M_2	28.98	x 1/0.956
M_3	43.48	x 1/0.911
M_4	57.97	x 1/0.831

Tidal analysis

The method used to analyse the filtered data for the tidal constituents is the familiar least-squares method (Dronkers, 1964, p. 102). In this approach a unique set of amplitudes (and associated phases) is sought that reduces the differences between the sum of the squares of the deviations of the sinusoids of given frequencies and the measured tide data to a minimum. In choosing the frequencies it is necessary to take into account the length of the record: the longest unambiguously detectable period will be half the length of the record, and furthermore the separation between every pair of frequencies in cph must be greater than the reciprocal of the record length in hours. The constituents ultimately chosen for analysis are shown in Table II, along with their angular frequencies and correction factors.

Spectral analysis

The last process of importance is that of spectral analysis. This is applied to the original unfiltered data -- in this case the vector sum of the currents was chosen as the one-dimensional parameter to be investigated. Owing to the shortness of the records it was not necessary to resort to Fast Fourier Transform techniques. The form of the program used was taken from Jenkins & Watts (1969, pages 207 and 310). The autocovariance function was computed for 60 lags of 20 minutes each (i.e. a maximum lag time of about 1/10 of the total record). A Tukey spectral window was then used in the calculation of the spectra, which was computed for 150 frequency intervals up to a frequency of 1/(0.3333 x 2) cph i.e. up to 1.5 cph, the highest frequency ideally contained in the original data.

CHAPTER III

THE PERIOD 3-9 DECEMBER 1971

Description of the tides

In order to provide a basis for comparison between the tides and measured currents, the tides of Port Valdez were predicted (using the constants in Table I) for the period corresponding to that over which the currents were measured: 3-9 December 1971. The tide curve is shown in Figure 8. It should be noted that there is no proof that this is the real tide curve, since no measurements of this type were attempted; however the curve is the best estimate available. It is obvious that at this time the tides were definitely of the 'mixed' type, and this will be reflected in the appearance of the current meter records.

As mentioned earlier, on account of the shortness of the current meter records, it proved reasonable to only analyse them for four tidal constituents (in addition to the mean value). To make quantitative comparisons, the predicted tidal data (corresponding precisely in origin, number of data points, and spacing to the decimated and filtered current meter data) were analysed in the same fashion as were the current meter records to give a mean value, and to give the K_1, M_2, M_3, and M_4 constituents. The December 1971 tide data gave the results noted in Table III.

TABLE III. December 1971 tidal data.

	Amplitude, ft	Phase, degrees
M.S.L.	6.27	--
K_1	2.73	359.9
M_2	4.56	154.9
M_3	0.06	264.2
M_4	0.07	107.6

The time origin for the above phases is 09.67 hours (i.e. 09 hours 40 minutes) local time on 6 December 1971. The absence of significant contributions from the M_3 and M_4 constituents is noteworthy. This absence also occurs in the corresponding current analysis.

The current meter records

Unfortunately data for the 40 m current meter were not available. The raw data, and the decimated data (i.e., after being subjected to the low pass numerical filter having a cut-off frequency of 0.5 cph) are shown in Figure 9 through 12 in the form of true North and true East components.

As to the reasons behind the jagged appearance of the data (plotted at intervals of 20 minutes, as recorded) it is difficult to speculate. One reason is that the current meters were set for maximum currents of some 10 times greater than that actually encountered: thus, the current meters were not operating in the most favorable manner. Sluggishness, and somewhat erratic readings could result. However at times a considerable coherence exists between the spikes on, say, the 10 m and 20 m records.

As expected, the decimated records reflect the 'mixed' type of vertical tide that occurred during the period of observation. Although difficult to interpret, the results of the filtered decimated records are shown in Figures 13 through 16. As described earlier, these computer plots show from top to bottom:

1) 40°-true component of tidal frequency current, cm/sec
2) 130°-true component of tidal frequency current, cm/sec
3) magnitude of drift current, cm/sec
4) direction of drift current in degrees true.

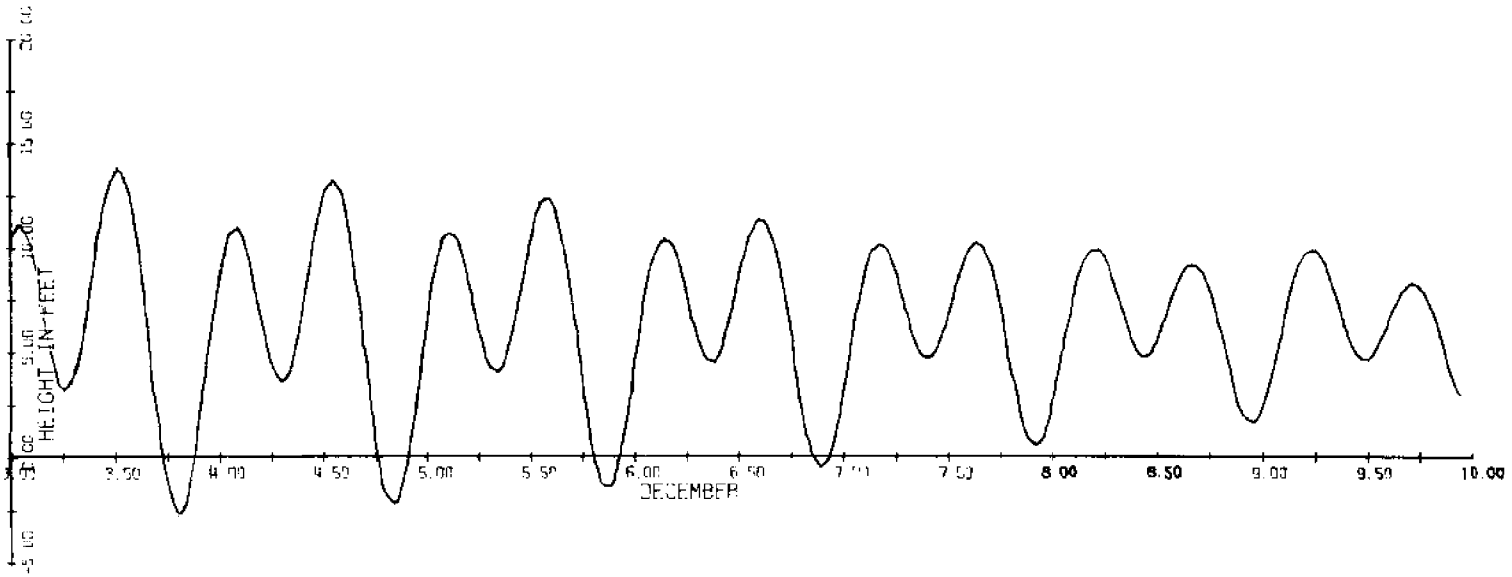

Figure 8. Computed tides of Port Valdez for the period 3 December 1971 to 10 December 1971

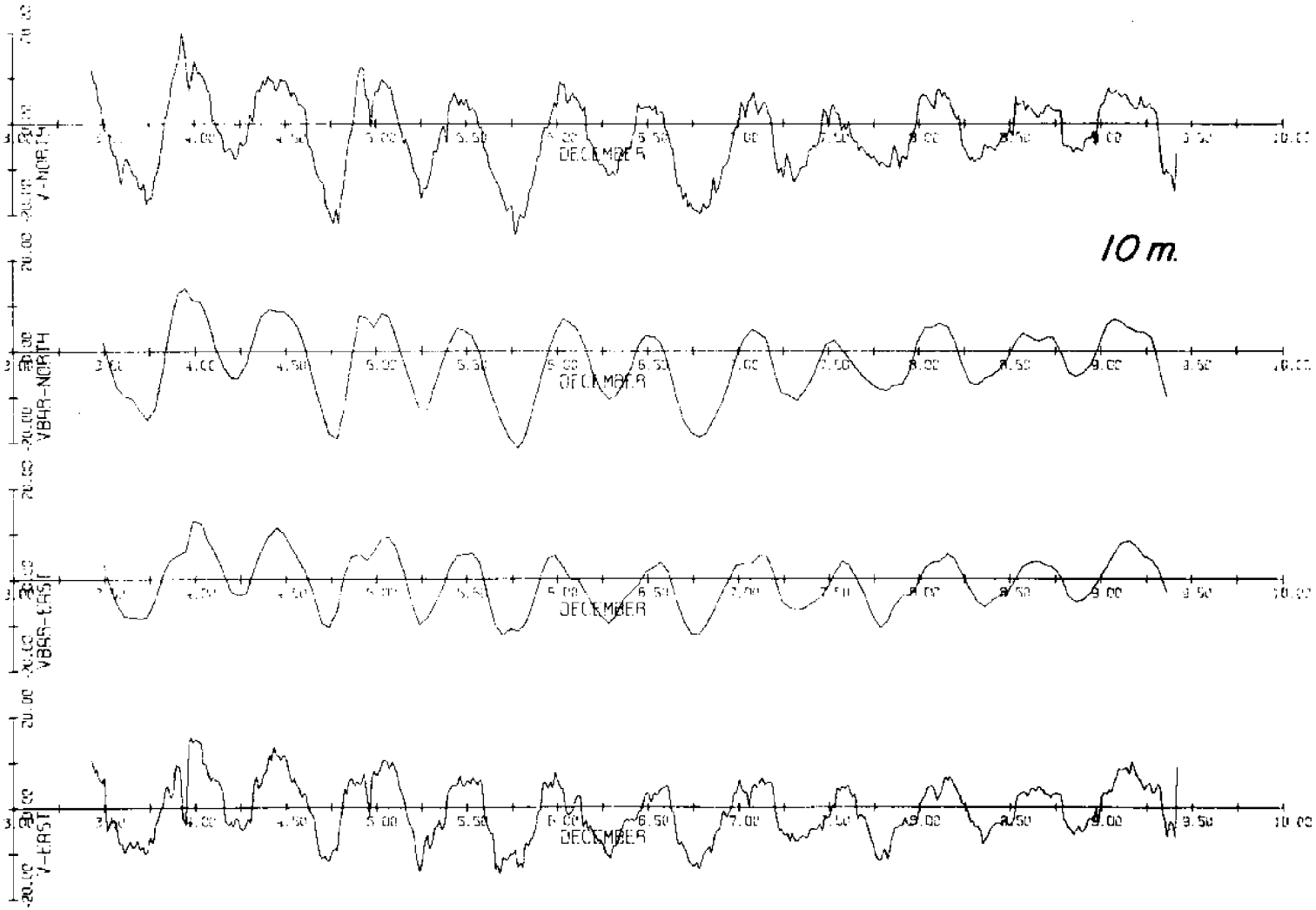

Figure 9. Original and decimated records for December 1971 - 10m

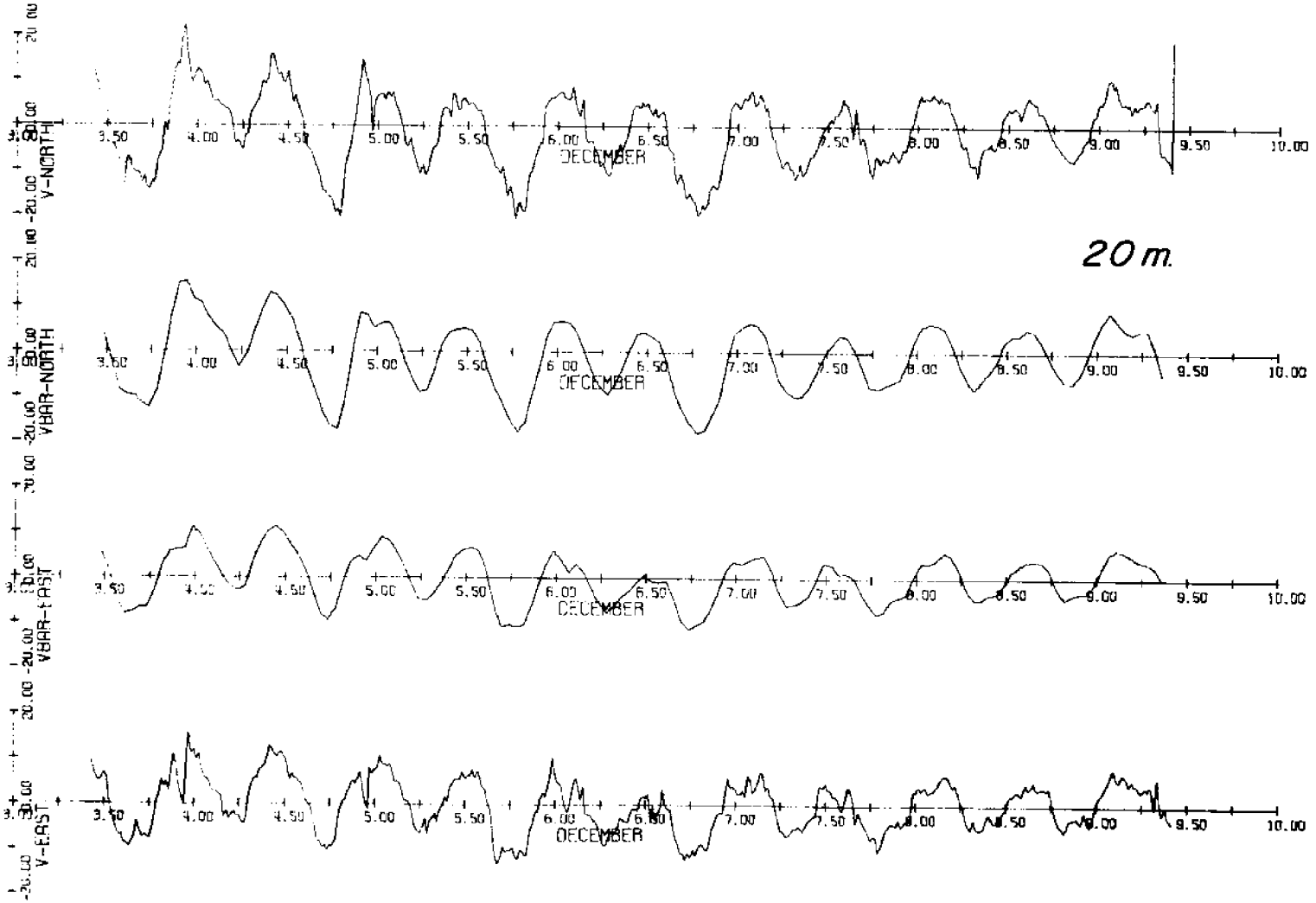

Figure 10. Original and decimated records for December 1971 - 20m

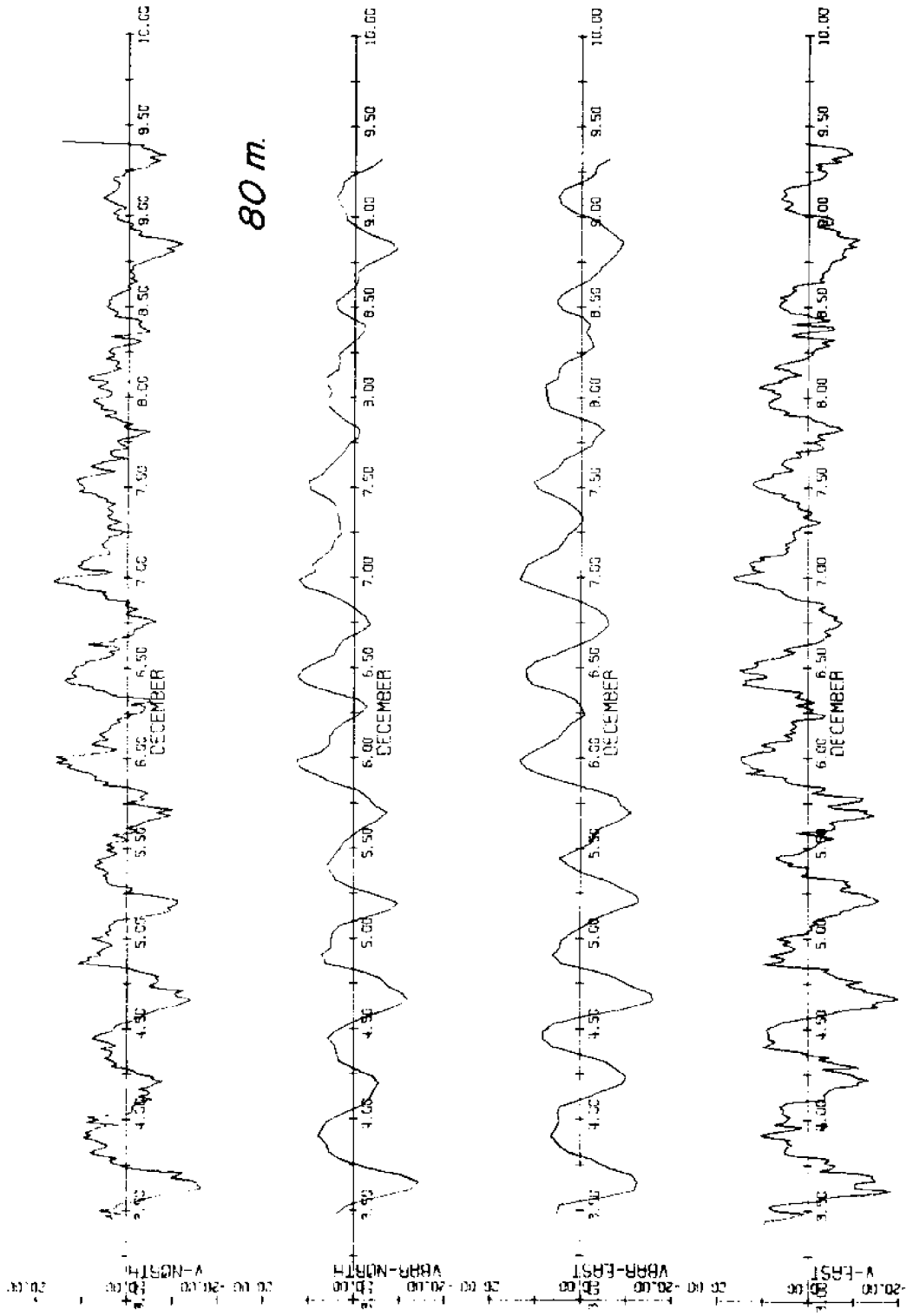

Figure 11. Original and decimated records for December 1971 - 80m

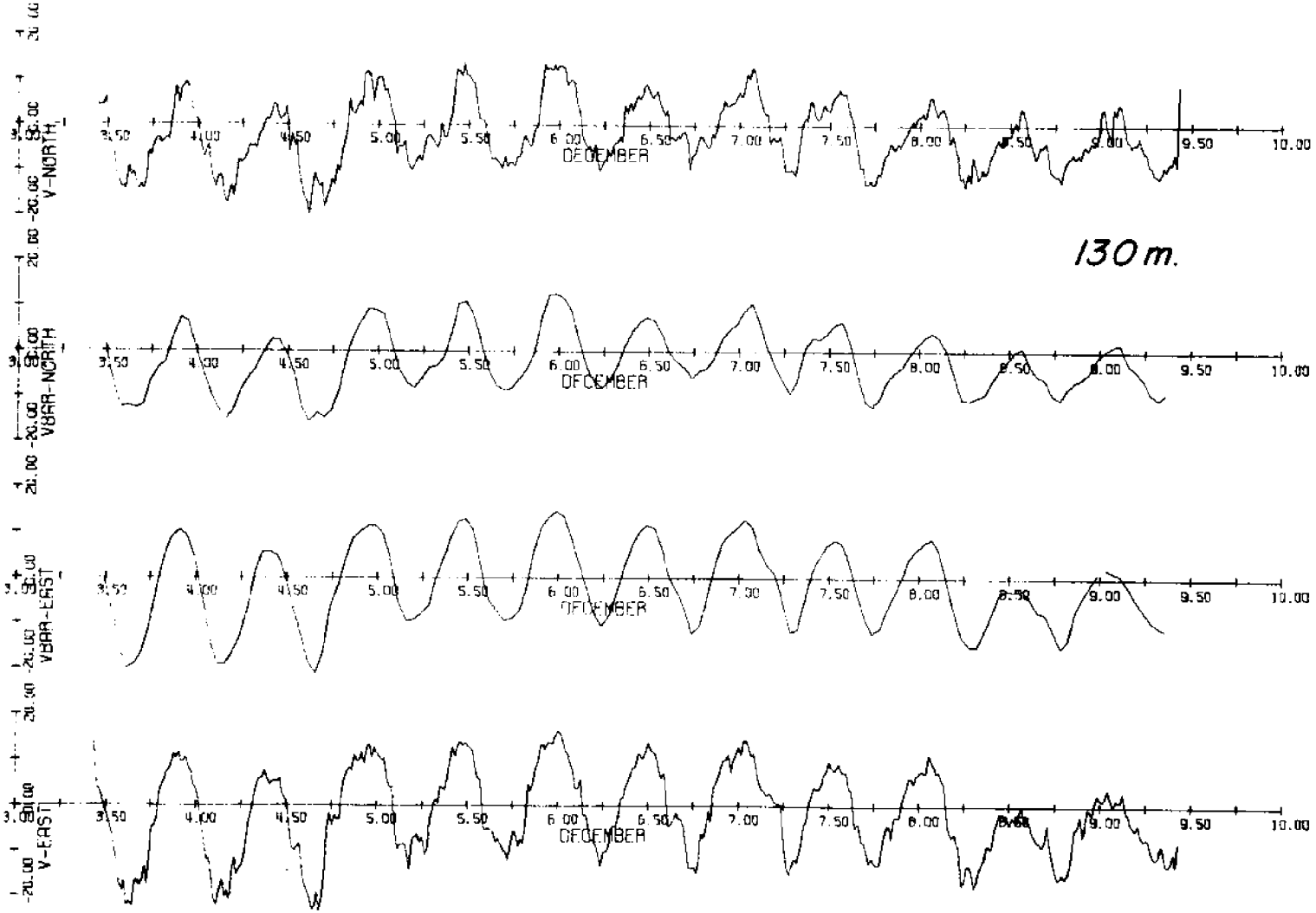

Figure 12. Original and decimated records for December 1971 - 130m

TABLE IV
December 1971 current meter analysis

semi-major and semi-minor axes
(maximum and minimum currents)

degrees/hour	K_1 15.04		M_2 28.98	
	max cm/sec	min cm/sec	max cm/sec	min cm/sec
10 m	4.2	0.5	12.2	0.1
20 m	4.4	0.3	11.5	0.5
80 m	2.7	0.1	9.9	0.7
130 m	3.0	0.5	14.4	0.6

phase (based on central time origin of December 6th 1971
9.67 hrs local time) and orientation of major axis

degrees/hour	K_1 15.04		M_2 28.98	
	phase degrees	orientation degrees T	phase degrees	orientation degrees T
10 m	294	27	94	37
20 m	294	35	92	34
80 m	273	50	65	53
130 m	232	54	60	53

The filtered currents: tidal components

The angle made by the axis of the channel at the entrance, in the inwards direction, is 40° true; hence the choice of component directions. The top graph in Figures 13 through 16 thus shows the tidal component of the current flowing into Port Valdez in the long-channel direction, and the second graph shows the cross-channel component. The fact that the latter exists at all is obviously an indication that the current is not always aligned with the channel axis. A cursory glance shows that the cross-channel components are erratic for the 10 to 20 m depths, but that there is considerable correspondence between the cross-channel and long-channel peaks in the 80 and 130 m records.

When the tidal component currents were analysed it was found that only the K_1 and M_2 constituents were of significance. The two components, when recombined so as to provide information on the current ellipses corresponding to each constituent, are shown in Table IV.

As can be seen, the ellipses are such that the maximum current is at the very least 6 times the minimum current. In the case of the M_2 constituent, the maximum and minimum current values when averaged from top to bottom are 12.0 and 0.5 cm/sec. The equivalent values for the K_1 constituent are 4.6 and 0.4 cm/sec.

From records of such short length it is difficult to say whether the changes that occur in the amplitudes from top to bottom are meaningful. In the opinion of the writer of this report they are not; i.e., longer records would be needed to ascertain if there is any real variation in amplitude.

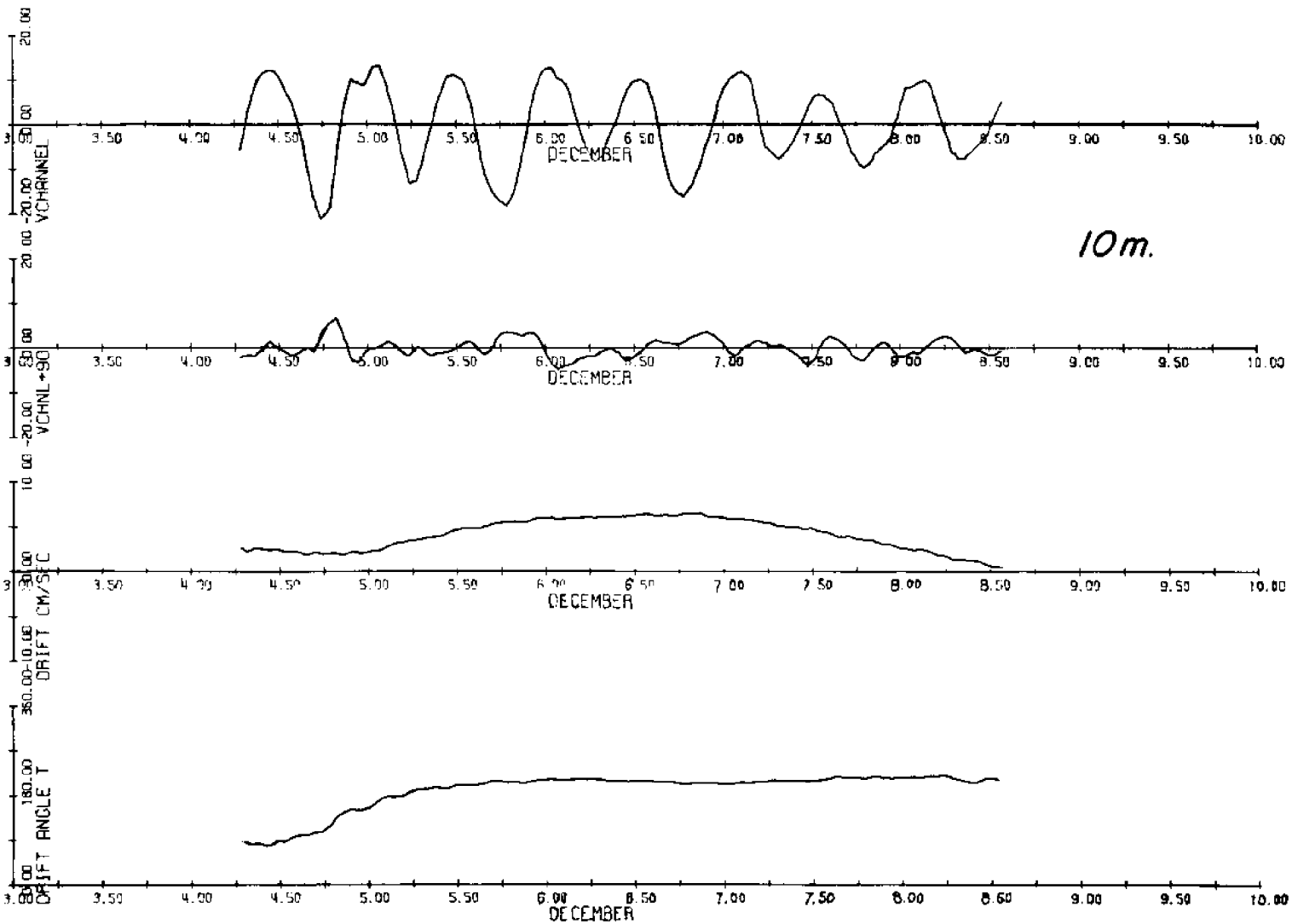

Figure 13. Long-channel and cross-channel components of tidal frequency currents, velocity and direction of drift currents, December 1971 - 10m

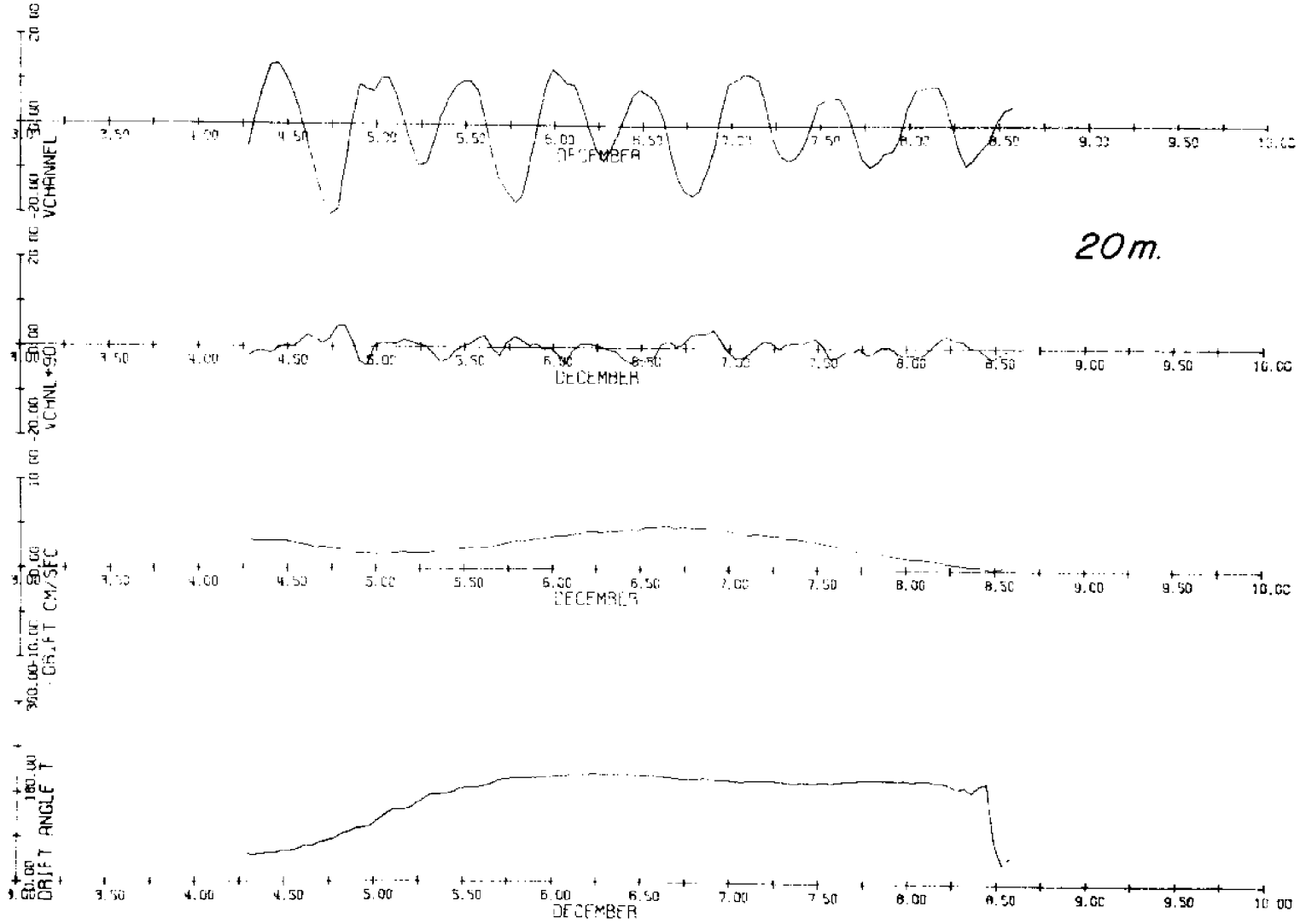

Figure 14. Long-channel and cross-channel components of tidal frequency currents, velocity and direction of drift currents, December 1971 - 20m

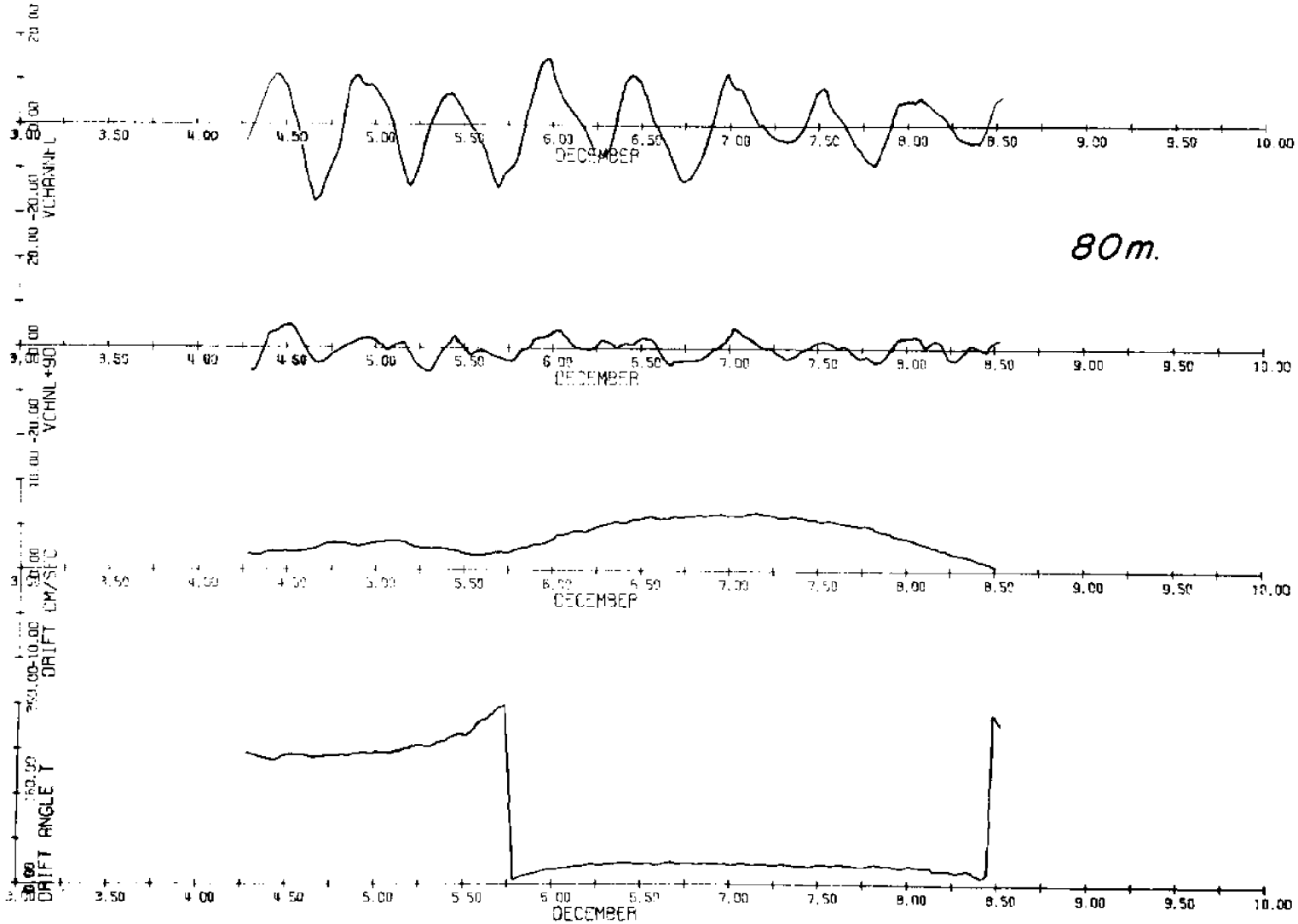

Figure 15. Long-channel and cross-channel components of tidal frequency currents, velocity and direction of drift currents, December 1971 - 80m

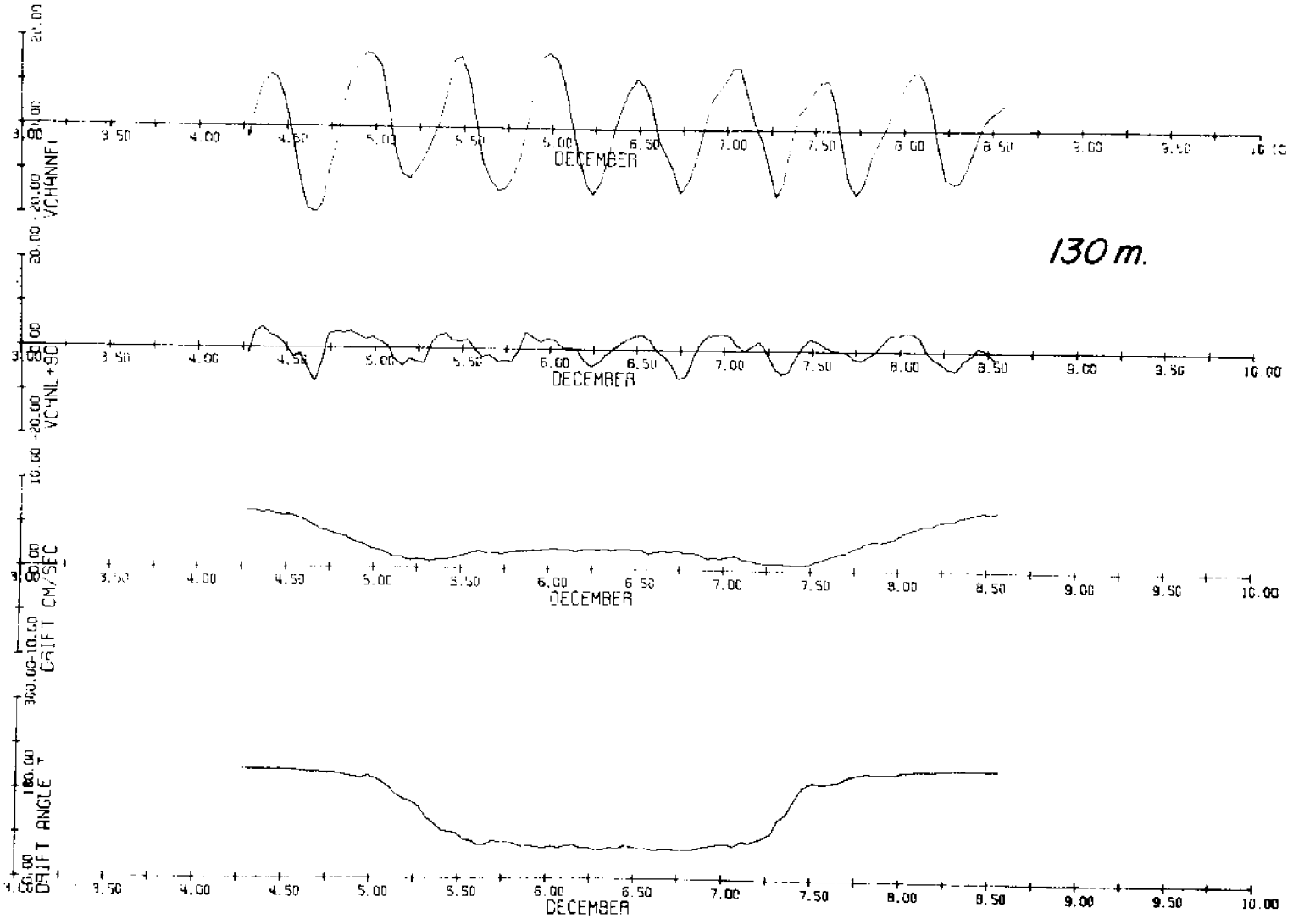

Figure 16. Long-channel and cross-channel components of tidal frequency currents, velocity and direction of drift currents, December 1971 - 130m

Turning to the phases of the maximum inwards current, shown in Table IV, one sees that for the M_2 tide, the values for the top two depths are about 90°, and for the bottom two depths about 60°. Since these values represent a difference of only one hour, the difference is probably not significant. (Note that if it is desired that such small differences in phase be accurately determined, the error rate of the timing mechanisms in each current meter must be carefully measured.) As a matter of interest, 'high tide' for the M_2 component of the short tide record, obtained earlier, occurred at about 150°; i.e., 60° later than the analysed maximum current constituent of the top pair of depths and 90° later than the bottom pair of depths (a 90° value corresponds to standing wave theory).

As to the orientations of the maximum inwards currents (in degrees true) for the M_2 constituent, the values of the upper and lower pairs of depths group into about 35° and 53° respectively. The entrance channel axis lies at about 40°, so one suspects again that the difference reflects mostly the short nature of the record -- although it is possible that the maximum tidal currents near the bottom could be a few degrees more clockwise than those at the top. Similar comments might be made for the K_1 constituent.

The filtered currents: drift components

The magnitude and direction of the drift currents derived by numerical filtering are shown in the bottom two graphs of Figures 13 through 16. The values are more meaningful than those of the tidal frequencies found above. One can clearly see that the 10 to 20 m records are very similar in form; e.g., between 1200 hrs on the 5th to slightly before 1200 hrs on the 8th the drift currents were wholly directed *outwards*, with values ranging as high as 5 cm/sec. The actual times of change from inwards to outwards, and *vice versa*, were somewhere around 0000 hrs on the 5th and 1200 hrs on the 8th.

The 80 m record shows currents that are essentially equal in magnitude to those above, however their directions are opposite -- i.e., from around 1800 hrs on the 5th to 1000 hrs on the 8th, the drift currents at the 80 m level were directed *inwards*.

Near the bottom, the 130 m record shows a different pattern, with small (2 cm/sec) *inwards* currents between the times 0600 hrs on the 5th and 0800 hrs on the 7th. At each end of the total record outwards drift currents of as high as 7 cm/sec were recorded. This is a significant fraction of the current associated with the vertical tide (i.e. 0.5 x the M_2 current amplitude).

To summarize the drift current findings for the period 3 December 1971 to 10 December 1971, from the 5th to the 8th, at 10 and 20 m, the drift currents were *outwards*, with velocities of up to 5 cm/sec, while at the 80 and 130 m levels the drift currents were essentially *inwards*, with values up to 5 cm/sec at 80 m, and up to 2 cm/sec at 130 m. Since the maximum currents due to tidal causes were of the order of less than 20 cm/sec, one sees that the drift currents (probably unpredictable well in advance) can be significant.

The spectra of the original data

The power spectra for the four current meter records are shown overlayed in Figure 17, and separately in Figures 18 through 21. The number and spacing of the data are such that it is not possible to properly separate the K_1 peak from the M_2 peak and still get meaningful results. The main peak, near 0.08 cph, is mostly due to the M_2 tide, and the next peak, at about 0.16 cph, is due to the M_4 component. Due to the short length of the records one should not put too much faith in the actual values of each peak, the overlayed records will, however, show up any frequency bands containing significant amounts of energy common to all the records. It is felt that the only significant bands of such a type are those associated with the tides. Due to the 20 minute spacing of the data it is not possible to check for the presence of oscillations with a period of less than 40 minutes, so it is possible that short-period seiches have been overlooked. On interpreting the records one should remember that the vertical axis is proportional to the quantity log(amplitude^2).

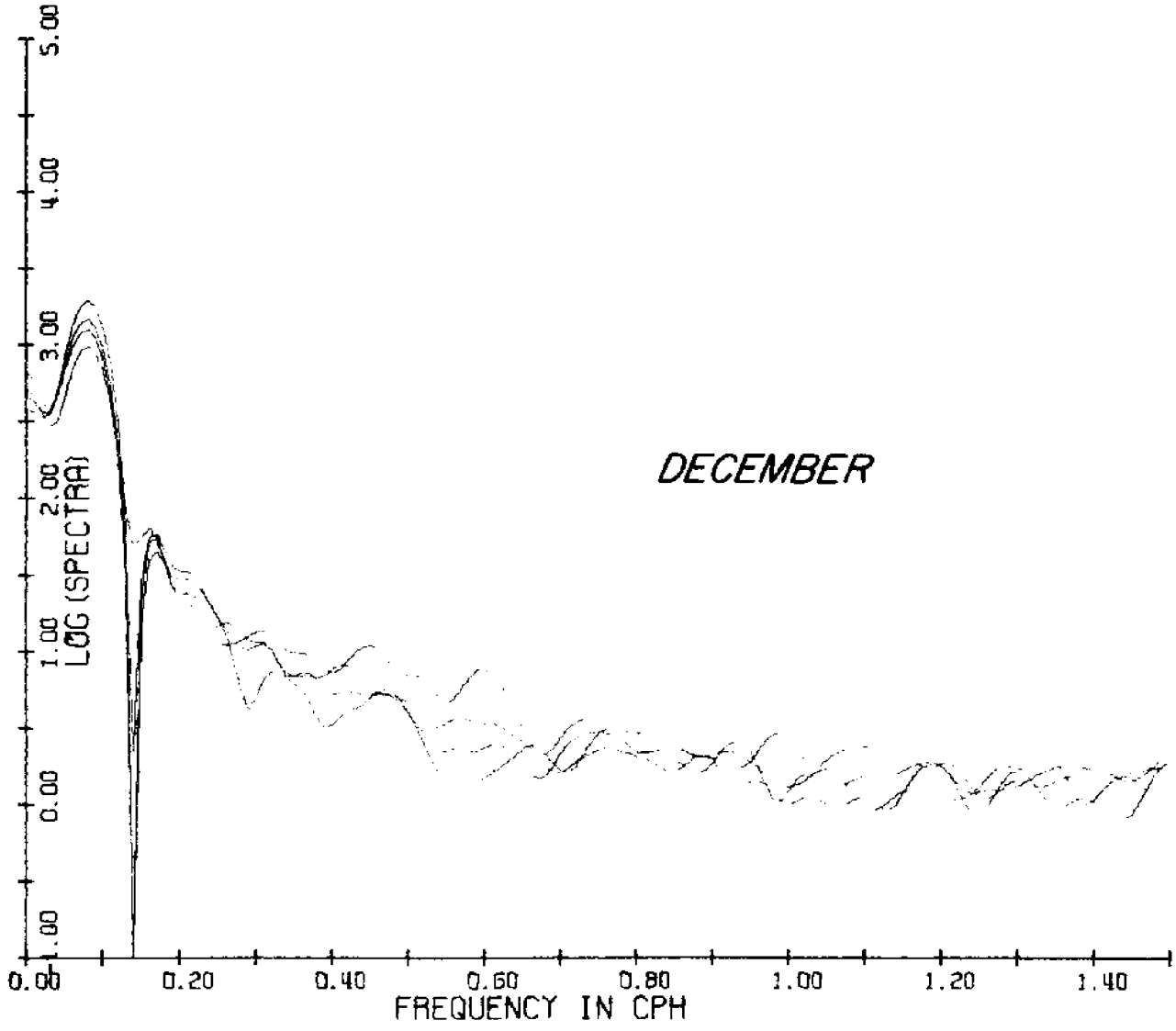

Figure 17. Overlayed spectra of original data for December 1971

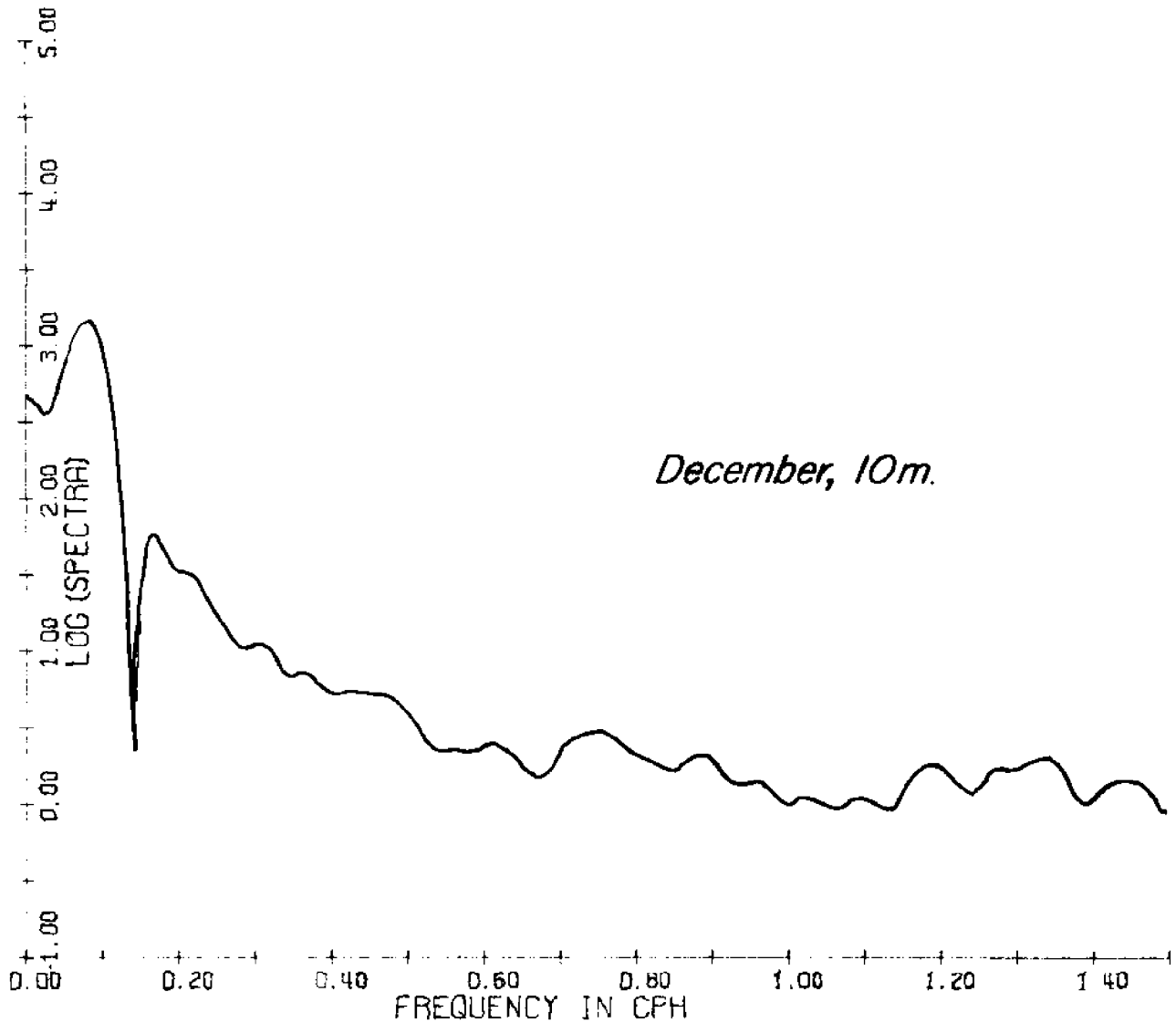

Figure 18. Spectra of original data, December 1971 - 10m

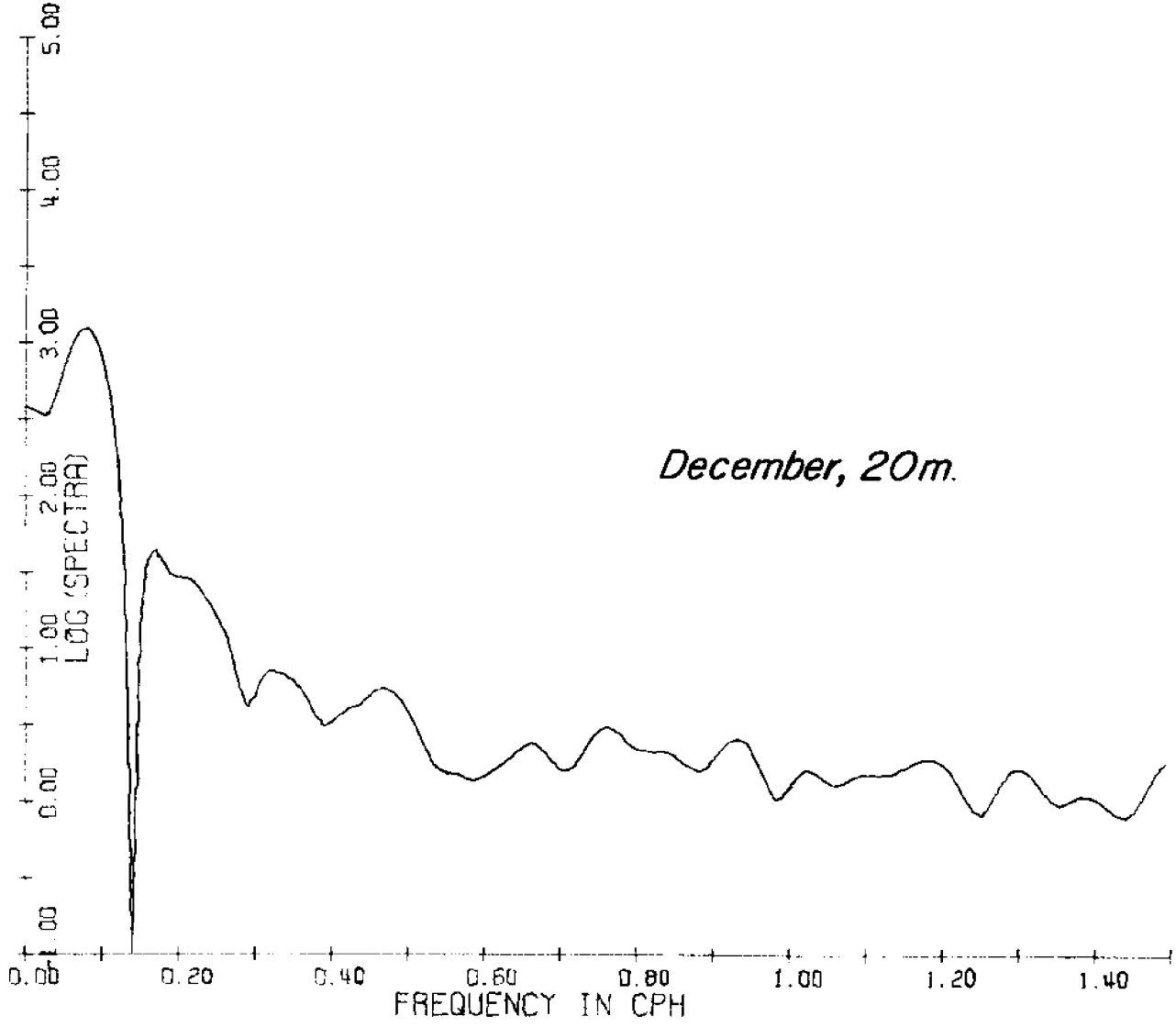

Figure 19. Spectra of original data, December 1971 - 20m

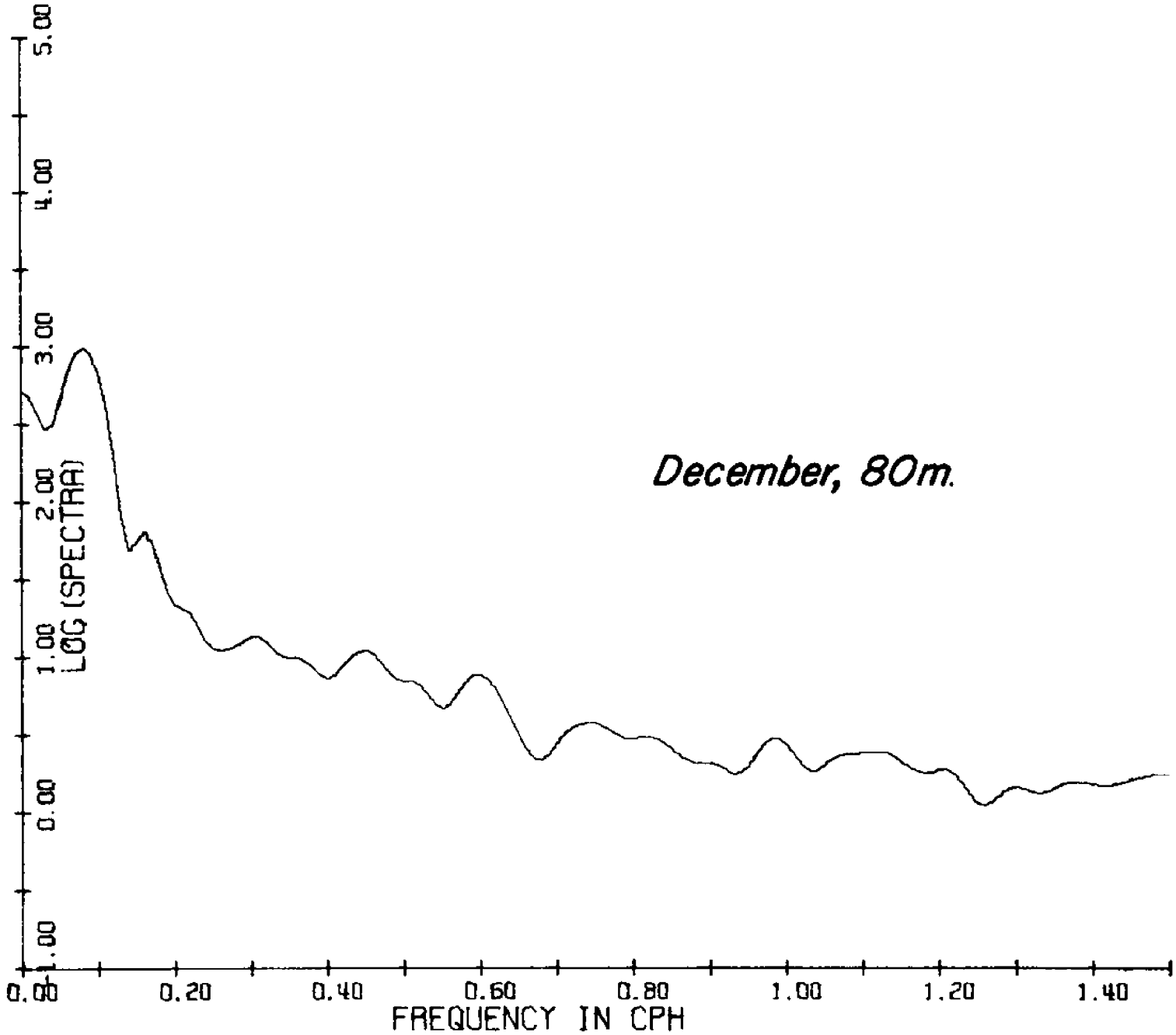

Figure 20. Spectra of original data. December 1971 - 80m

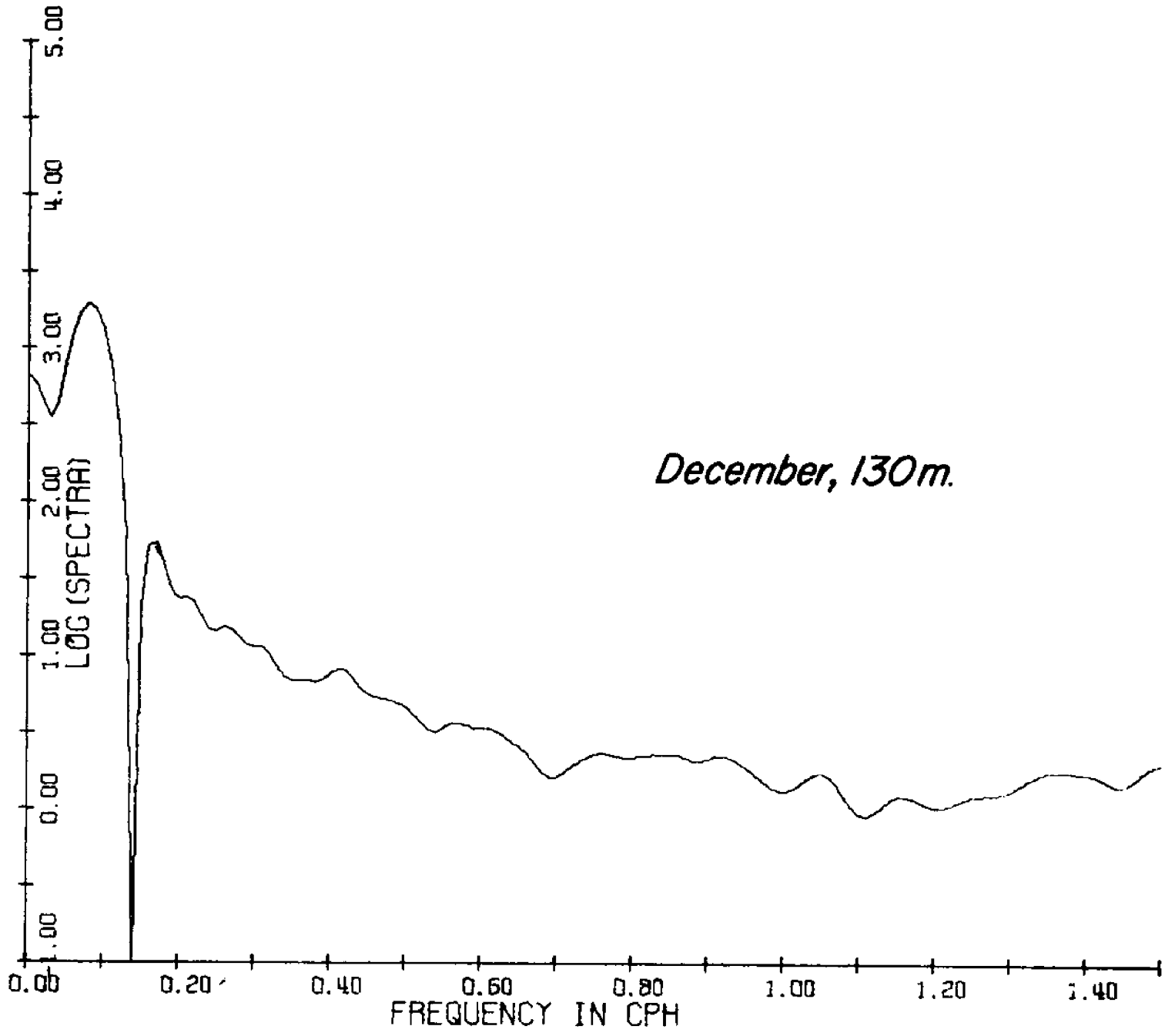

Figure 21. Spectra of original data, December 1971 - 130m

CHAPTER IV

THE PERIOD 12-18 MARCH 1972

The form of the predicted tide corresponding to the period of interest is shown in Figure 22. As can be seen, at this time the tide is essentially semidiurnal in form, as are the smoothed current meter records for this period. The predicted tide data, taken at times corresponding to those of the current meter readings, were analysed yielding the results noted in Table V.

TABLE V. Predicted tide data.

	Amplitude, ft	Phase, degrees
M.S.L.	6.27	--
K_1	0.28	197.1
M_2	6.80	52.0
M_3	0.08	269.3
M_4	0.12	266.8

The time origin for the above phases is 10.26 hours (i.e. 10 hours 16 minutes) local time on March 15th 1972. As in the December record, the absence of important contributions from the M_3 and M_4 constituents is clear. Note also the dominance of the M_2 constituent.

The current meter records

The raw data and the decimated data for the five current meters, again in the form of true North and true East components, are shown in Figures 23 through 27. As with the December 1971 records, there appears to be some coherence in the spikes appearing in the 10 and 20 m records and to a certain extent in the 40 m record. It is felt that the spikes are mostly artefacts and represent poor behavior on the part of the meter.

Little needs to be said about the decimated records, other than that they are obviously semidiurnal in form.

The results of filtering the decimated records using the Doodson filter are shown in Figures 28 through 32. These computer plots show from top to bottom:

1) 40°-true component of tidal frequency current, cm/sec
2) 130°-true component of tidal frequency current, cm/sec
3) magnitude of drift current, cm/sec
4) direction of drift current in degrees true.

The direction of the channel leading to the fjord, at the current meter string location, is 40° true.

The filtered currents: tidal components

The filtered records cover approximately four days. The top graphs in Figures 28 through 32 are very similar for the 10, 20, and 40 m records. The 80 m record differs somewhat in form, and the 130 m record is yet again different. Of visual interest are the second graphs in Figures 28 through 32 -- the cross-channel tidal-frequency component. These records, for the top three meters seem somewhat random. The 80 m record shows slightly more regularity. However the bottom (130 m) record shows a very noticeable M_2 component, indicating that the current is becoming more elliptical in shape. The time of maximum is delayed slightly, so the current is clockwise.

When the components were analysed, it was found that the next constituent of significance after the M_2 component was that of the M_4. This could have been anticipated from the tidal 'analysis', as it was demonstrated earlier that maximum currents depend partly on the quantity (tidal amplitude x frequency). For this reason only the M_2 and M_4 values of the ellipse components are shown in Table VI.

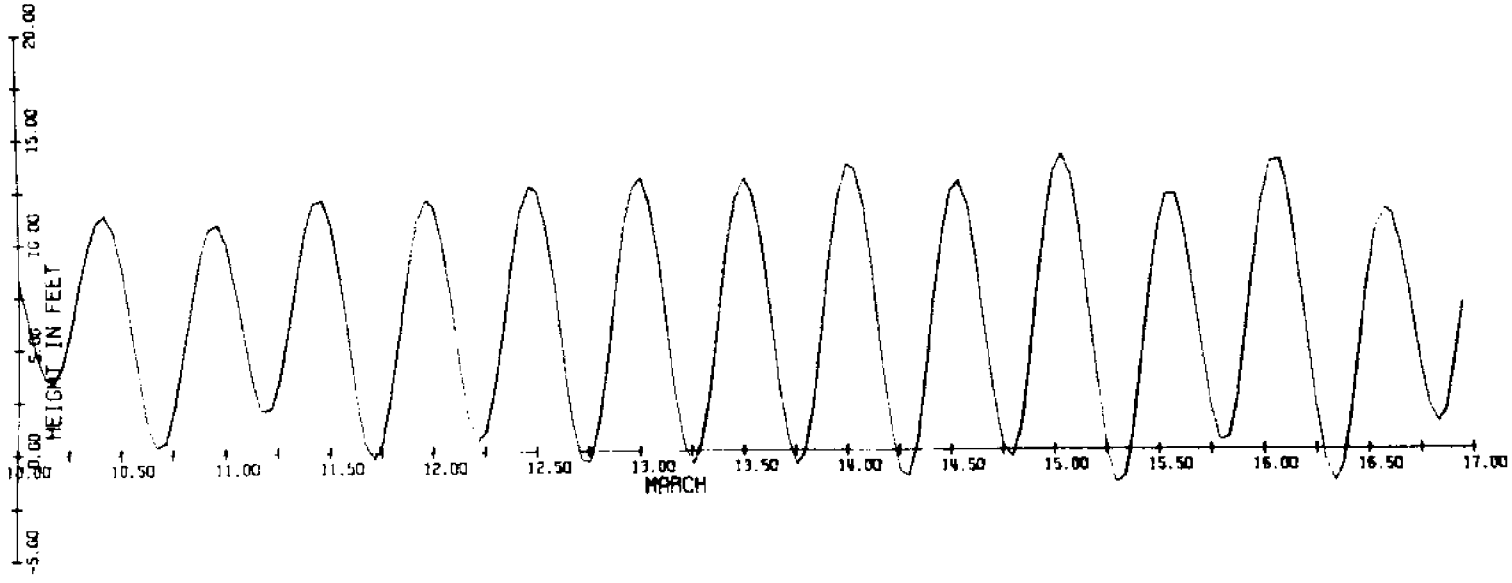

Figure 22. Computed tides of Port Valdez for the period 10 March 1972 to 17 March 1972

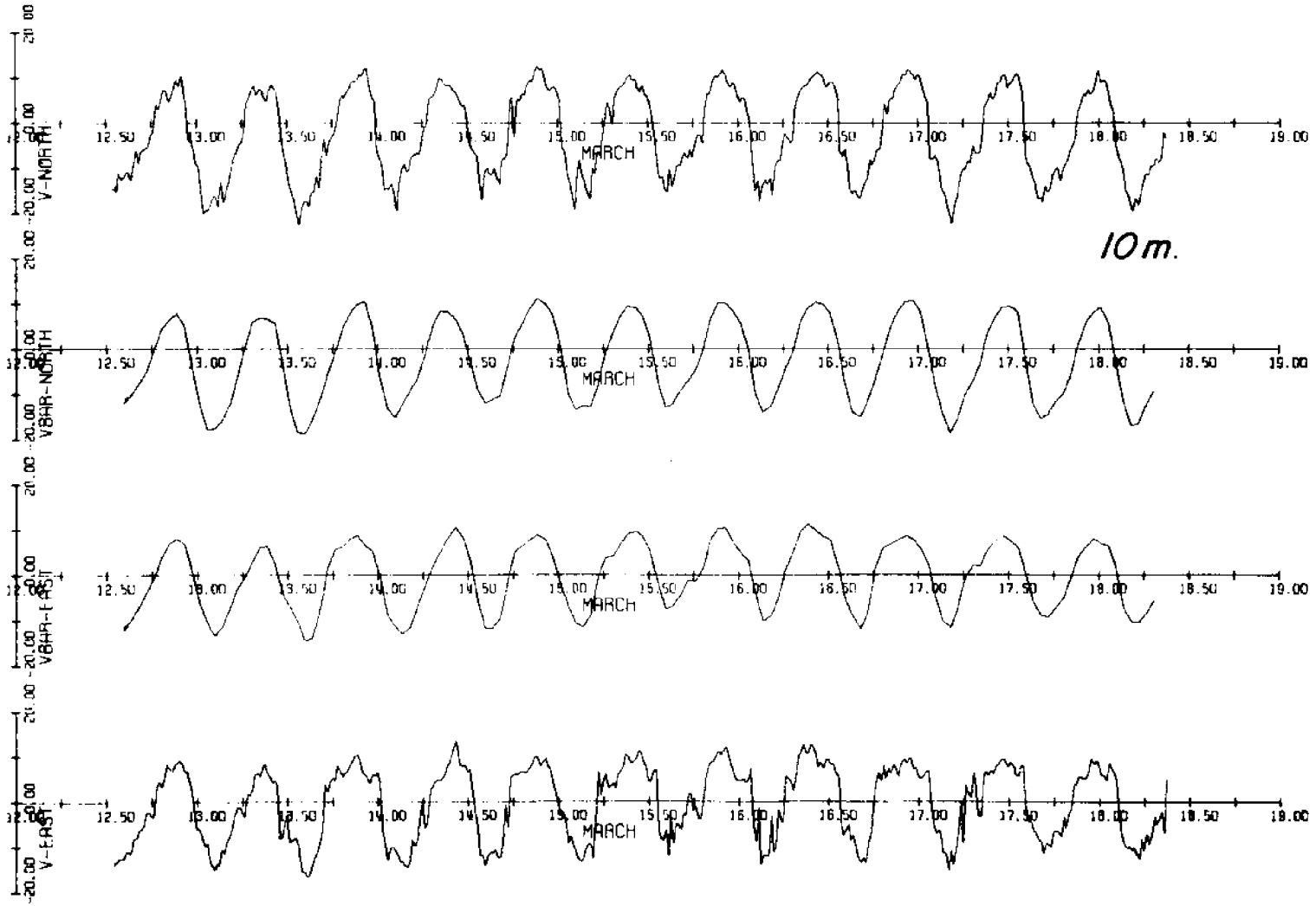

Figure 23. Original and decimated records for March 1972 - 10m

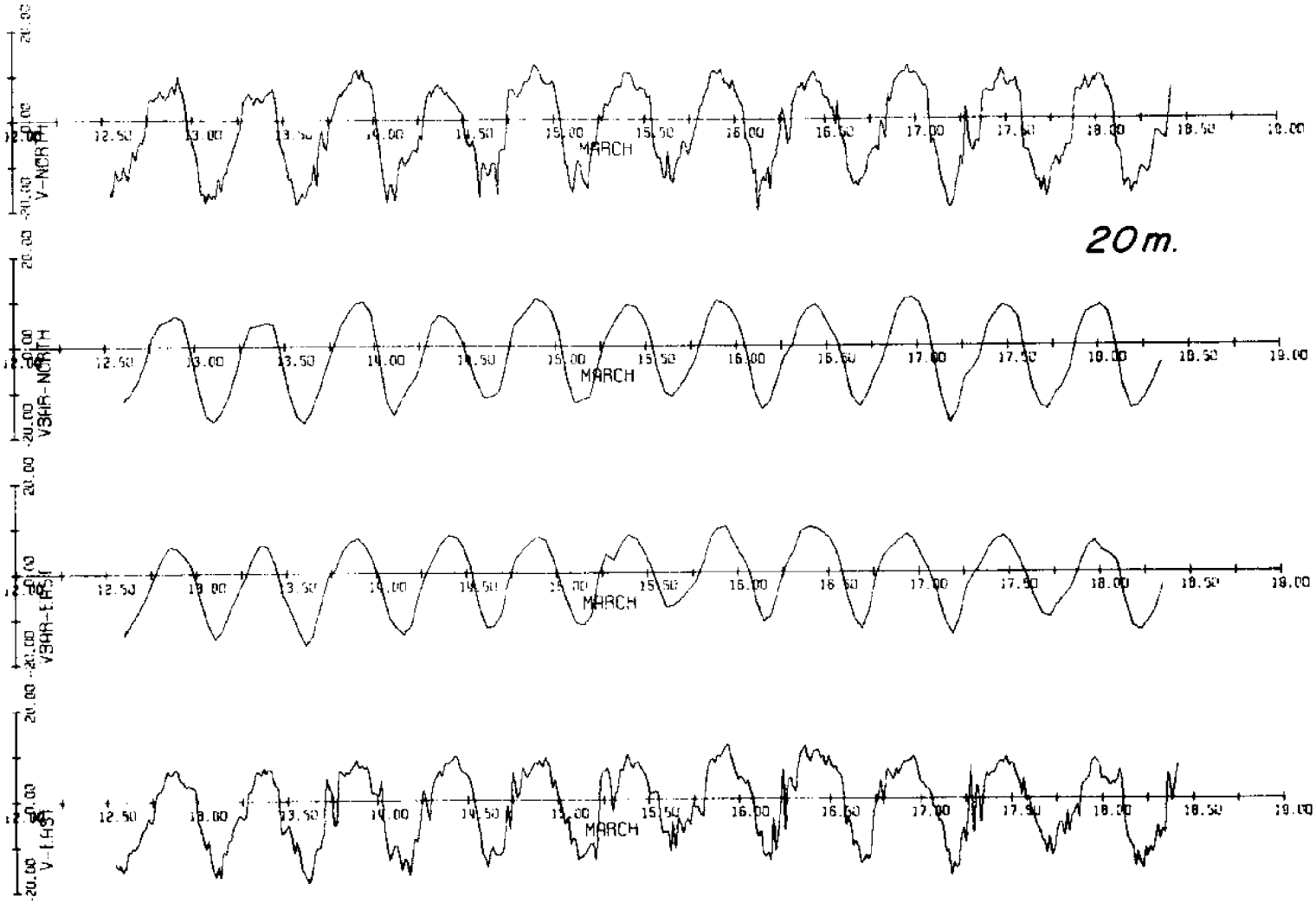

Figure 24. Original and decimated records for March 1972 - 20m

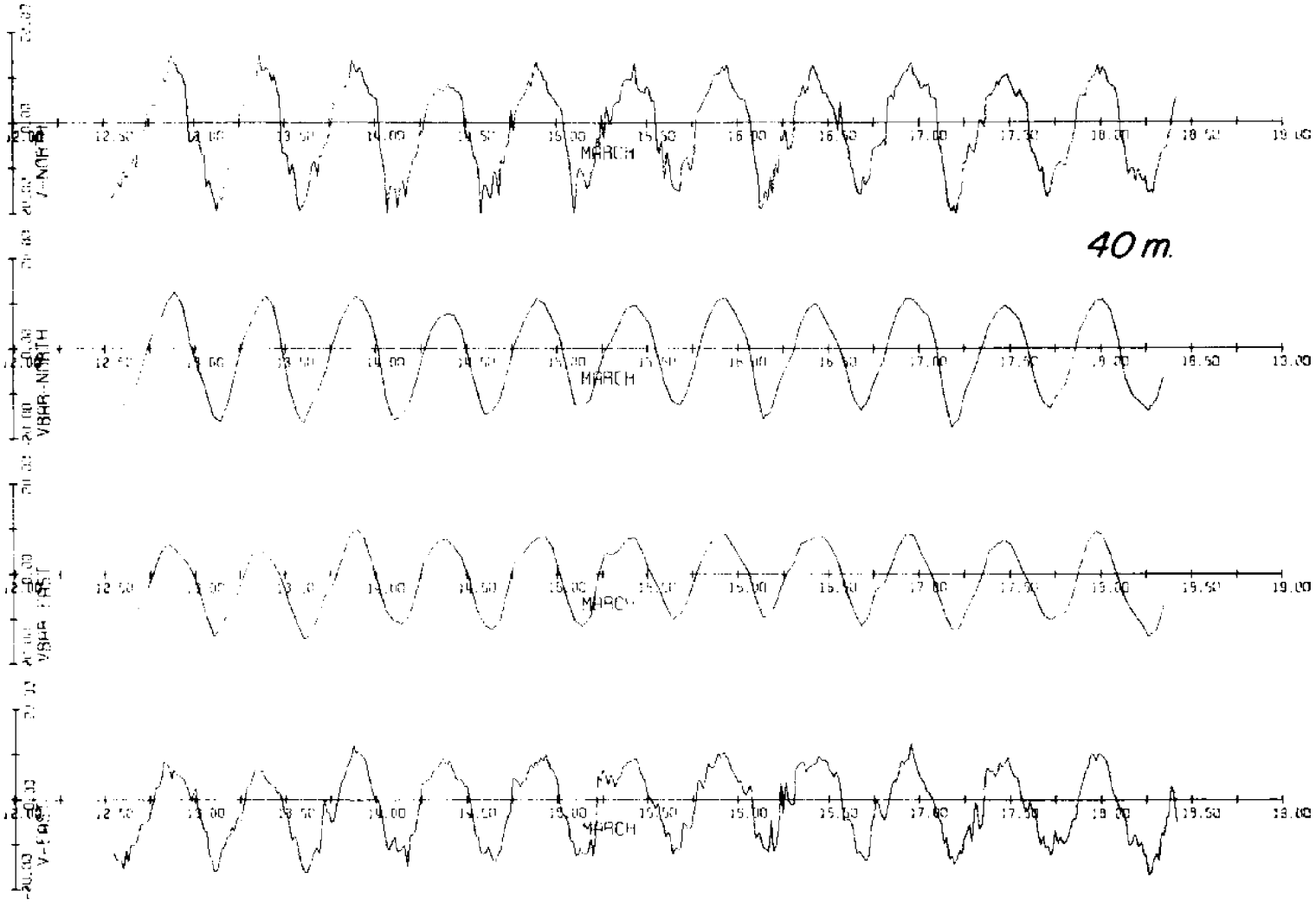

Figure 25. Original and decimated records for March 1972 - 40m

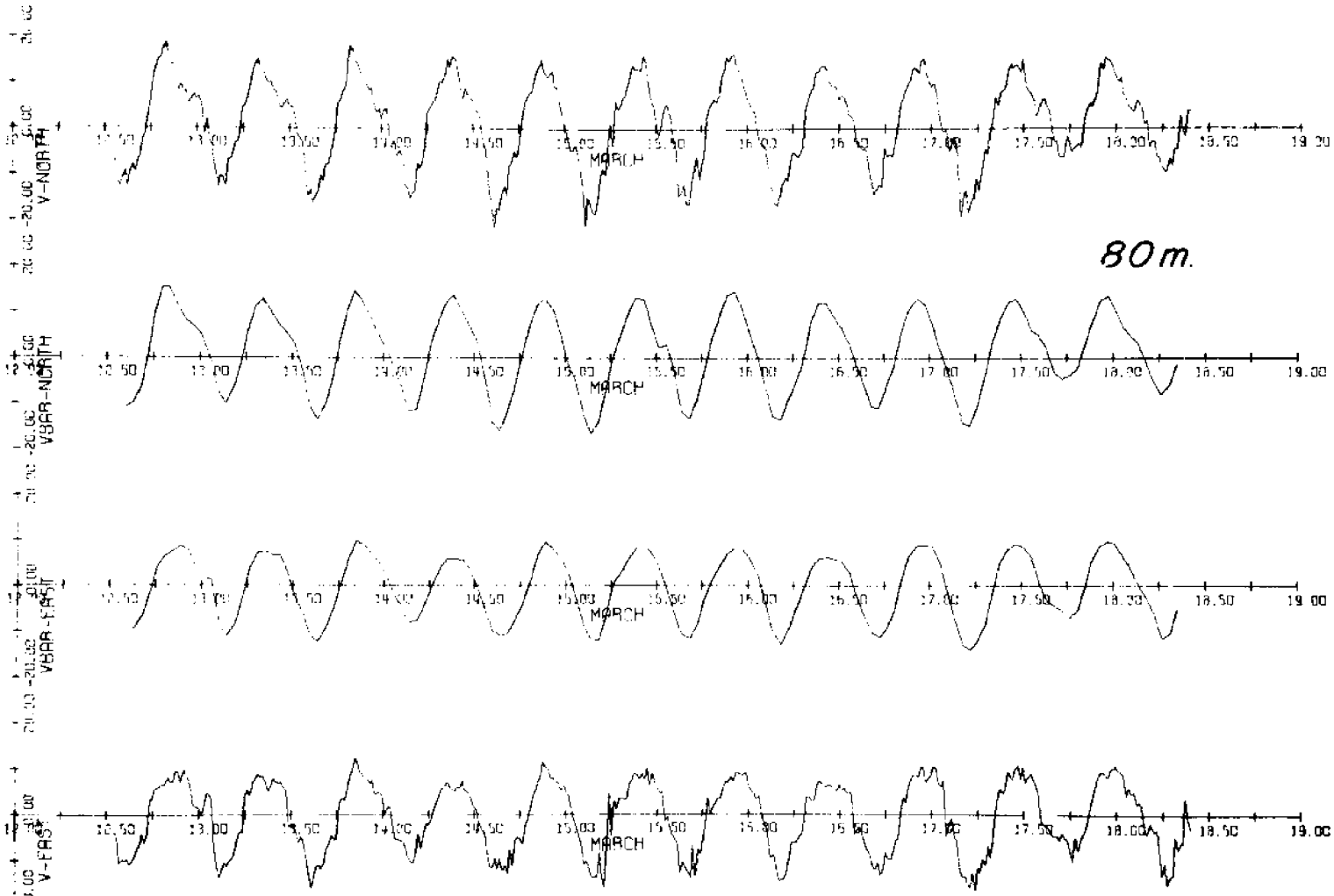

Figure 26. Original and decimated records for March 1972 - 80m

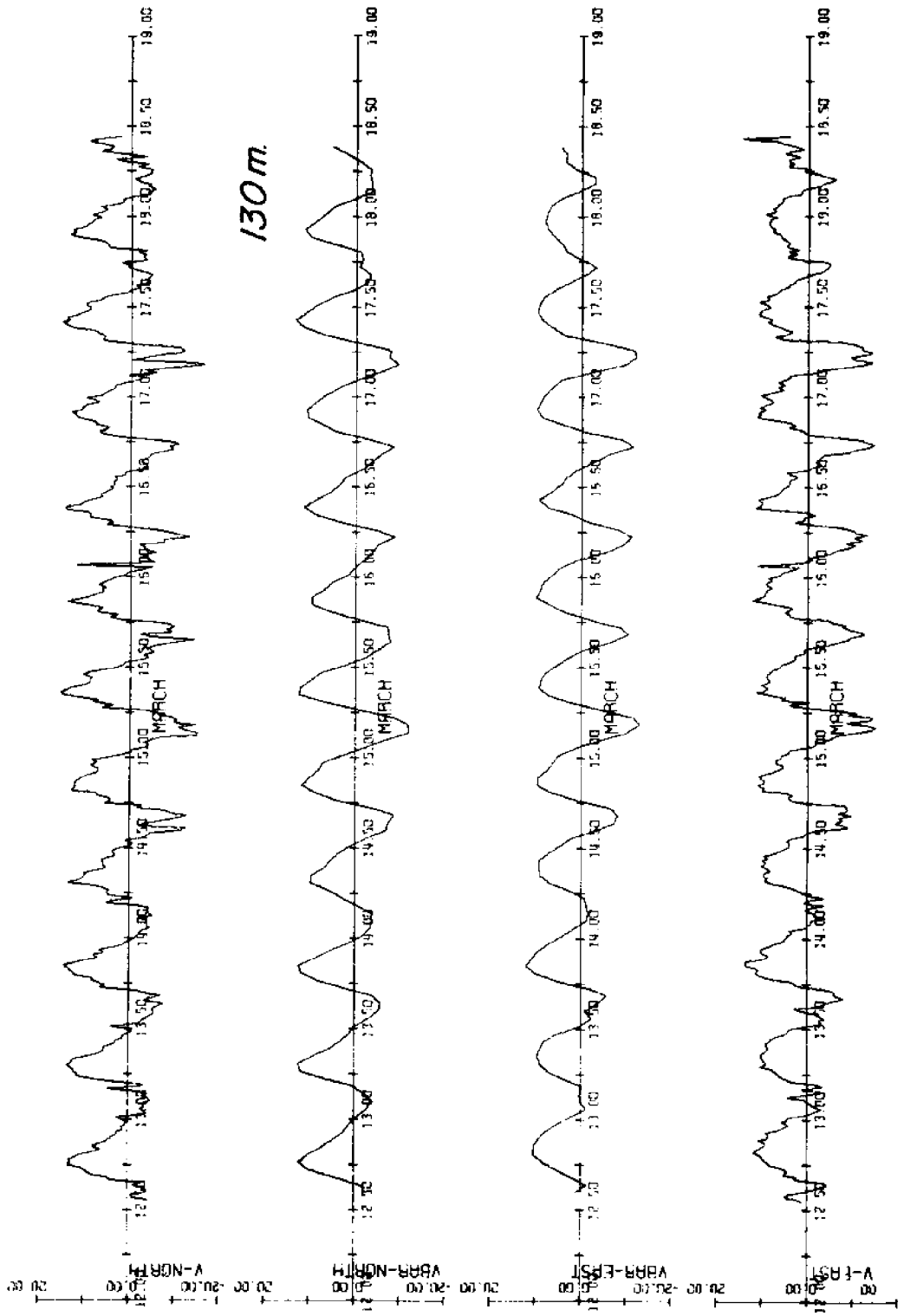

Figure 27. Original and decimated records for March 1972 - 130m

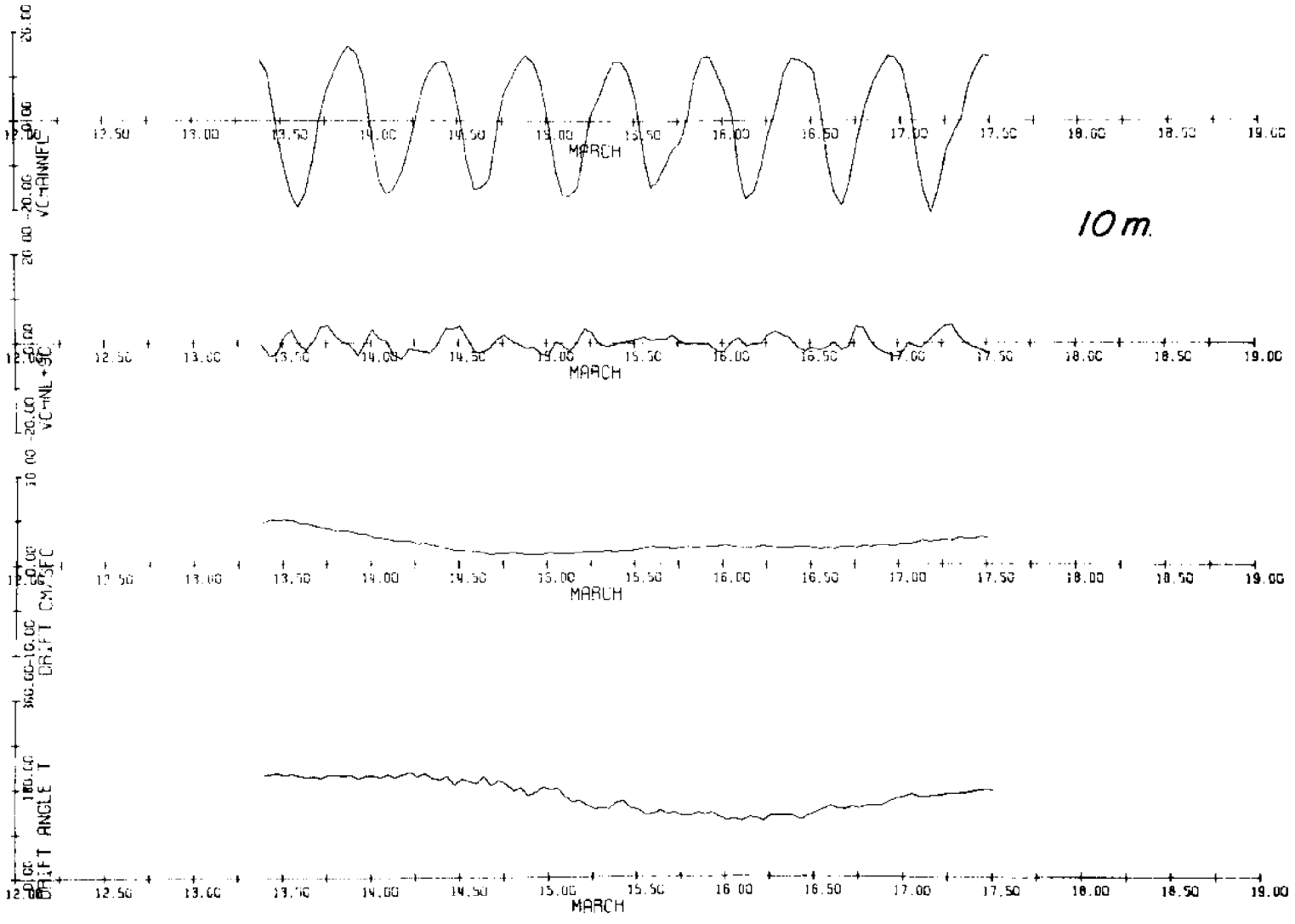

Figure 28. Long-channel and cross-channel components of tidal frequency currents, velocity and direction of drift currents, March 1972 - 10m

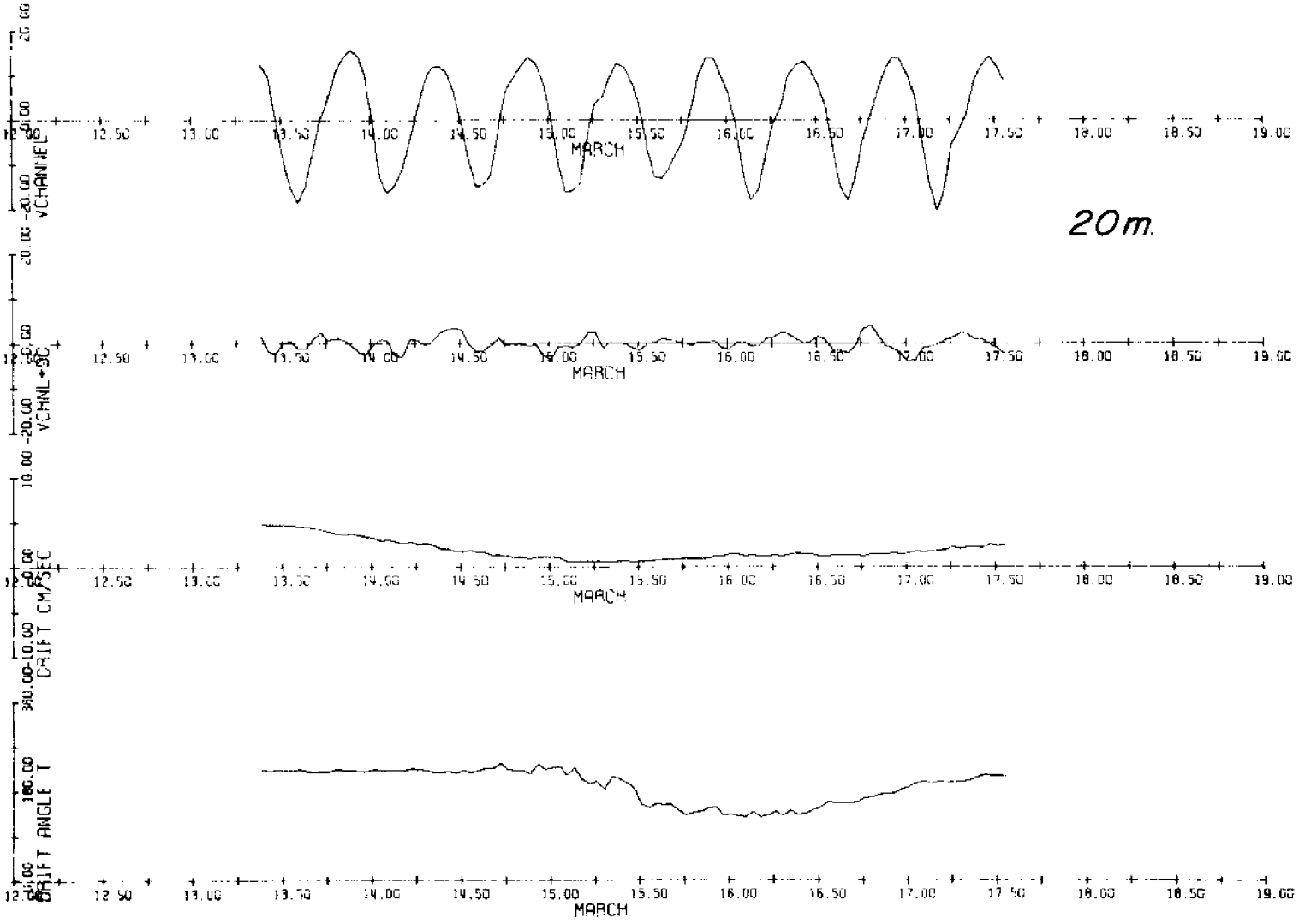

Figure 29. Long-channel and cross-channel components of tidal frequency currents, velocity and direction of drift currents, March 1972 - 20m

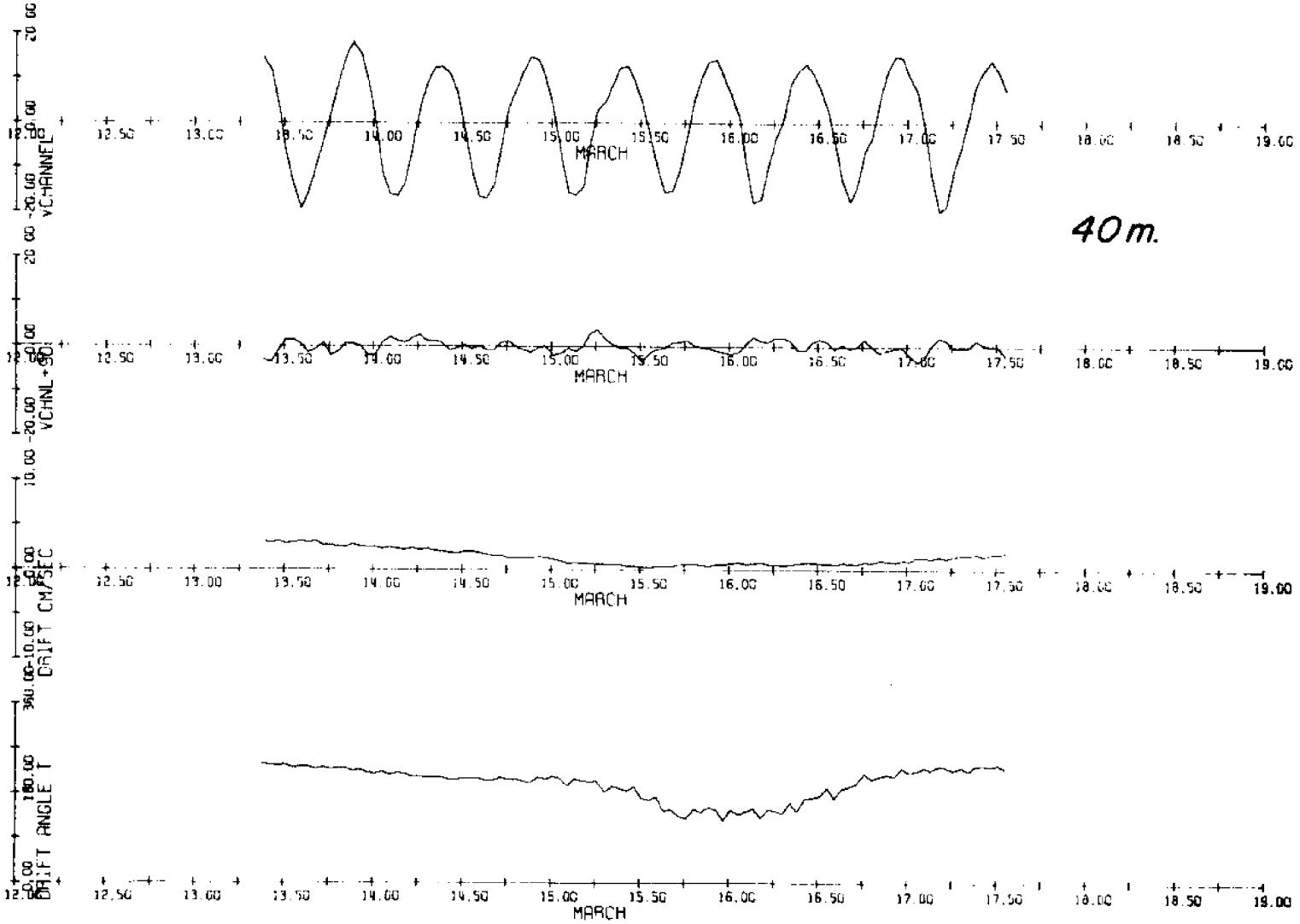

Figure 30. Long-channel and cross-channel components of tidal frequency currents, velocity and direction of drift currents, March 1972 - 40m

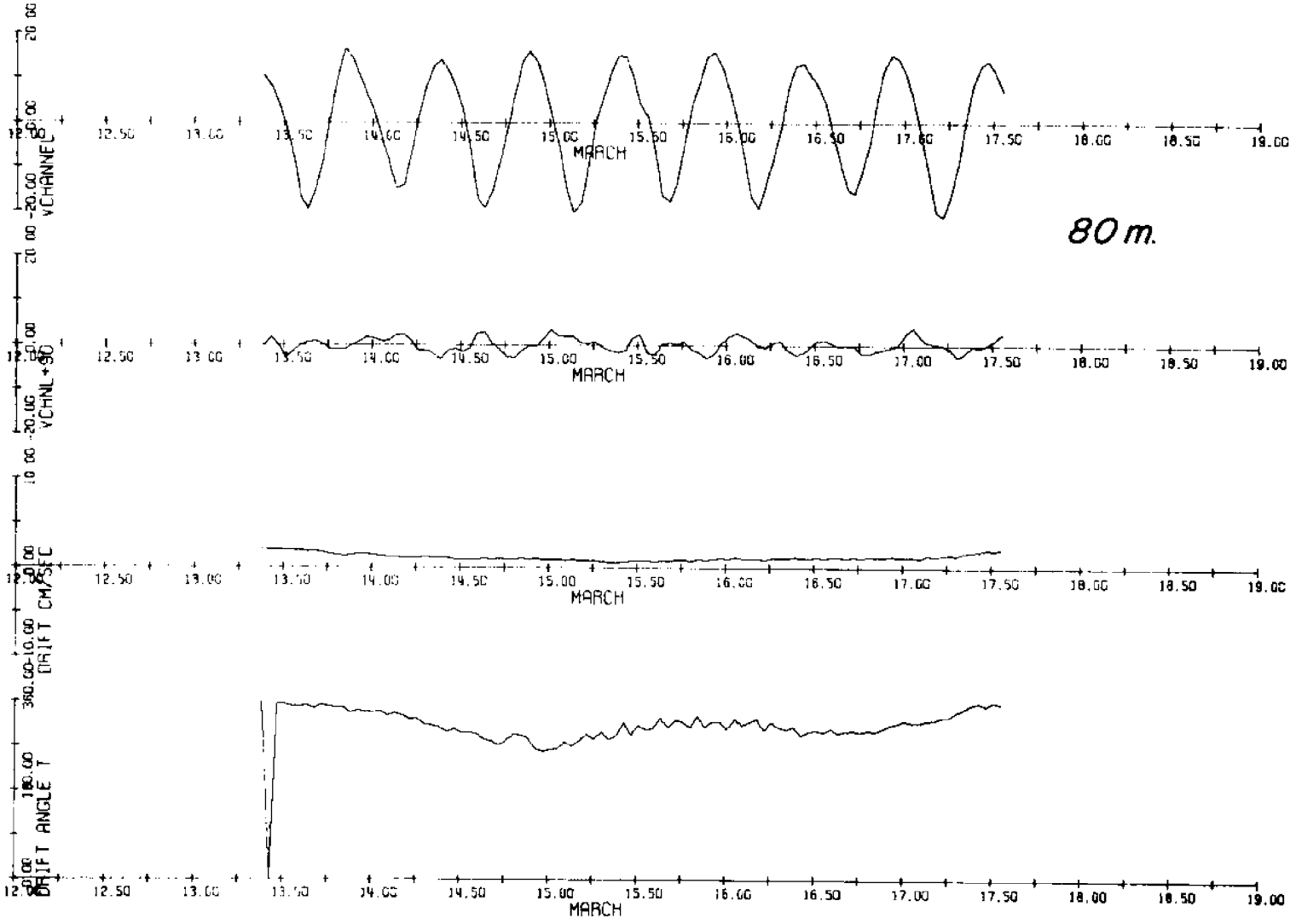

Figure 31. Long-channel and cross-channel components of tidal frequency currents, velocity and direction of drift currents, March 1972 - 80m

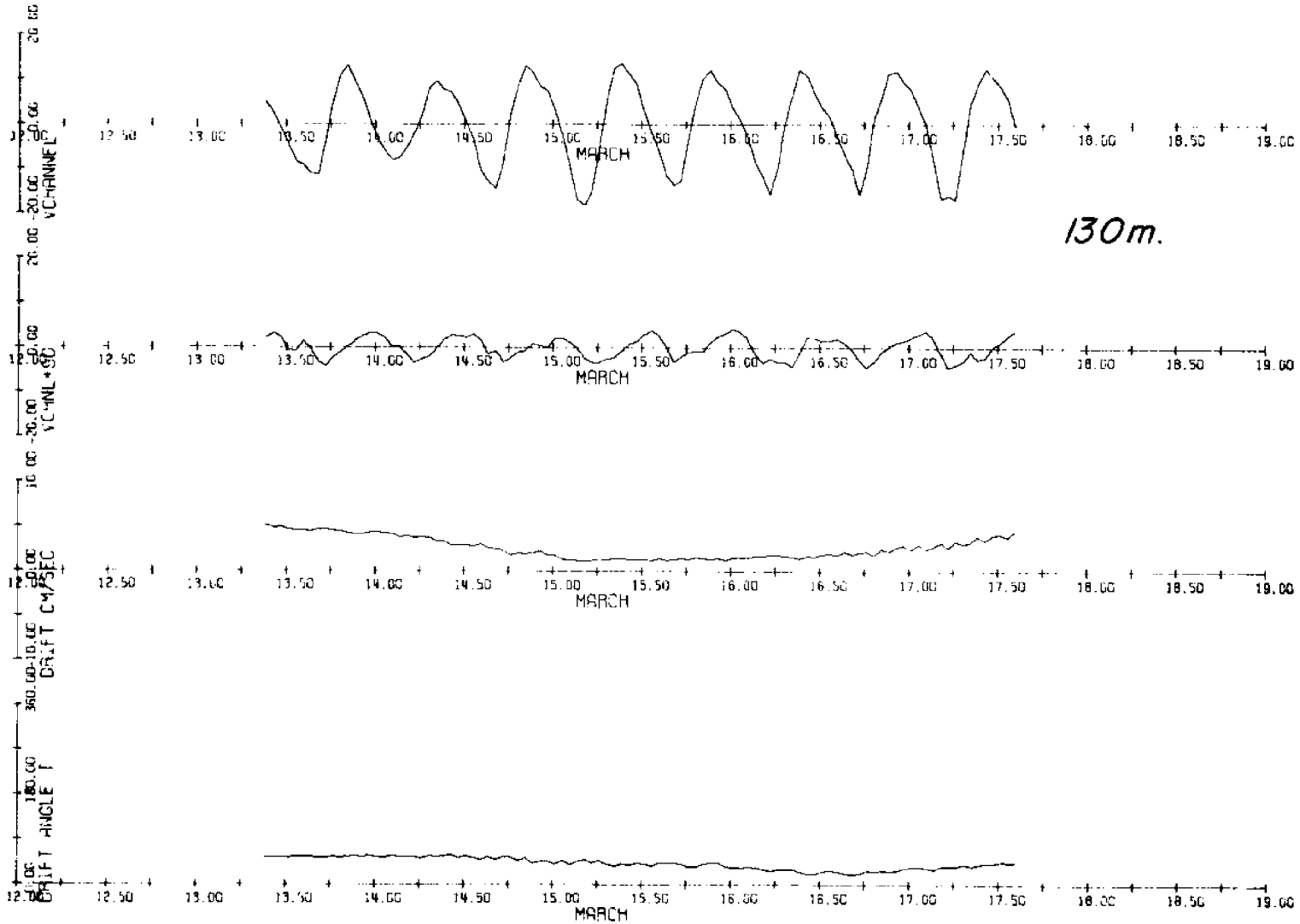

Figure 32. Long-channel and cross-channel components of tidal frequency currents, velocity and direction of drift currents, March 1972 - 130m

TABLE VI
March 1972 Current Meter Analysis

Semi-major and semi-minor axes
(maximum and minimum currents)

degrees/hour	M_2 28.98		M_4 57.97	
	max cm/sec	min cm/sec	max cm/sec	min cm/sec
10 m	16.3	0.6	2.8	0.7
20 m	15.4	0.9	2.6	0.1
40 m	16.1	0.9	2.5	0.1
80 m	16.5	0.9	2.0	0.7
130 m	12.9	2.8	3.0	0.1

phase (based on central time origin of March 15th 1972
10.26 hrs local time) and orientation of major axis

degrees/hour	M_2 28.98		M_4 57.97	
	phase degrees	orientation degrees T	phase degrees	orientation degrees T
10 m	339	38	90	48
20 m	338	41	98	46
40 m	344	38	115	34
80 m	349	38	193	31
130 m	345	45	213	44

As regards the M_2 ellipse, it is clear that the current ellipse is similar in shape and orientation for the 10, 20, 40, and 80 m records. As was visually observed, the 130 m record is considerably different, being 'fatter', and being aligned some 5° to the right of the channel axis. Unlike the December 1971 record situation, the phases of the maximum inwards currents differ by 11° at most (about 20 minutes), and, taking a mean value as 343°, the maximum inwards current for the M_2 constituent occurs some 70° before the theoretical high water for the M_2 constituent.

The filtered currents: drift components

The magnitude and direction of the drift currents is shown in the bottom two graphs of Figures 28 through 32. The records for the top three meters (10, 20, and 40 m) are very similar in form, *being directed outwards at all times.* The velocities decrease with increasing depth. Maximum velocities occurred at the ends of the records, the values for the 10, 20, and 40 m records being 5.0, 3.0; 4.8, 2.5; and 3.1, 1.9 cm/sec at the start and end of each respective record.

The 80 m record is different in character, in that the current is *always directed inwards,* but the velocity profile is similar to those above, with maximum velocities of about 2.0 cm/sec.

The 130 m record is such that the drifts *are always inwards,* with velocities being larger than those of the 80 m record - the maximum velocities at the ends being 5.1 and 4.4 cm/sec.

Comparison between December 1971 and March 1972 drift records

In as much as it is clearly difficult to make meaningful comparisons for such short records - at the entrance, the following are apparent:

1) In both sets of records the division between depths at which drift currents were in or out at any moment was somewhere between 20 and 80 or 40 and 80 (since, unfortunately, data was lacking for the 40 m December depth).

2) The highest drift velocities were of the order of 5 cm/sec.

3) The maximum drift velocities may be compared with maximum tidal-frequency currents of around 20 cm/sec.

It may be possible, using the simultaneous oceanographic data (including current drogue measurements) recorded during these two periods, to find some relation between the drift directions and, say, the density structure inside and outside the entrance, or the wind field.

As a final comment, it must be remembered that these measurements were taken at the entrance and current values within the fjord should be a factor of 10 or so less, unless the drift currents concentrate (1.0 cm/sec ≡ 36 m/hour ≡ 864 m/day).

The spectra of the original data

The combined spectra for the March 1972 records are shown in Figure 33, and are shown separately in Figures 34-38. When compared with Figure 17, which shows the December 1971 combined spectra, the difference in the form of the broad peaks around 0.08 cph will be seen. This difference is due to the almost complete absence of the K_1 tide in the March 1972 record.

More clearly than in Figure 17, in Figure 33 one can clearly see the presence of harmonics of the M_2 tide. Easily identifiable are those corresponding to the 2nd, 3rd, and 4th harmonics (the 2nd harmonic is the M_4 tide), and a 5th harmonic is also distinguishable. Bearing in mind the fact that the vertical axis is in terms of log(amplitude^2), these figures approximately represent amplitudes of between one-tenth and one-twentieth of the M_2 amplitude. Thus, for precise work, one should analyse the records for harmonics as high as the M_8 component.

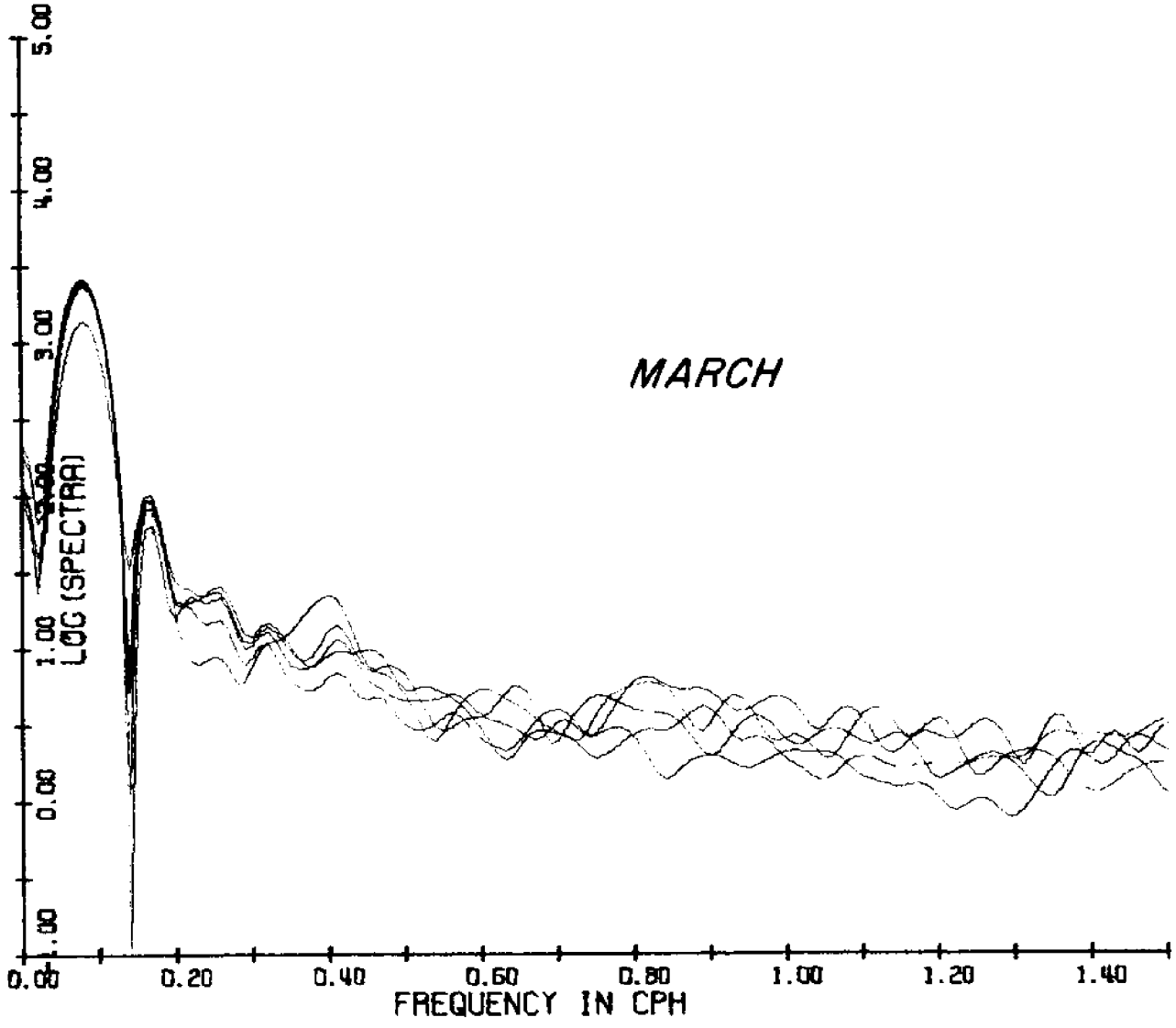

Figure 33. Overlayed spectra of original data for March 1972

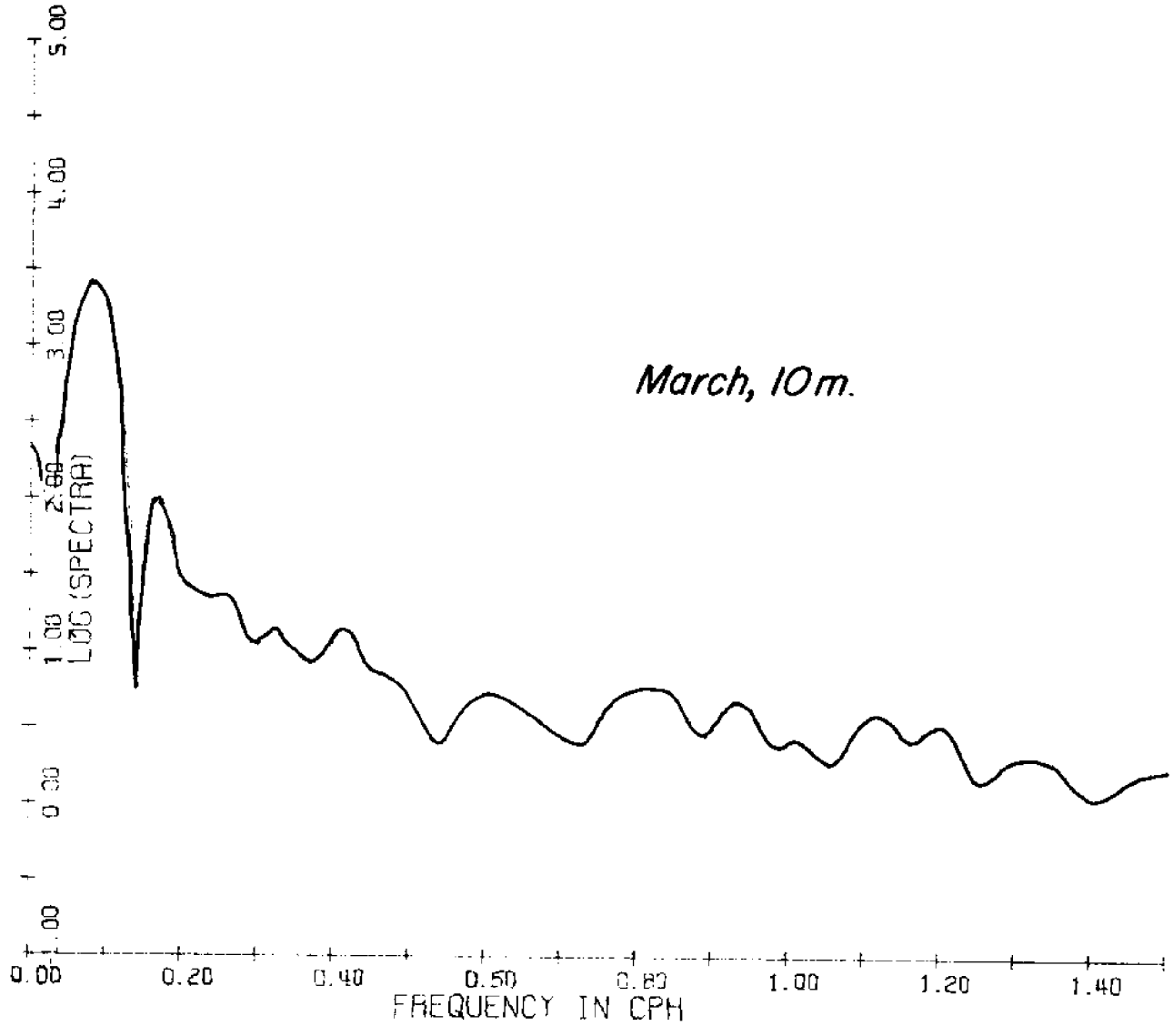

Figure 34. Spectra of original data, March 1972 - 10m

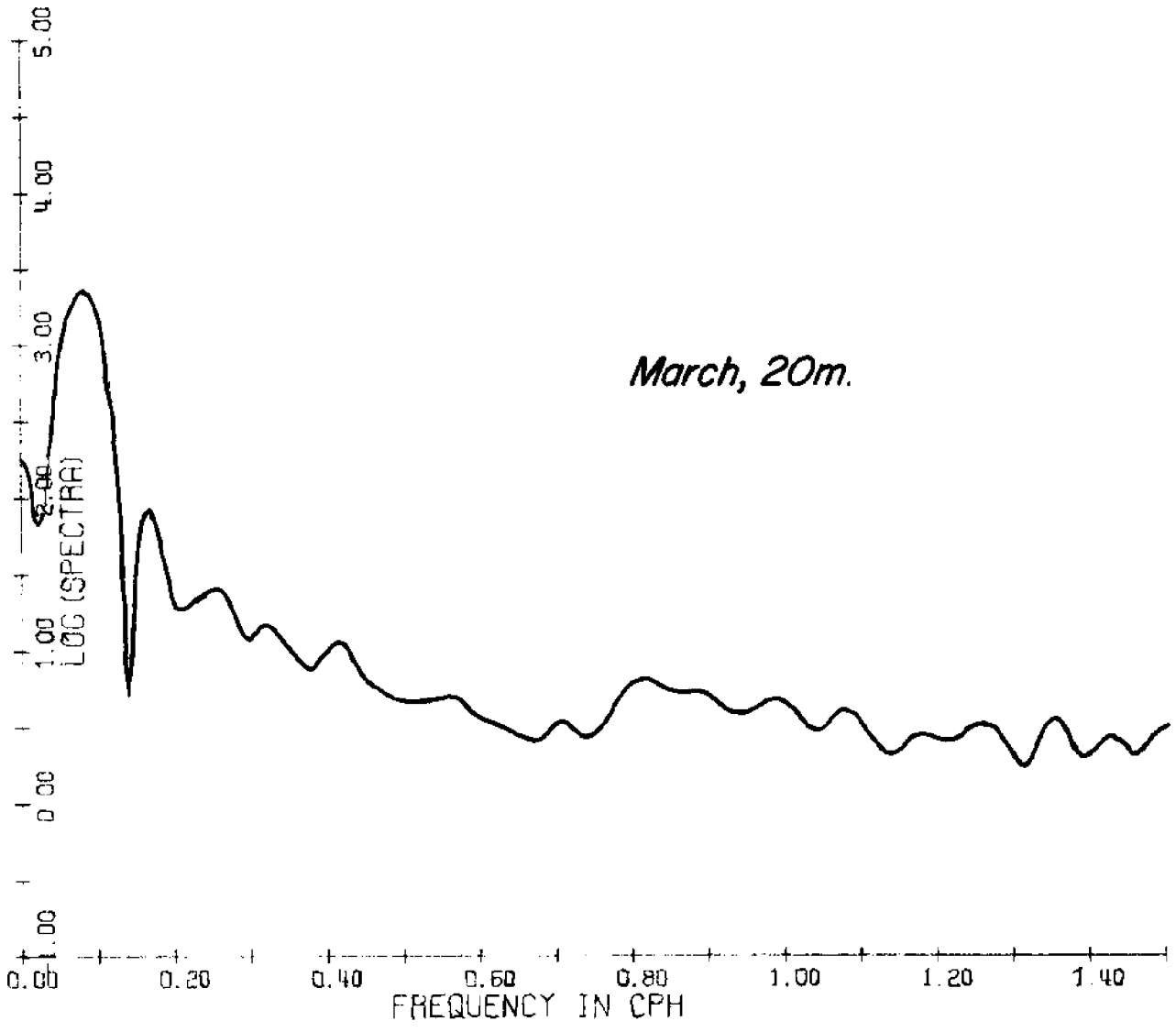

Figure 35. Spectra of original data, March 1972 - 20m

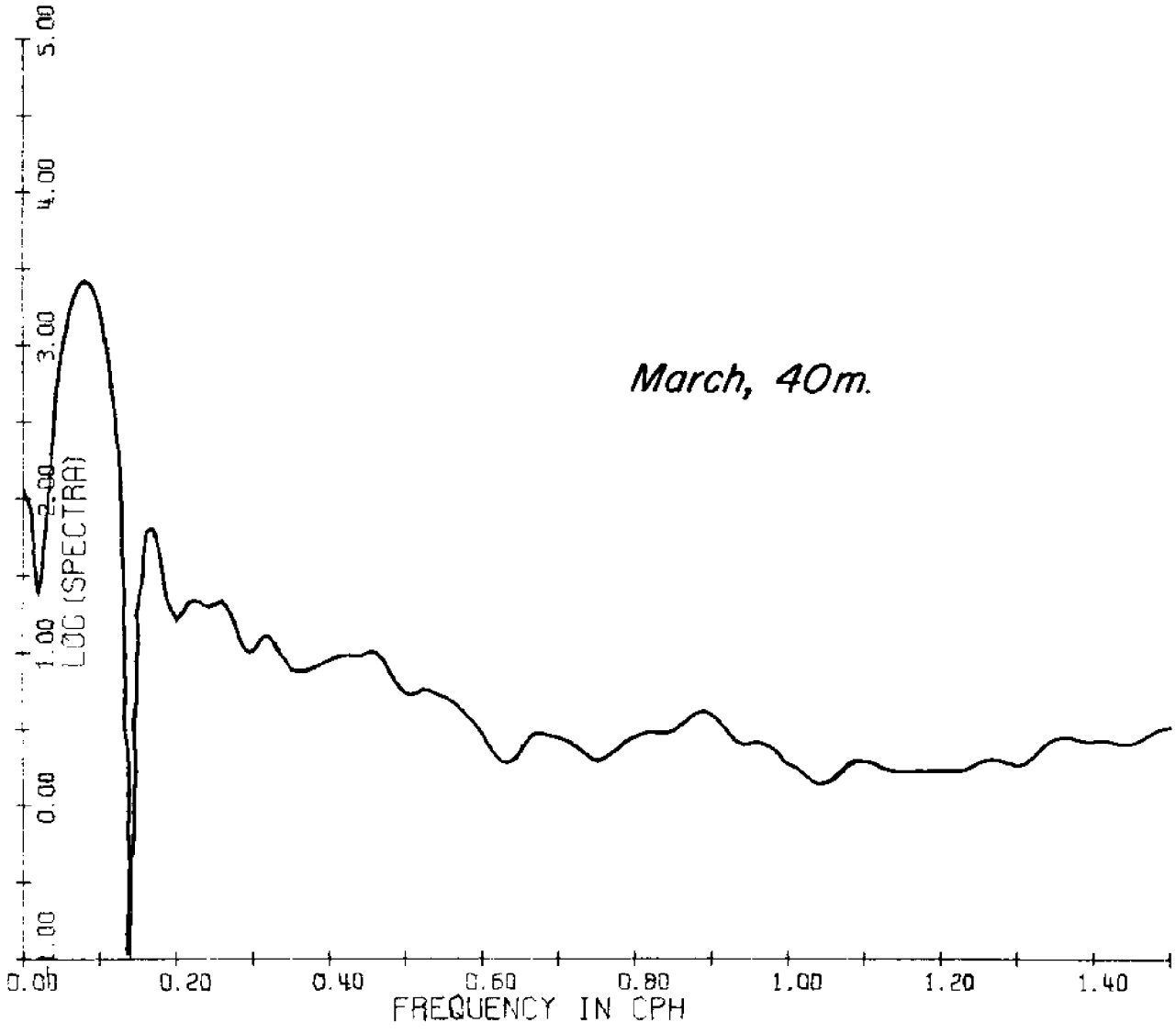

Figure 36. Spectra of original data, March 1972 - 40m

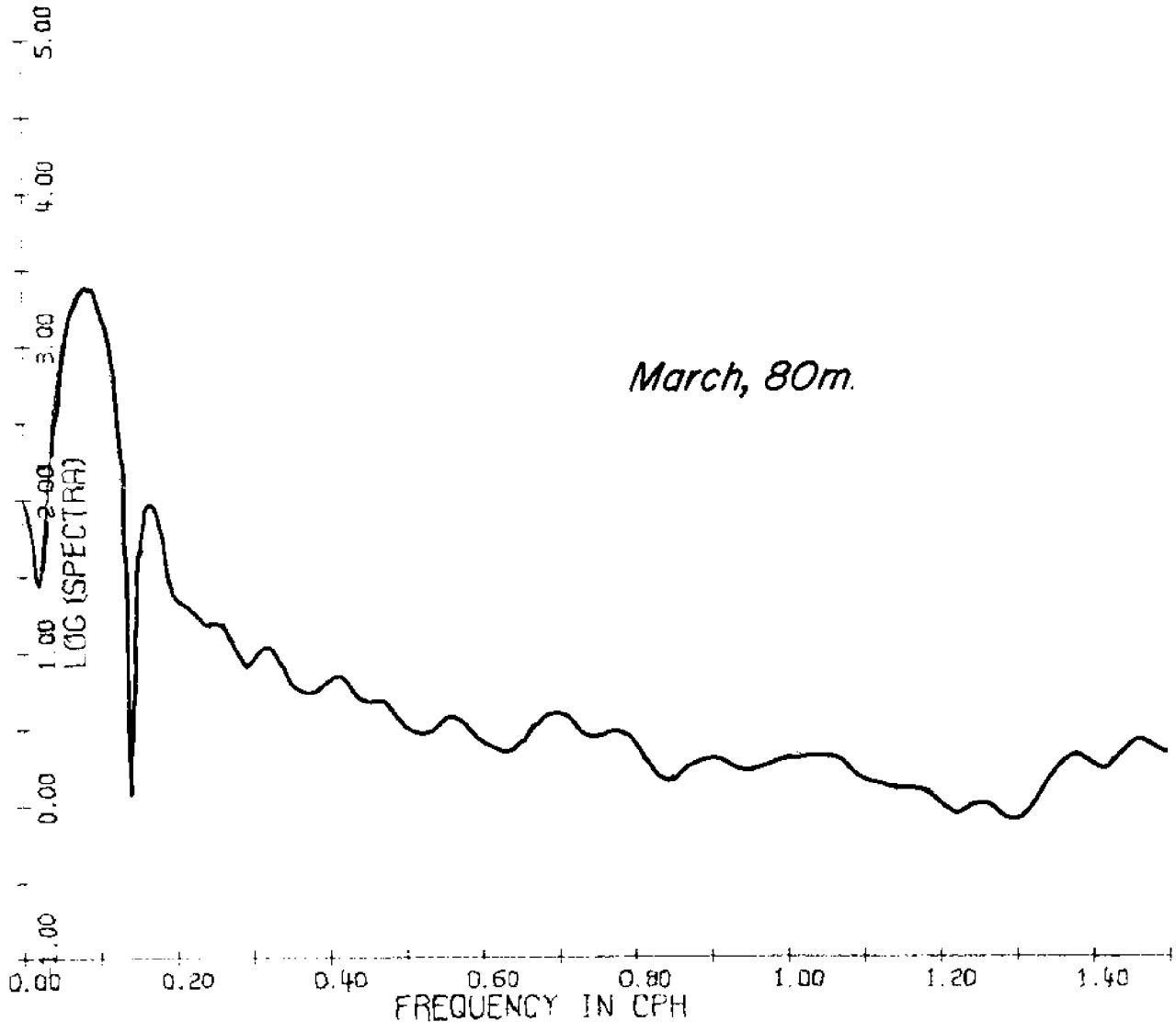

Figure 37. Spectra of original data, March 1972 - 80m

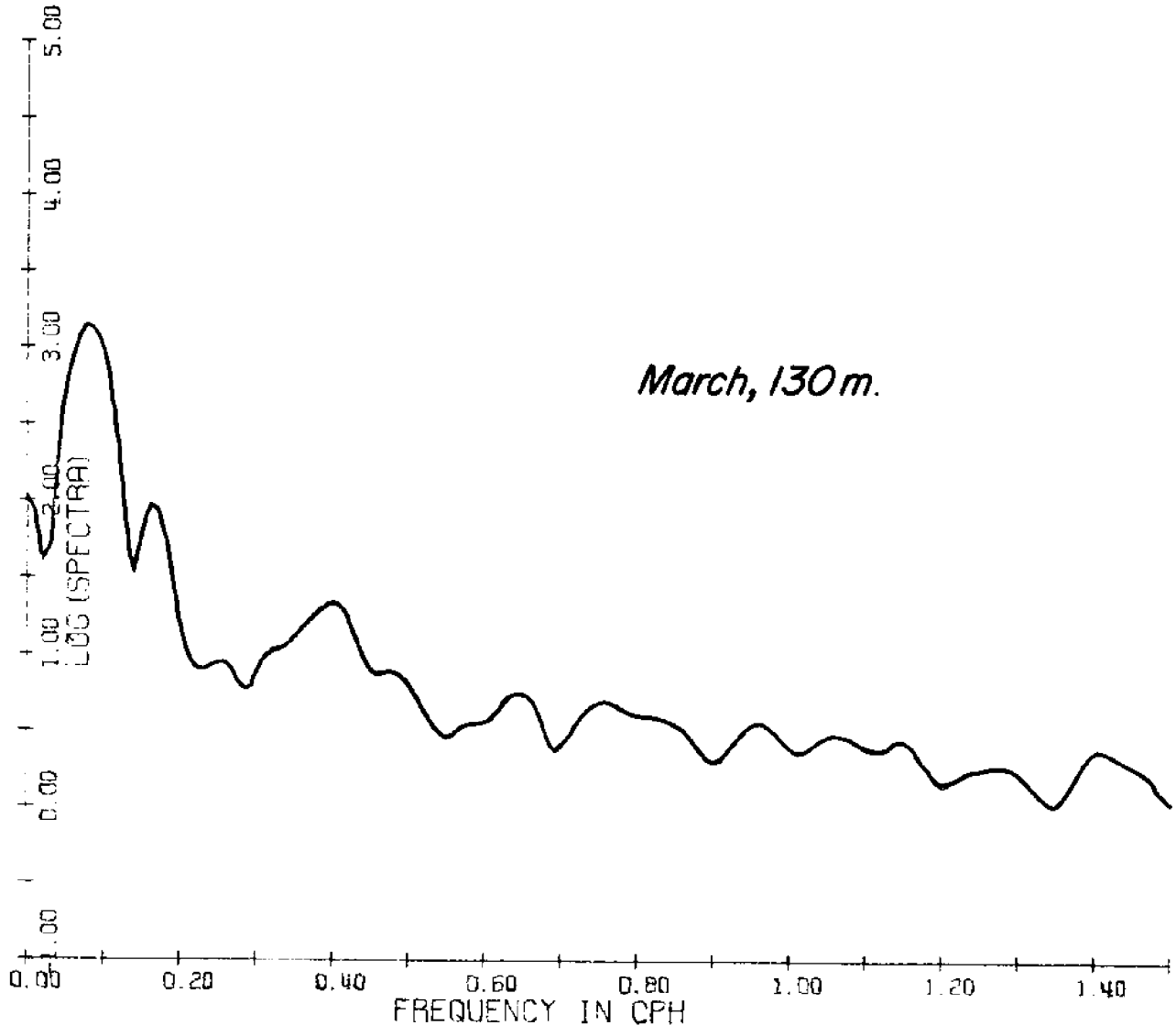

Figure 38. Spectra of original data, March 1972 - 130 m

CHAPTER V

NUMERICAL TIDAL MODEL OF PORT VALDEZ

Before making any extensive investigations as to the current regime of Port Valdez it is of interest to obtain as much information as possible on the tidal currents of the fjord. The currents studied by the model to be described in this chapter are the depth-mean currents $\bar{u}$ and $\bar{v}$ described by:

$$\bar{u} = \frac{1}{h+\eta} \int_0^{h+\eta} u \, dz ,$$

where u is the actual horizontal current at depth z (in the +x direction), h is the sea floor depth below mean sea level, and η is the sea-surface height above mean sea level. A similar equation holds for $\bar{v}$, in the +y direction. The depth-mean current will essentially be due to the slope of the sea surface and in the study that follows no attempt is made to take into account the effects of wind and density differences.

As mentioned in Chapter I, currents, except at the entrance to Port Valdez, are going to be very small and furthermore will be approximately 90° (one-quarter of a period) out of phase with the tide heights. In order to obtain more precise information as to the point-to-point distribution of the current amplitudes and phase lags, it is necessary to make use of the hydrodynamic equations of motion and continuity. For the purposes of this study, these are taken to be

$$\frac{\partial \bar{u}}{\partial t} = f\bar{v} - g\frac{\partial \eta}{\partial x} - g\frac{\bar{V}\bar{u}}{C^2(h+\eta)}$$

$$\frac{\partial \bar{v}}{\partial t} = -f\bar{u} - g\frac{\partial \eta}{\partial y} - g\frac{\bar{V}\bar{u}}{C^2(h+\eta)}$$

$$\frac{\partial \eta}{\partial t} = -\frac{\partial \bar{u}(h+\eta)}{\partial x} - \frac{\partial \bar{v}(h+\eta)}{\partial y} ,$$

where $\bar{V} = (\bar{u}^2 + \bar{v}^2)^{1/2}$.

In the above equations the sense of rotation of the x and y axes is counter-clockwise in the horizontal plane, $\bar{u}$ and $\bar{v}$ are the depth-mean currents in the x and y directions respectively, and f is the Coriolis parameter $2\Omega \sin$ (latitude) where Ω is the angular velocity of the earth's rotation. C is the friction coefficient of de Chezy and g is the acceleration due to the earth's gravity.

It will be noted that in the above equations convective acceleration terms have been neglected. It is considered that, except at the entrance, this assumption is justified on the grounds that the fjord is regular in shape (rectangular cross-section, little depth-variation).

The above equations in general constitute a mixed initial value/boundary value problem. Although it is theoretically possible to reduce the equations to a single elliptic partial differential equation in η (assuming a periodic solution and linearized equations -- very reasonable assumptions in this case), it is simpler to treat the problem as time dependent and to solve the equations by using finite-differences for ∂t, ∂x, ∂y, etc. In this case initial values are provided in the form of zero currents and a single overall high tide level. A cosine behavior of the tide at the entrance is specified and after several tidal cycles the model settles down to a periodic set of answers.

The finite-difference forms of the equations are often obtained in an explicit form. A disadvantage of such forms is that a stability criterion of the type $\Delta t < \sqrt{\Delta x / g(h+\eta)}_{max}$ must be used (Δt is the time step and Δx is the grid spacing). In the case of Port Valdez, with maximum depths of around 240 m and a necessary grid interval of around 1000 m, Δt would have to be of the order of 20 seconds -- which would in turn require considerable computer time. To escape partly from this restraint, and to take advantage of a recently-developed method which

allows one to use a grid made up of unequally spaced perpendicular lines, an implicit numerical tidal model was used (Mungall, 1973).

The finite-difference grid (selected as giving the best compromise between coastline-fit and computer time) for Port Valdez is shown in Figure 39. It should be noted that the grid does indeed allow a good fit to the coastline given the constraint of a limited number of rectangles. Considerable care was taken in evaluating the depths required at each side of each computational rectangle. Since these depths are critical to the correct numerical evaluation of the equation of continuity, mean depths were computed from graphs of bottom depth vs distance along the grid lines.

The entrance, represented by a single open-sided computational rectangle, was given special attention in order that the computed currents through the entrance should be as realistic as possible. To this end the effective cross-sectional area of the entrance rectangle was made equal in value to that of a section drawn from a point (lying 300 m NE of the left hand side of the model entrance) on the western side of the entrance perpendicularly to the other side, and such that the line passed through the current meter string location.

The quantity finally selected as being of most interest for modeling was the M_2 tide of the inlet, as this is the dominant constituent. Its amplitude is 4.5 ft, and the value 4.5 cos (ωt) was specified at the entrance, with $\omega = 2\pi/12.42$ and t being time in solar hours. The tidal cycle was divided up into 720 time intervals, so that each time step was equivalent to 1 lunar minute (which resulted in a saving in computer time per run of x 3). A value of 70 $m^{1/2}$ sec^{-2} was used for C.

The tidal model was run on the University of Alaska's IBM 360/45 computer, with sample values of height and current being printed out every time step (to serve as a check on convergence, etc.), and during the last tidal cycle (the 8th) every value of tide height and current computed was output onto magnetic tape. These values were then analysed for the M_2 constituents (thus, eliminating any small amounts of distortion present) of the tide height and current components. The same program that performed these analyses then combined the $\bar{u}$ and $\bar{v}$ current component information into more useful quantities of vector current amplitude and phase.

As was expected there was no distinguishable change in the amplitude or phase of the height components anywhere in the inlet (to repeat, this is a consequence of there being zero current and hence, zero Coriolis force across the inlet at the time of high water, and of there being little to cause a longitudinal change of phase or amplitude). No figures for tide height amplitude or phase are thus shown.

The M_2 current amplitudes are shown in Figure 40. It will be noted that they are all small, of the order of 1 cm/sec in the middle of the fjord, and slightly greater than 10 cm/sec at the entrance (actual value 11 cm/sec). Also to be seen is the fact that the current amplitudes are slightly greater on the right hand side (southside of the inlet).

The phase lead in degrees of the maximum inwards M_2 current over the time of high water is shown in Figure 41. It can be seen that the current along the long axis of the fjord reaches its maximum one quarter of a tidal period in advance of high water. Maximum current on the north side occurs some 10 minutes earlier than the maximum current along the axis, and 20 or so minutes earlier than that on the south side (360° corresponds to 12.42 hours, so 5° corresponds to approximately 10 minutes).

In order to permit easy prediction of the depth-mean currents at any position and time, the following technique was used: Currents corresponding to neap and spring tides are assumed to bear the same relationship to the M_2 currents as do neap and spring ranges to the M_2 tidal amplitude x 2. Thus, to obtain neap and spring current amplitudes, the M_2 current amplitudes computed above were multiplied respectively by the factors 6.23/9.028 and 12.53/9.028 and their phases were assumed to be equivalent to those of the M_2 current constituents. The magnitudes and directions of these quantities were computed and plotted by computer for the times of High Water (HW), HW $\pm$ 1, HW $\pm$ 2, HW $\pm$

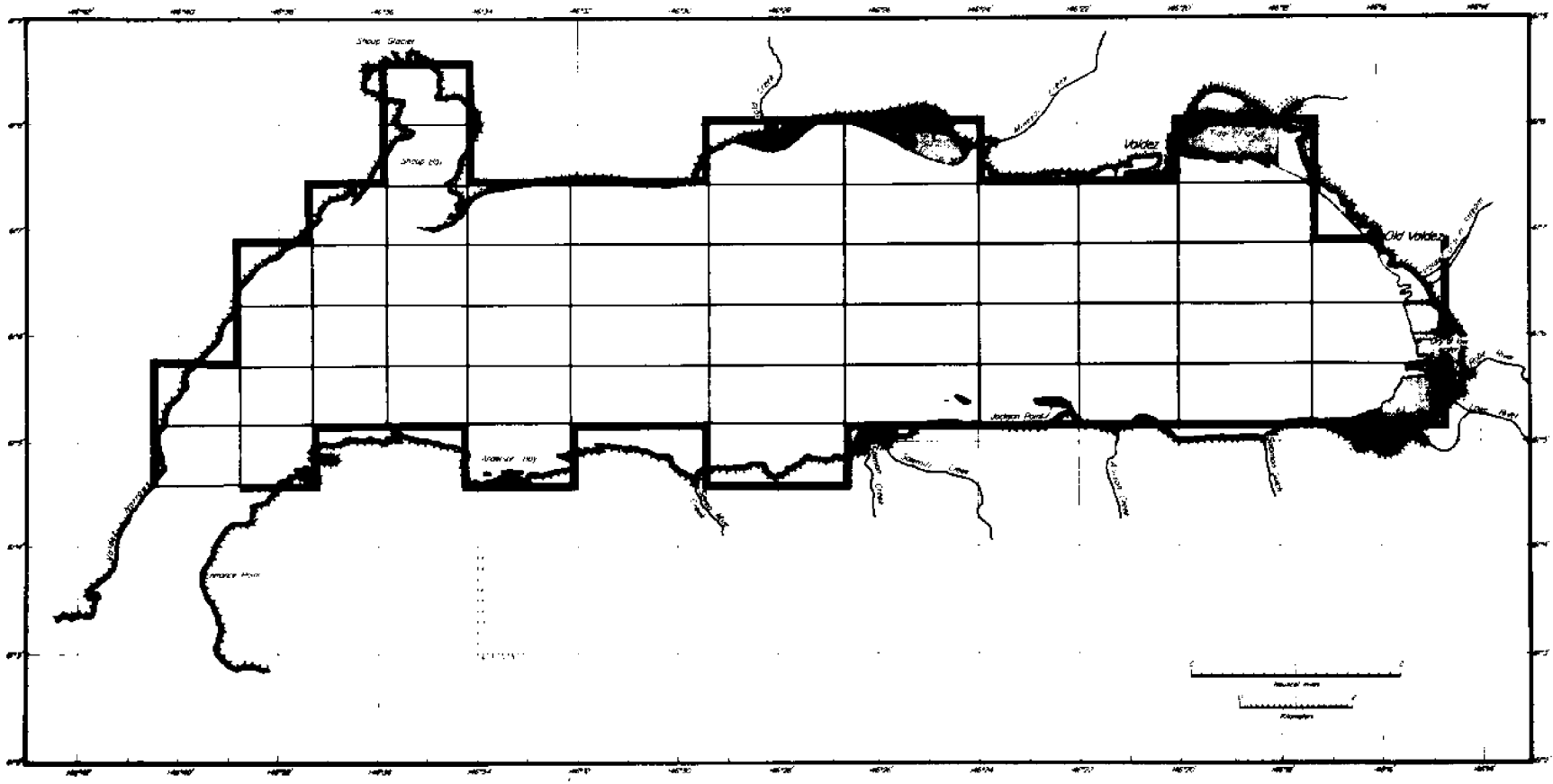

Figure 39. Grid used for hydrodynamic numerical tidal model of Port Valdez

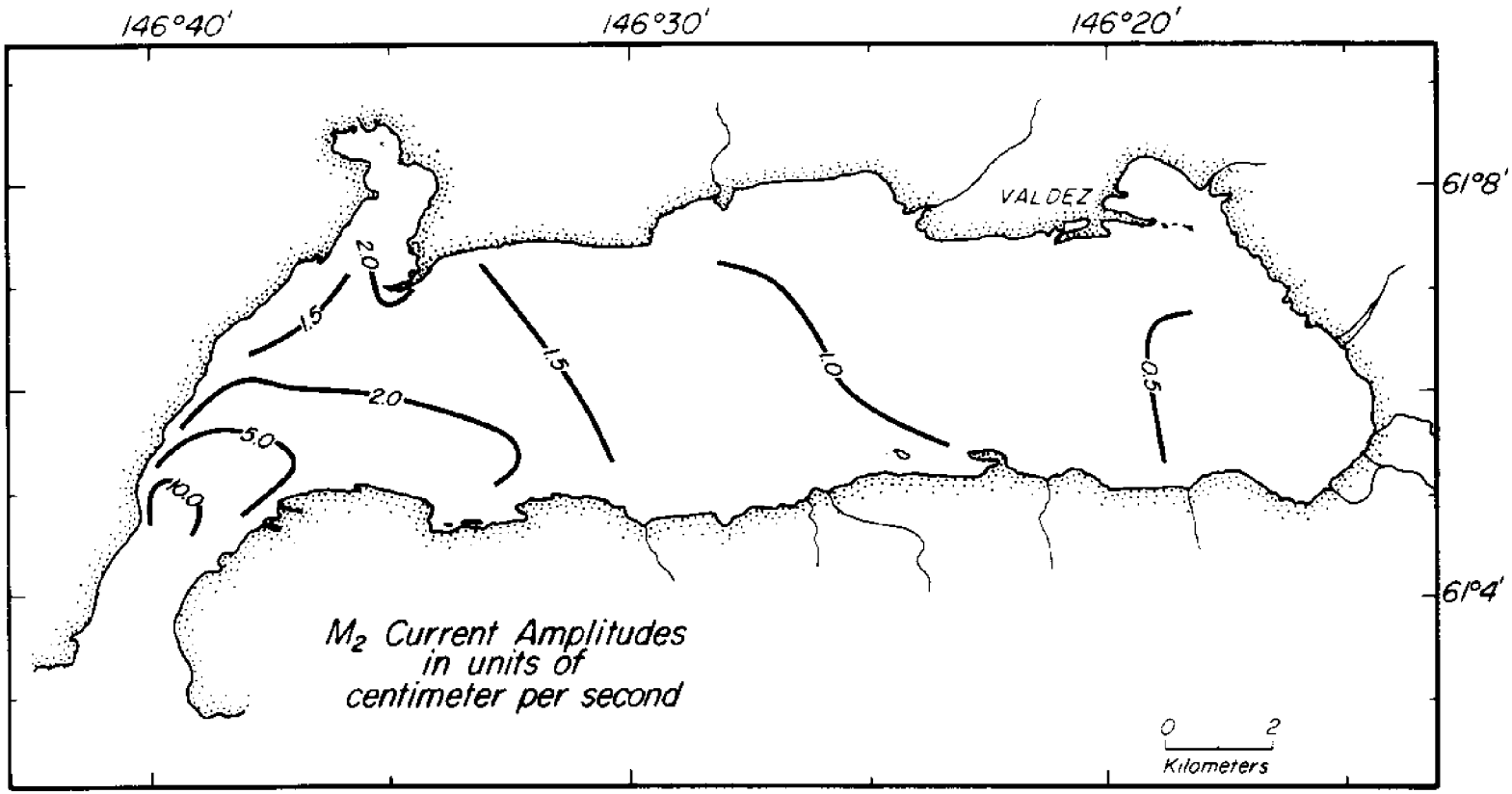

Figure 40. Results of Port Valdez tidal model calculations: current amplitudes

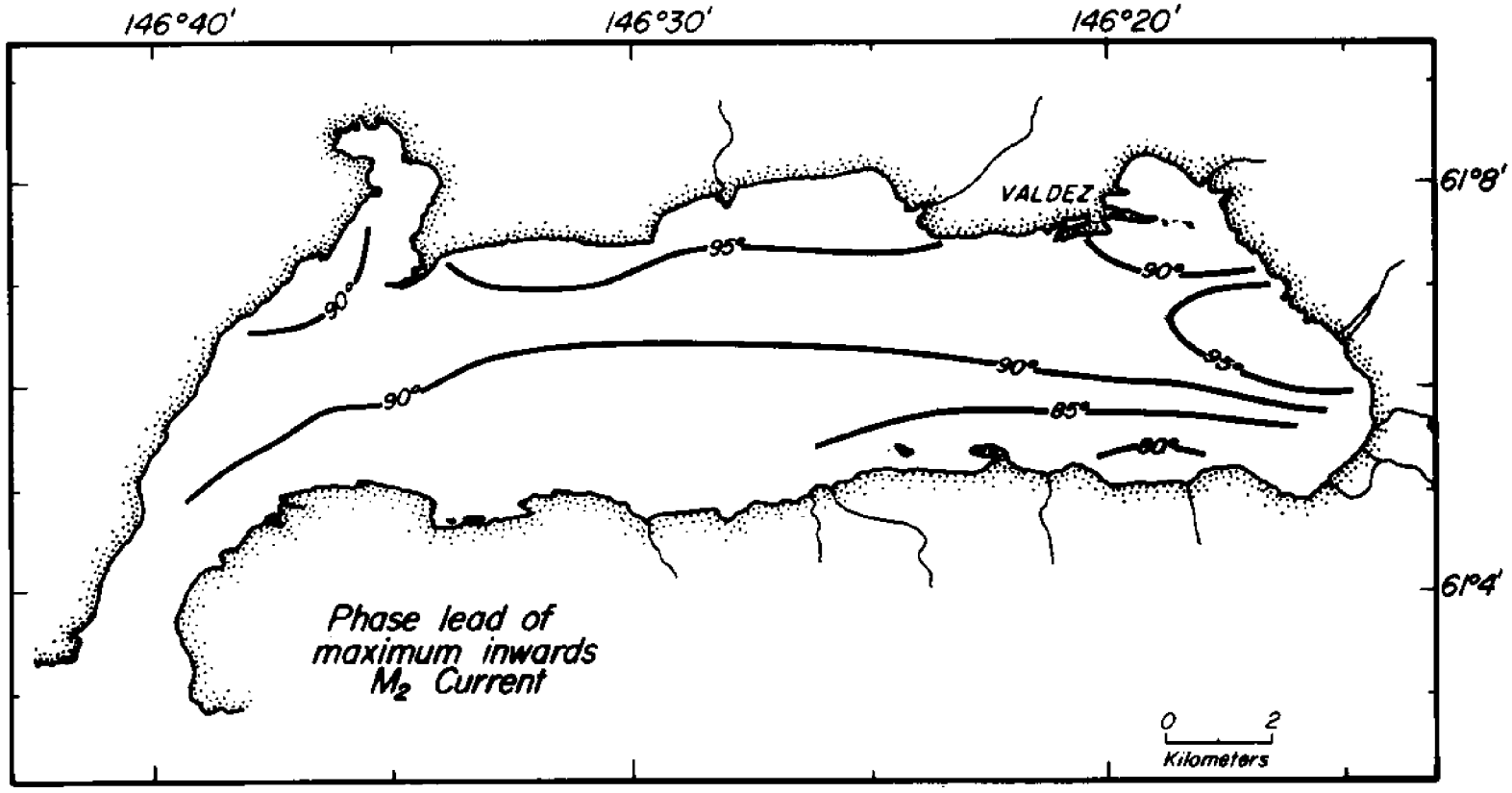

Figure 41. Results of Port Valdez tidal model calculations: lead of maximum inwards current before time of high water

3, HW ± 4, HW ± 5, and HW ± 6 hours. These values, shown in the form:

neap current (cm/sec) x 10,
spring current (cm/sec) x 10

can be seen in Figures 42 to 54. The final vectors were drawn by hand so as to give a better visual representation. The numbers correspond to conditions at a location in the middle of the arrow that points to the numbers.

To compute an actual value, one selects from a tide table the times and heights of the high and low waters that encompass the time of the prediction. The difference between the two heights gives the effective tidal range of that tide (the nearer the time difference between them is to 6.21 hours, the better the prediction). The number of hours of the prediction time before or after high water is also computed.

Next one selects the tidal stream chart corresponding to the appropriate time. At the required position on the chart the nearest (or interpolated) neap and spring current values are obtained. These values, along with the effective tidal range, are used as entries in Figure 55 or 56.

Placing a straight-edge at approximately 45°, one joins the two numbers recorded above -- the smaller value being located on the left column (corresponding to neap tide conditions) and the larger value being located on the right column (corresponding to spring tide conditions).

The intercept between the straight-edge and a vertical line corresponding to the effective tidal range gives the predicted current.

For example, suppose one requires the value of the current at 1100 hrs at 61°06'N - 146°32'W given the following tide table data:

LW	0800 hrs	4 ft
HW	1400 hrs	14 ft

The effective range is 10 ft, and the time for the prediction is 3 hours before high water. Consulting Figure 45, one obtains the quantity 10,20. Making use of Figure 55, on joining the numbers 10 and 20, one finds a value of 16 (1.6 cm/sec) at the point of intersection of the straight-edge and the vertical line through 10 ft.

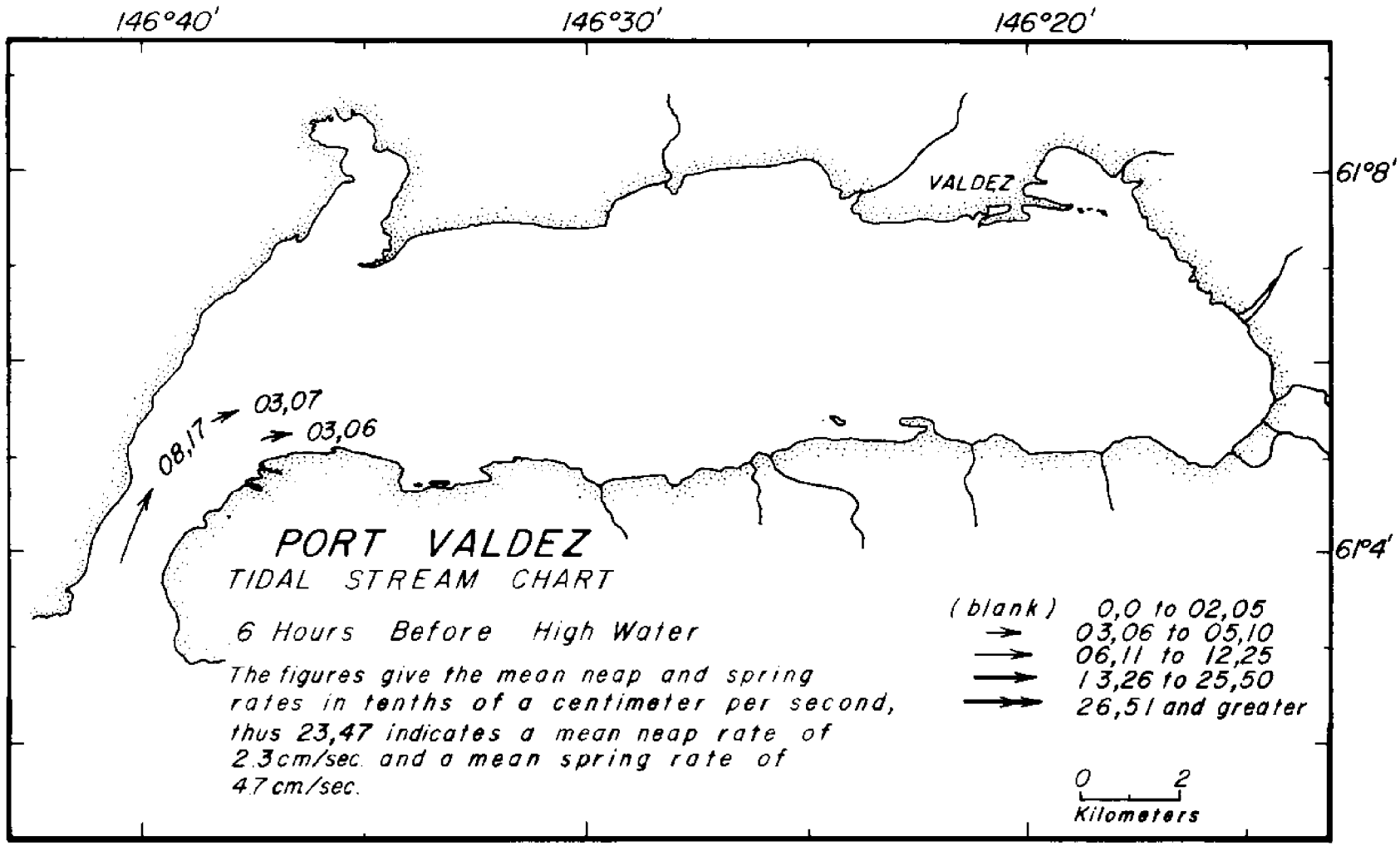

Figure 42. Port Valdez tidal stream chart, 6 hrs prior to high water

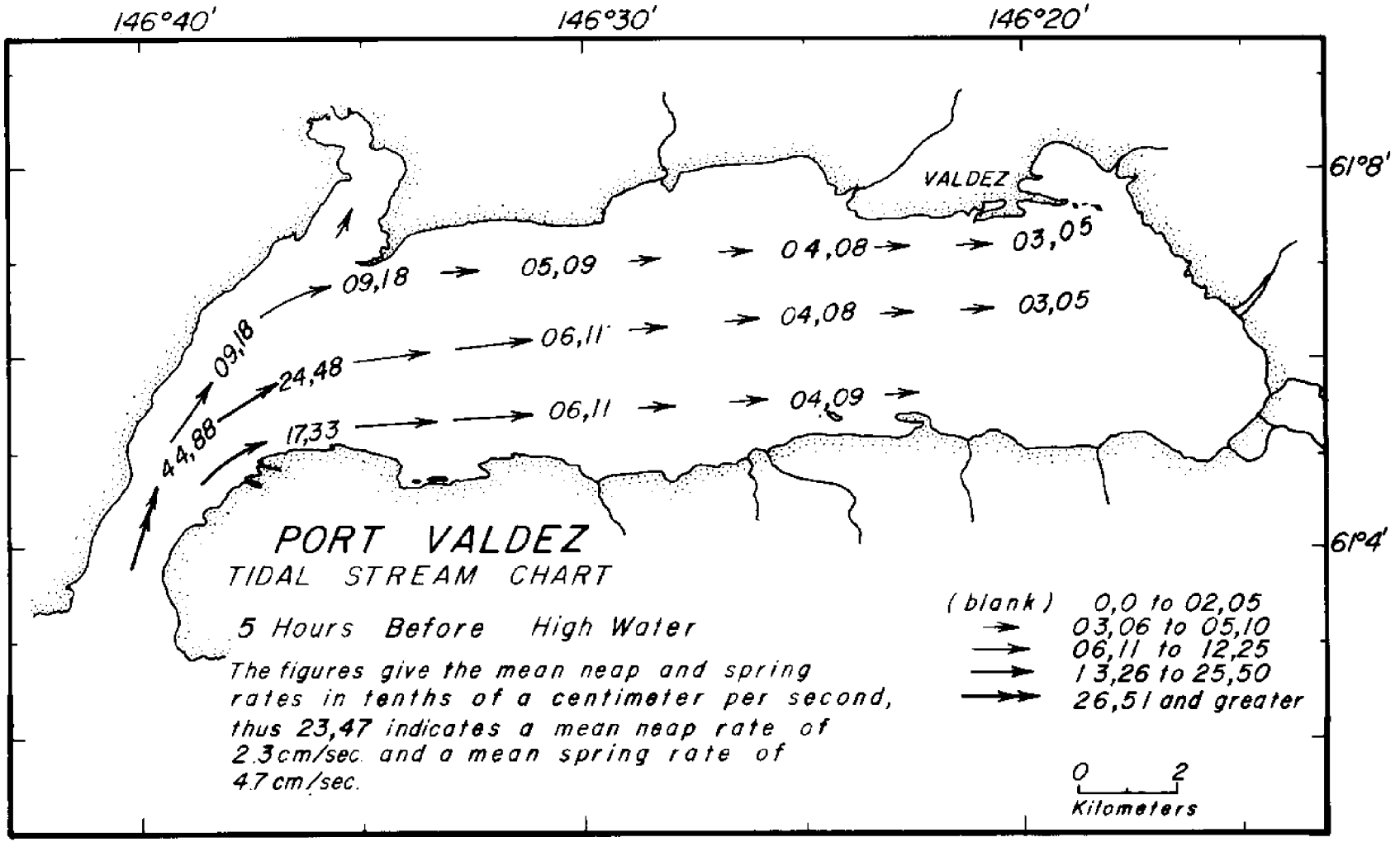

Figure 43. Port Valdez tidal stream chart, 5 hrs prior to high water

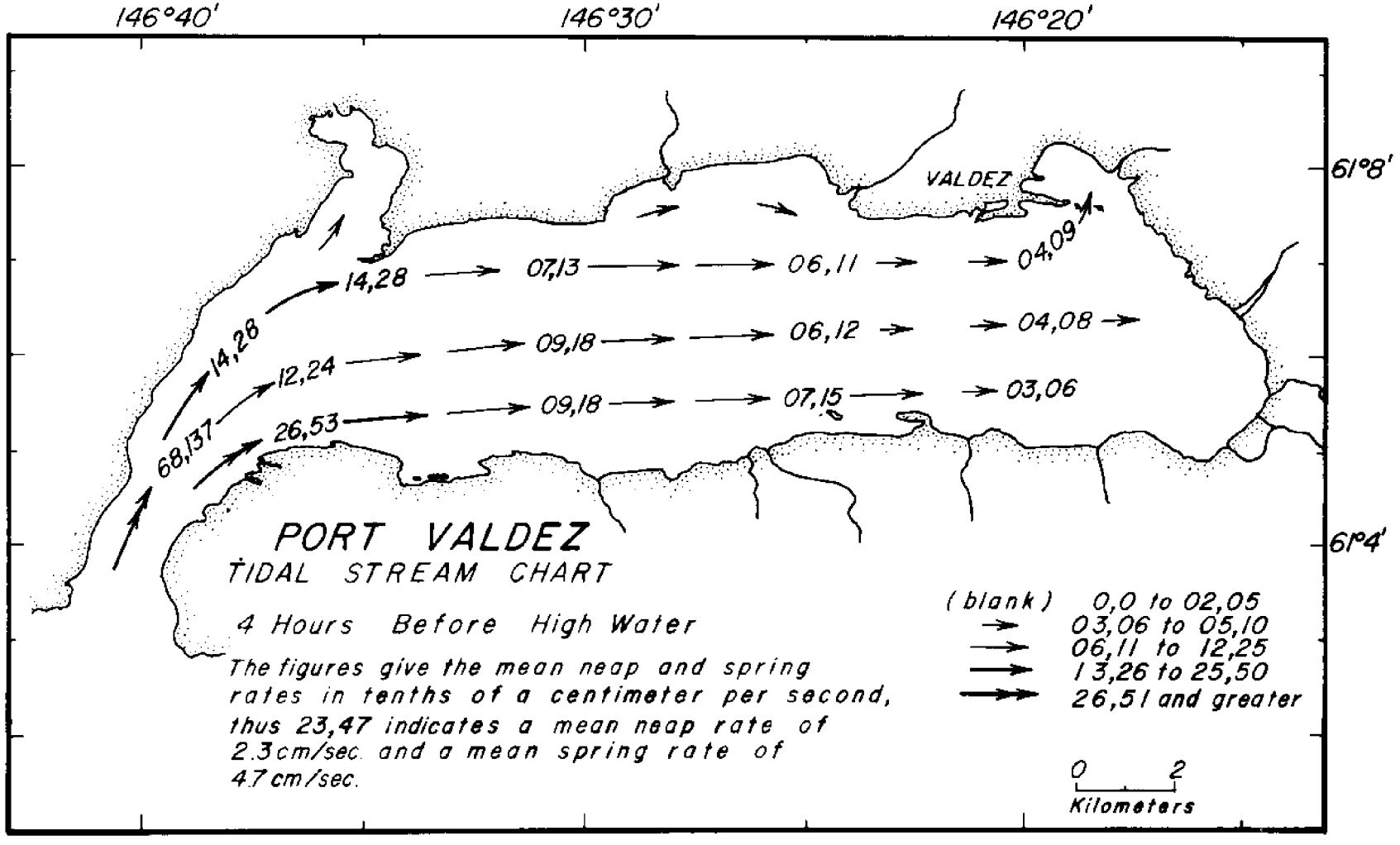

Figure 44. Port Valdez tidal stream chart, 4 hrs prior to high water

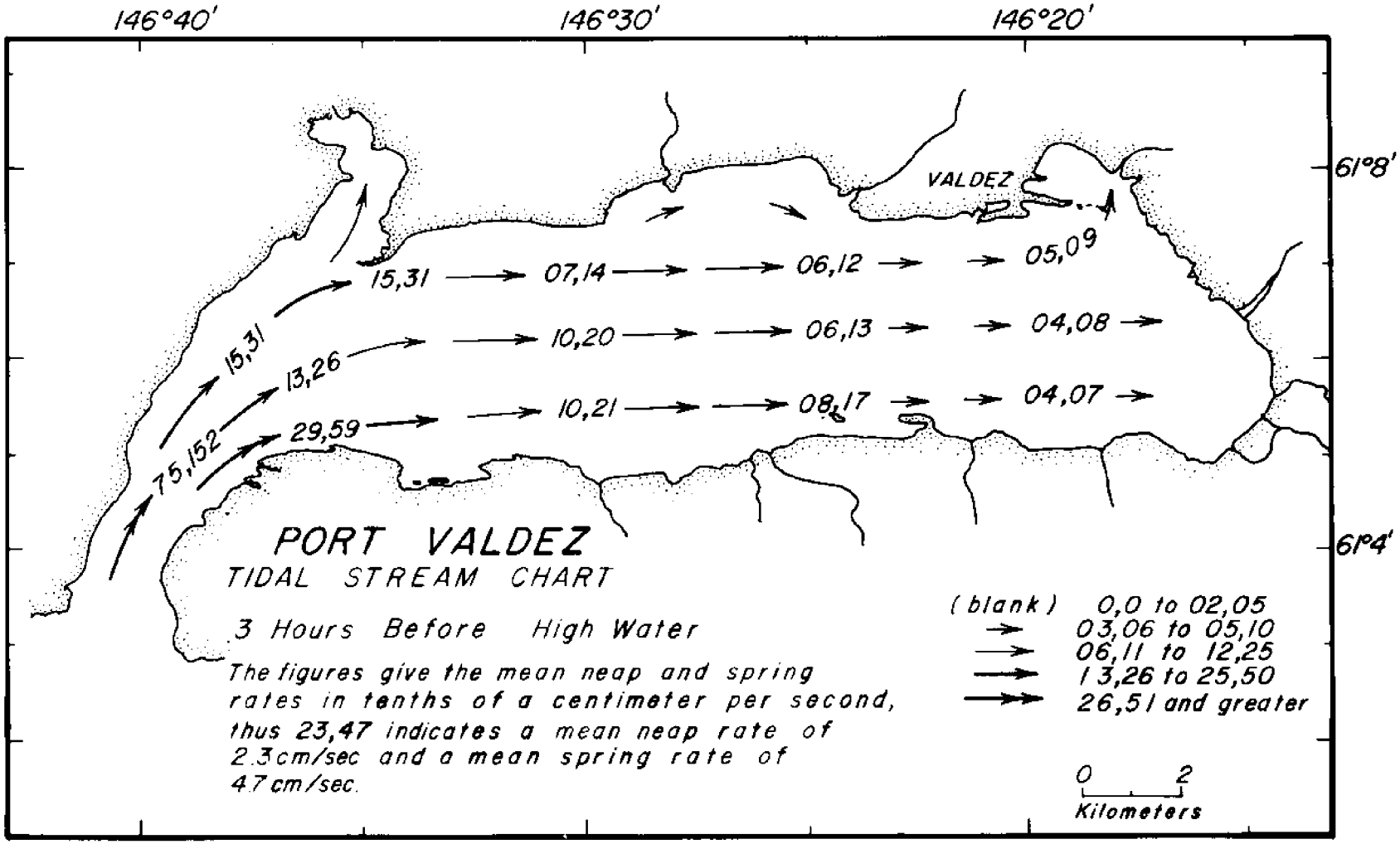

Figure 45. Port Valdez tidal stream chart, 3 hrs prior to high water

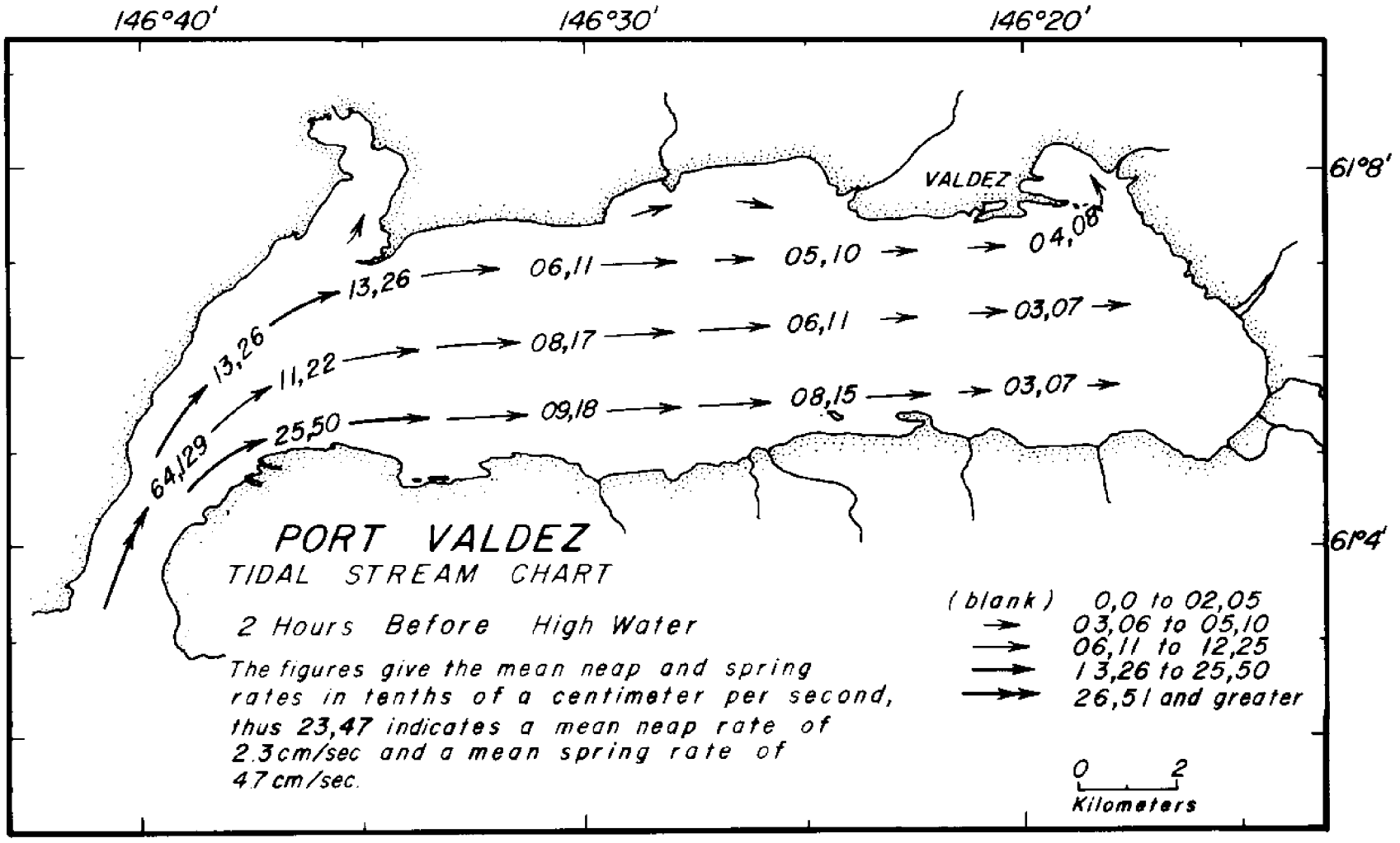

Figure 46. Port Valdez tidal stream chart, 2 hrs prior to high water

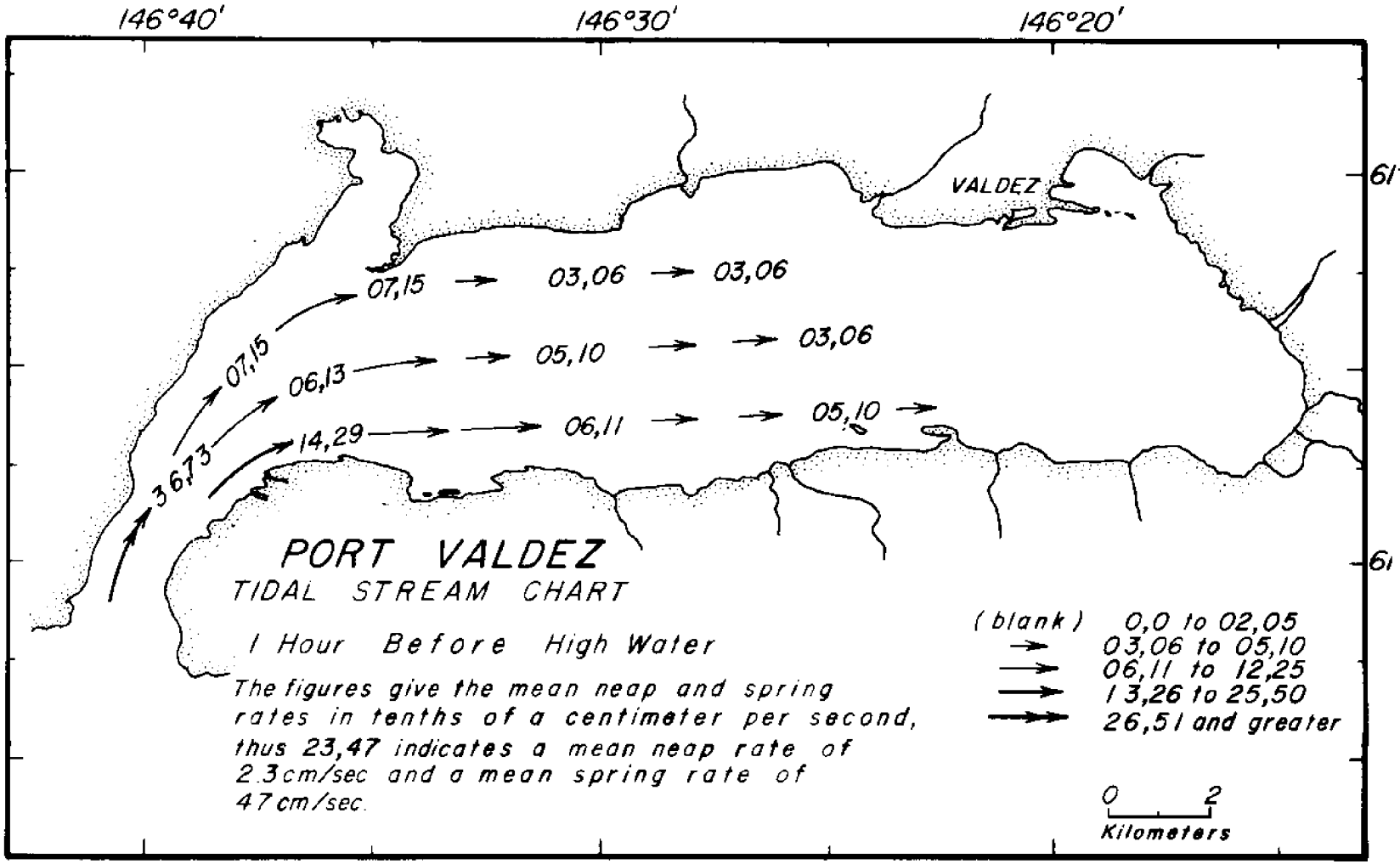

Figure 47. Port Valdez tidal stream chart, 1 hr prior to high water

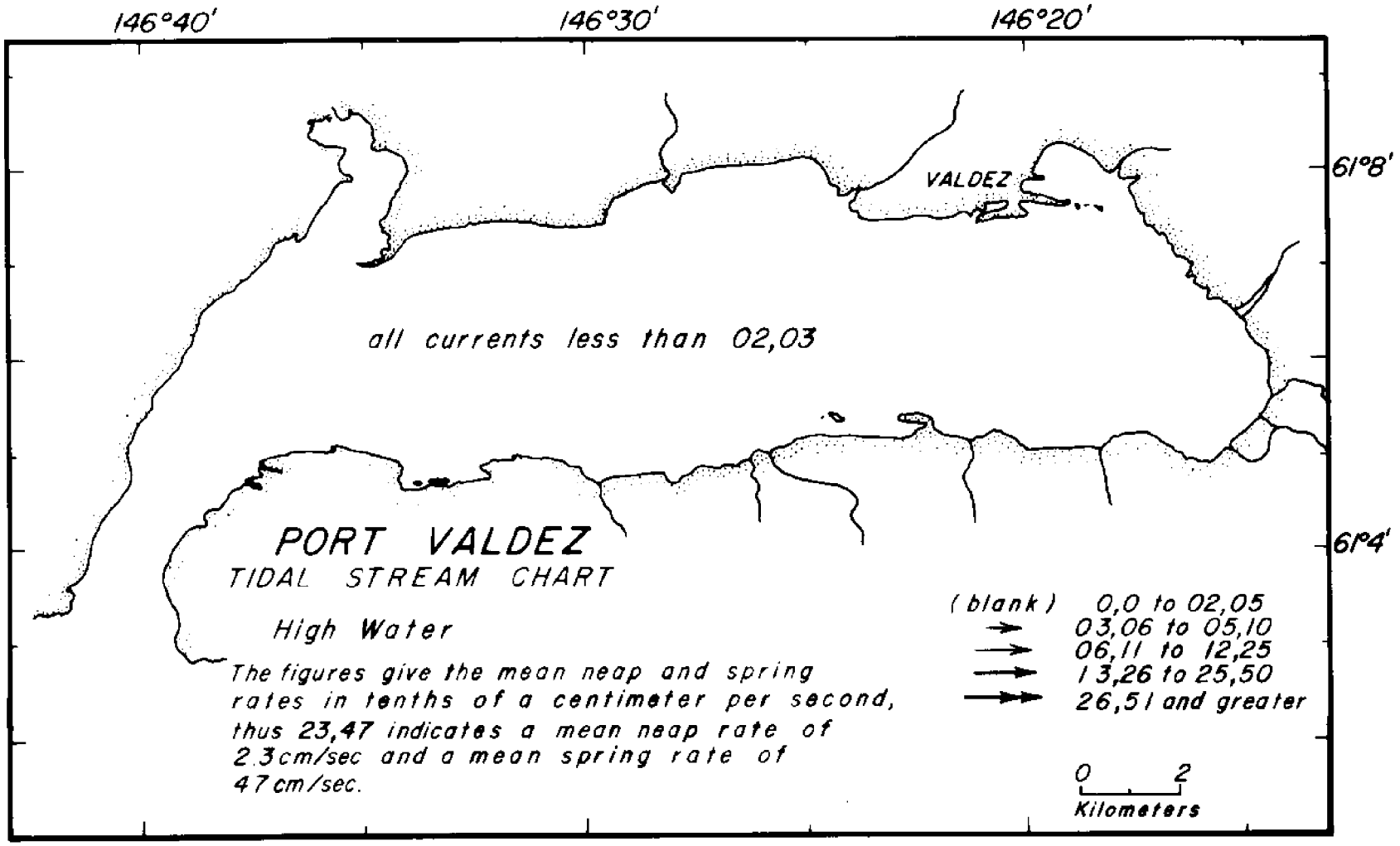

Figure 48. Port Valdez tidal stream chart, at high water

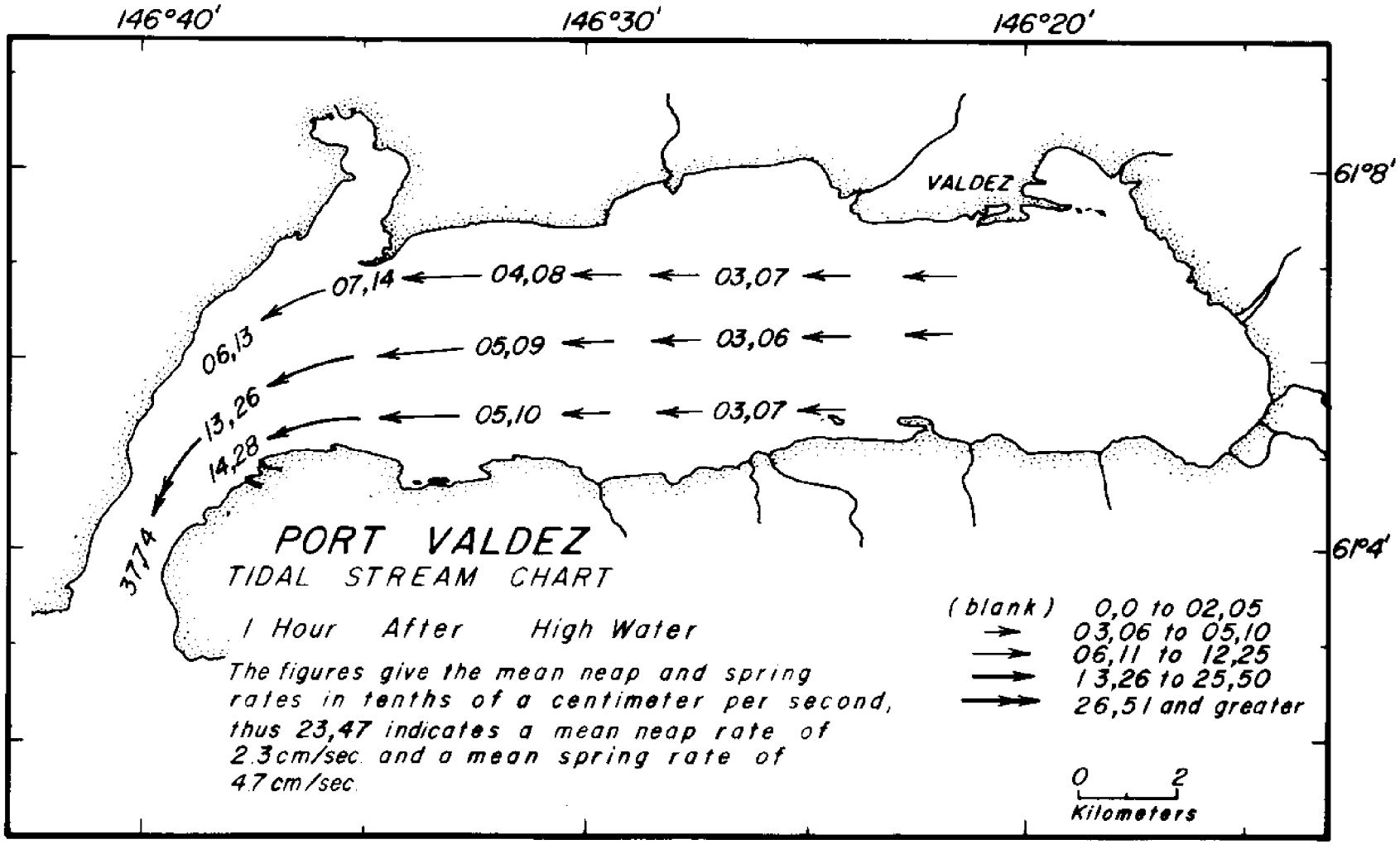

Figure 49. Port Valdez tidal stream chart, 1 hr after high water

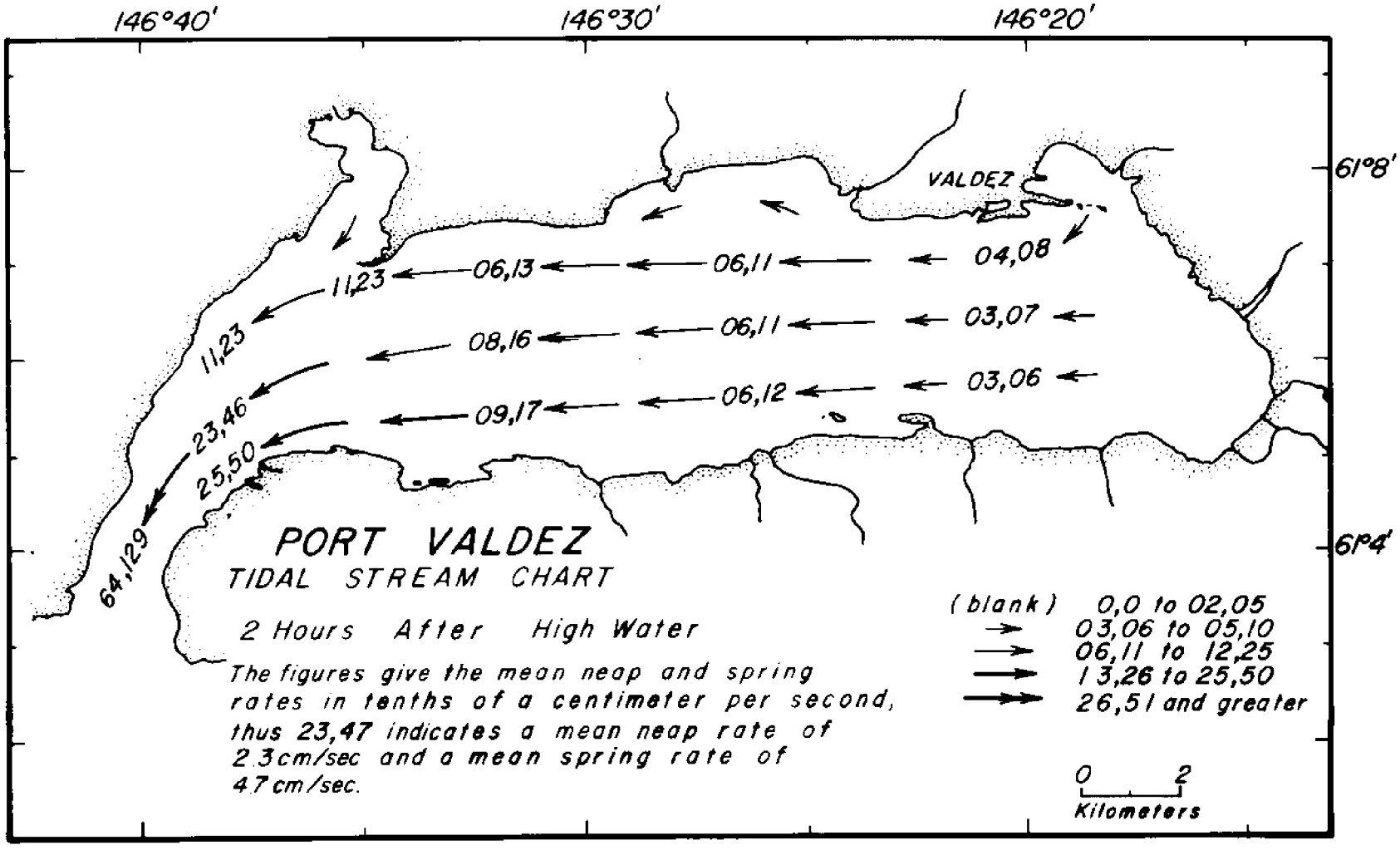

Figure 50. Port Valdez tidal stream chart, 2 hrs after high water

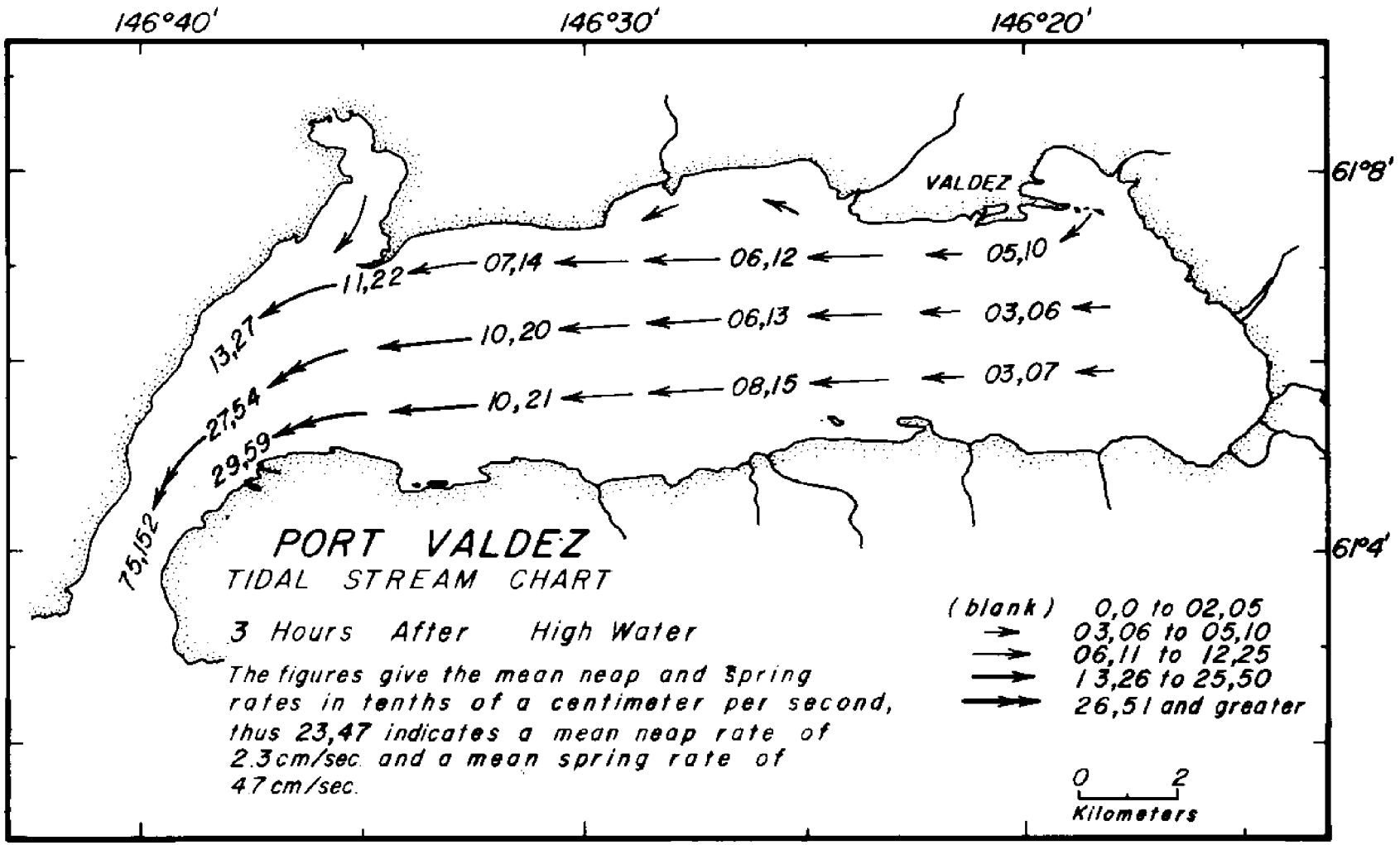

Figure 51. Port Valdez tidal stream chart, 3 hrs after high water

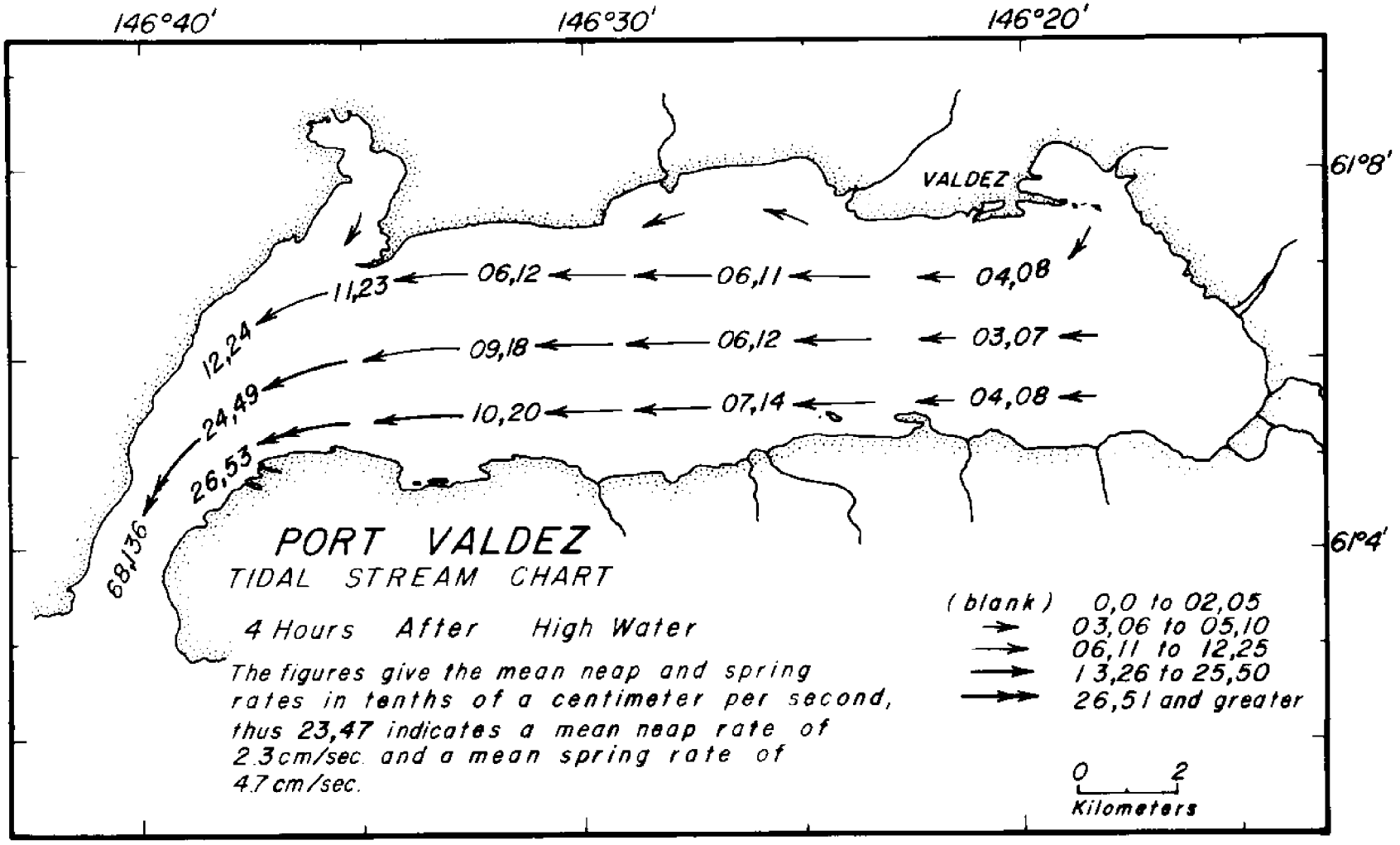

Figure 52. Port Valdez tidal stream chart, 4 hrs after high water

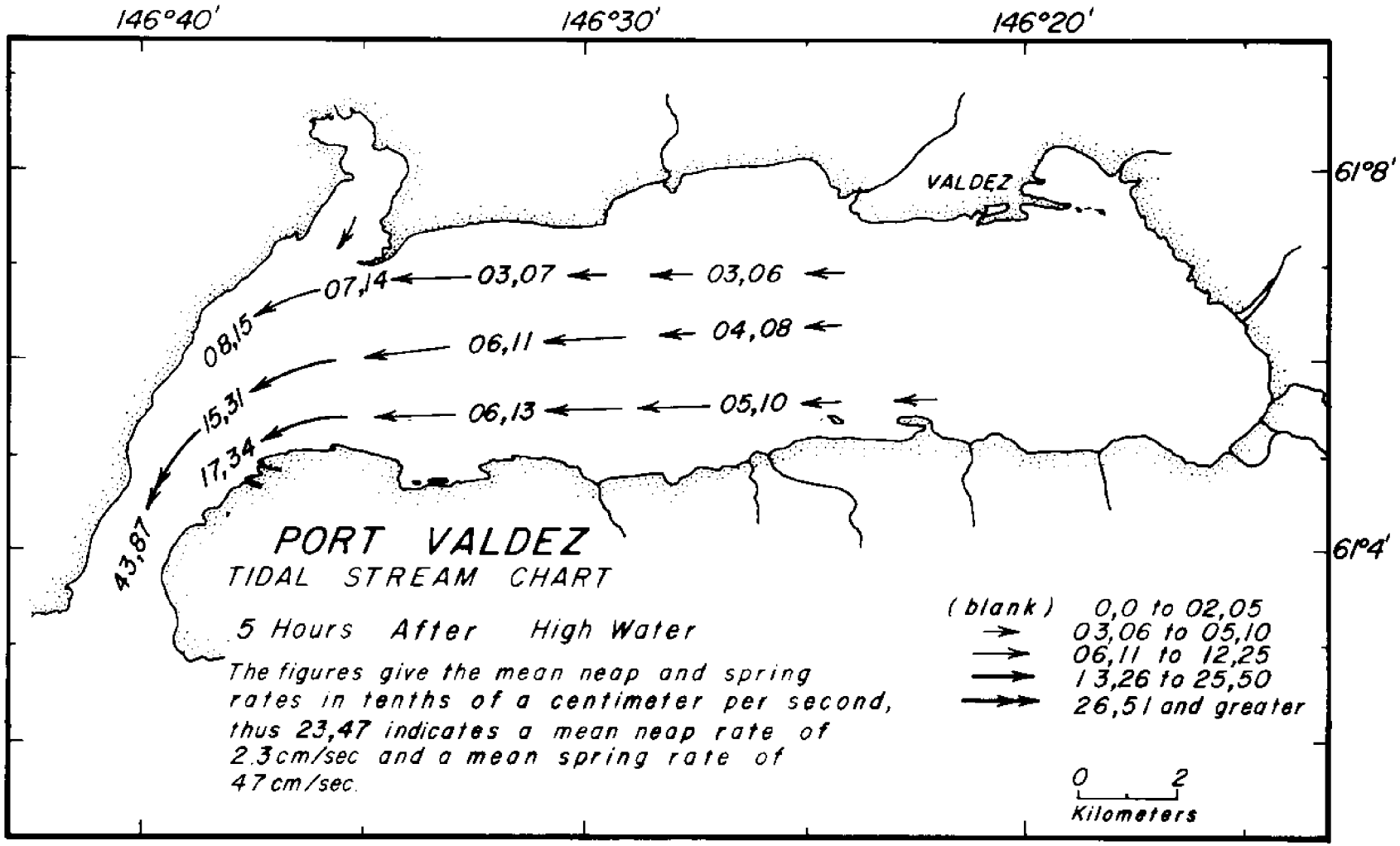

Figure 53. Port Valdez tidal stream chart, 5 hrs after high water

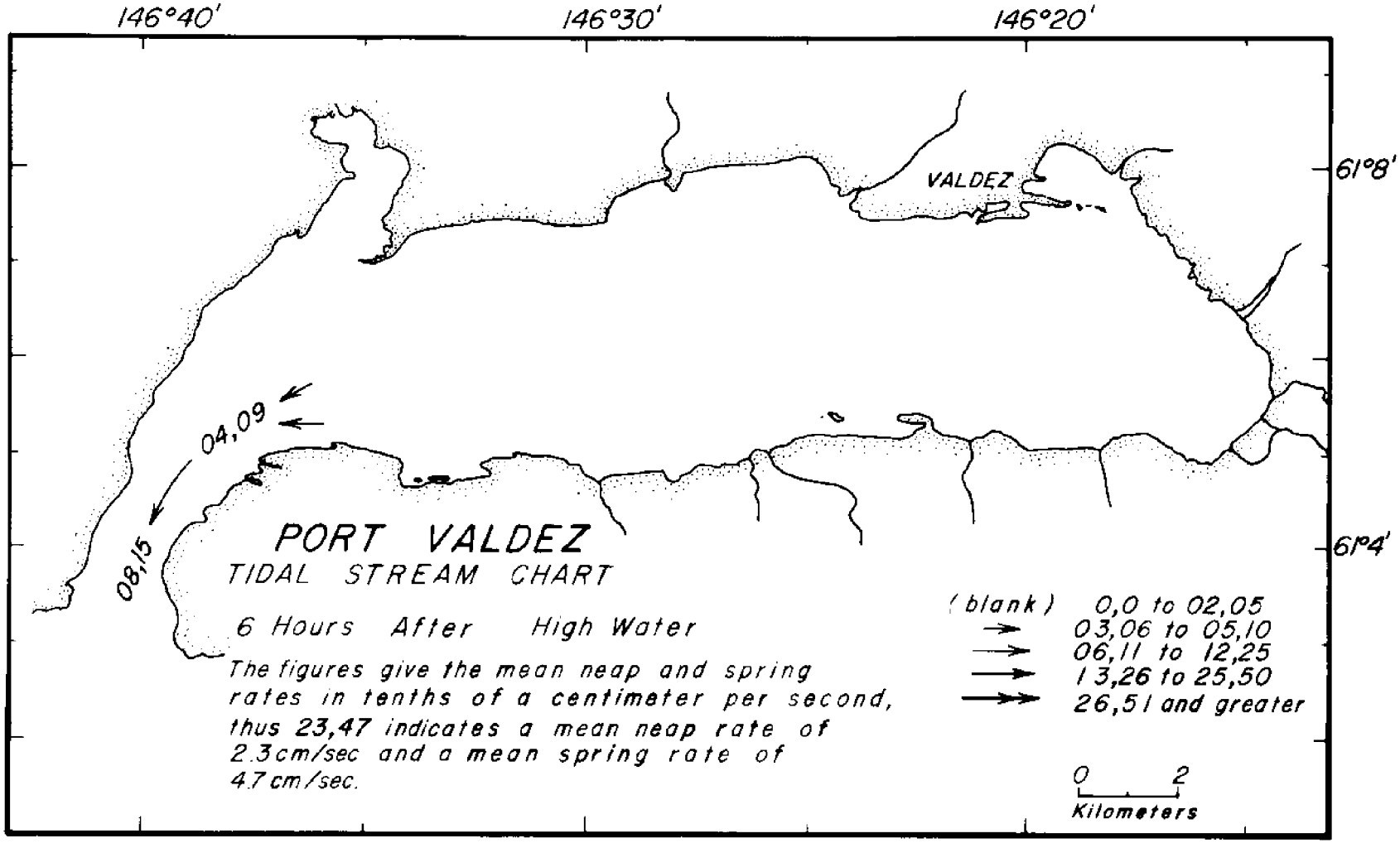

Figure 54. Port Valdez tidal stream chart, 6 hrs after high water

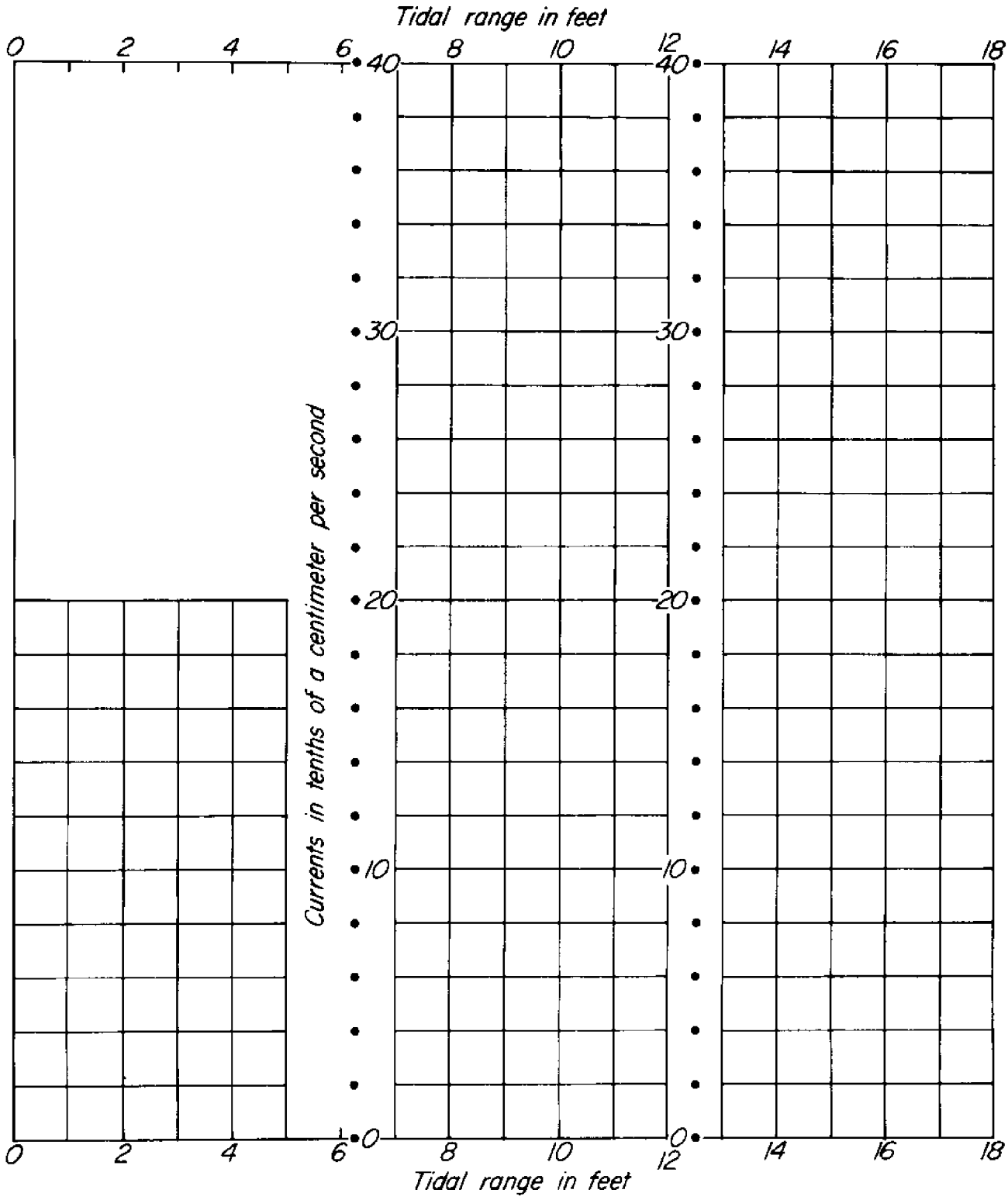

Figure 55. Prediction diagram for currents less than 15.30

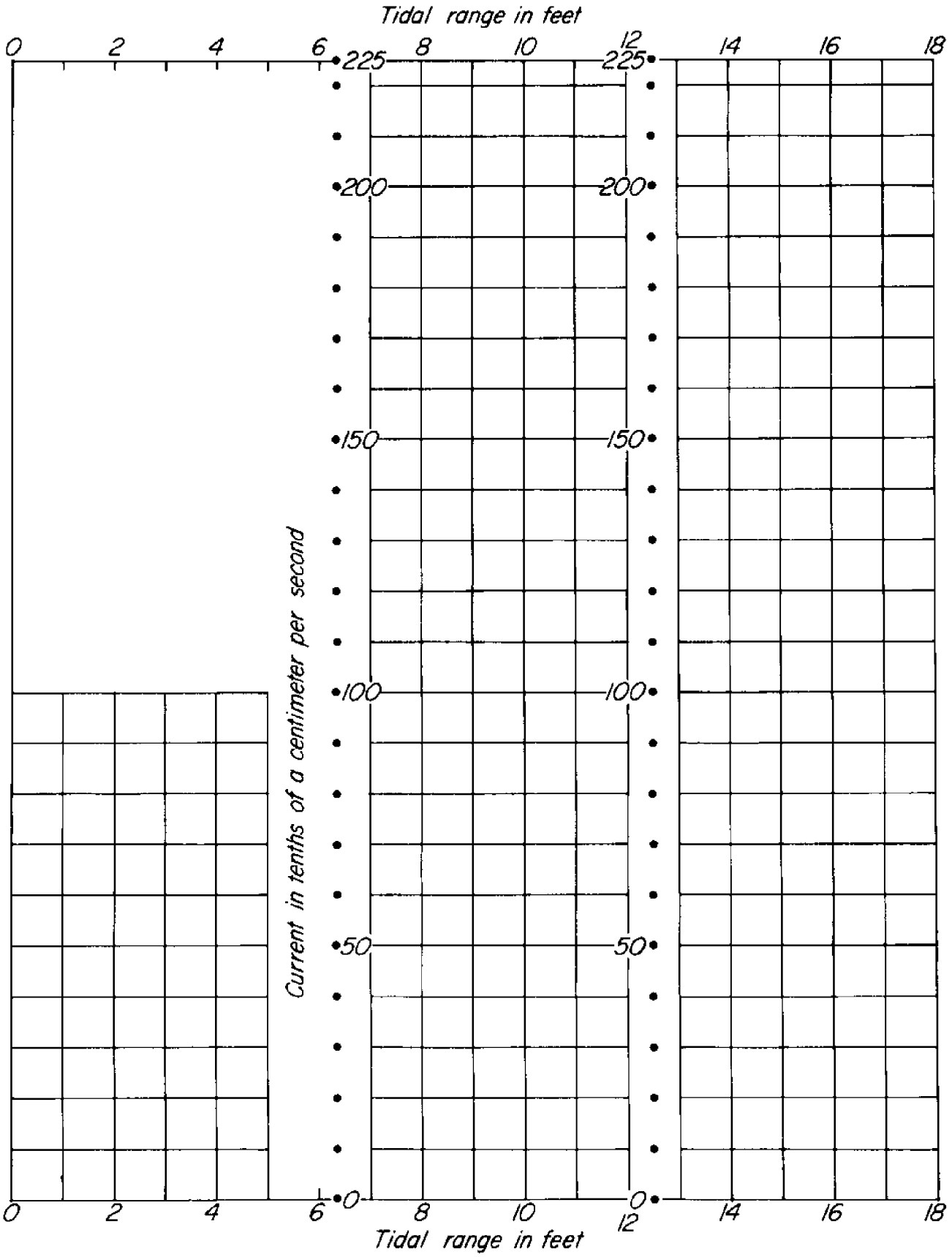

Figure 56. Prediction diagram for currents greater than 15.30

CHAPTER VI

SUMMARY AND CONCLUSIONS

The purpose of this brief chapter is to summarize the results of the current meter data analyses and to combine these, where possible, with the results of the numerical tidal model. Owing to the shortness of the current records it has not been possible to produce any precise results concerning the change of the current constituents (in the form of ellipse and phase information) with depth. Should such information be desired it is felt that a 29-day series of hourly data should be available for tidal analysis.

The major current constituent at the entrance is that associated with the M_2 tide. For the December 1971 data, the average amplitude was 12.0 cm/sec (for an 'effective' M_2 tide amplitude of 4.56 ft) and for the March 1972 data was 15.4 cm/sec (for an 'effective' M_2 tide amplitude of 6.80 ft). Thus, at the entrance, one expects an M_2 current amplitude of about 2.5 cm/sec per foot of M_2 tide amplitude, or about 11 cm/sec for the M_2 constituent. By the tidal model the computed current amplitude for the entrance was also 11 cm/sec; thus the model appears reasonable.

At the entrance, except for the 130 m currents, the ellipses are probably similar in shape and in phase: the M_2 ellipses are uniformly thin, with maximum currents in the cross-channel direction being less than a tenth of the long-channel values. It seems that as one approaches the bottom, the direction of the maximum current swings some 5 to 10 degrees clockwise.

The drift currents encountered during the two series of observations were considerable, with maximum values of around 5 cm/sec. It was noticeable that the direction of the drift currents changed from being outwards to inwards, or *vice versa*, slightly less than 80 m below the surface. Drift currents *above* this depth were mostly directed *inwards* in the December 1971 series, and *outwards* in the March 1972 series.

The chief results of the numerical tidal model study are clearly shown in Figures 16 and 17. No phase change occurred in the M_2 constituent over the region, and no change in the amplitude of the M_2 constituent was found. These results were expected due to the standing wave nature of the tides. The tidal current prediction charts shown in Figures 42 through 54 are of interest, and allow one to predict currents for any point at any time -- the accuracy being greatest when the interval between the nearest high and low water is equal to 12.42 hours.

To conclude, it is felt that if further knowledge concerning the tidal currents and drift currents is considered desirable, note should be taken of the following:

1) Tidal and drift currents throughout the region are very small -- the current meters used must be chosen and calibrated accordingly.

2) Should information be sought on the current constituents, the timing mechanisms of the meters must be carefully calibrated, and all relevant times must be noted. A current meter deployment of at least 31 days is considered desirable. A tide gauge should be operating concurrently.

3) It may be worth investigating seiche motion -- local knowledge would be of help in this respect. Data should be taken at very short intervals.

4) Obtaining drift information without wind and density information will probably not assist predictive capability.

5) It is not known whether the critical depth for current reversal near 80 m, is appropriate for other times or locations. If such information could be obtained, it might make the positioning of current meters in future studies a less expensive task.

REFERENCES

Doodson, A. T., and H. D. Warburg, *Admiralty Manual of Tides.* Her Majesty's Stationery Office, London, 1941.

Dronkers, J. J., *Tidal Computations in Rivers and Coastal Waters.* North-Holland Publishing Company, Amsterdam, 1964.

Jenkins, G. M., and D. G. Watts, *Spectral Analysis and its applications.* Holden-Day, San Francisco, 1969.

Mungall, J. C. H., Numerical Tidal Models with Unequal Grid-Spacing. Technical Report R73-2, Institute of Marine Science, University of Alaska, College, Alaska, 1973.